2022

Phenomic and Genetic Controls of the Drought Stress Response in Sorghum

Melissa A. Lehrer
malehrer@mix.wvu.edu

PHENOMIC AND GENETIC CONTROLS OF THE DROUGHT STRESS RESPONSE IN *SORGHUM*

Melissa Axelrod Lehrer

Dissertation submitted to
the Eberly College of Arts and Sciences
at West Virginia University

in partial fulfillment of the requirements for the degree of
Doctor of Philosophy in Biology

Jennifer Hawkins, Ph.D., Chair
Vagner Benedito, Ph.D.
Edward Brzostek, Ph.D.
Jonathan Cumming, Ph.D.
Timothy Driscoll, Ph.D.

Department of Biology
Morgantown, West Virginia
2022

Keywords: *Sorghum bicolor*, drought stress, hydraulic safety, recombinant inbred line population, quantitative trait loci, domestication, root system architecture, water acquisition, plant hormone signaling

ABSTRACT

Phenomic and Genetic Controls of The Drought Stress Response in *Sorghum*

Melissa Axelrod Lehrer

Drought, one of the most common abiotic stressors, is a result of the precipitation and temperature fluctuations influenced by climate change. As consistent weather patterns are crucial for the maintenance of crop yield, drought threatens food security through its impact on plant growth and development. It is essential to ensure the quality, availability, and affordability of grain-based products in the face of climate change due to expectations of population growth. Therefore, shedding light on the mechanisms associated with drought tolerance is integral to maintaining agricultural production under water-limited conditions. My dissertation work aimed to uncover the morphological, physiological, and genetic controls of drought resistance in *Sorghum*, a C4 grain crop grown for food, feed, and biofuel. In Chapter 3, two *Sorghum bicolor* accessions that differ in their pre-flowering responses to drought were evaluated following long-term drought exposure across juvenile and adult vegetative stages. Findings from this work emphasized accession-specific responses to drought, indicating that morphological/histological and physiological strategies both play roles in promoting hydraulic safety in response to drought, and these mechanisms may be mutually exclusive. Chapter 4 expanded upon the findings of Chapter 3 by uncovering the evolutionary origins of the morphological and physiological responses associated with drought exposure. Using quantitative trait loci (QTL) mapping in a *Sorghum* recombinant inbred line (RIL) population, eight QTL unique for drought exposure were detected. *S. bicolor* alleles controlled reductions in height and enhanced aboveground biomass, emphasizing the impact of grain *Sorghum* varieties (i.e. TX7000) on drought-responsive phenotypes. These biological impacts may be influenced by the candidate genes with these QTL, specifically those involved in reproductive processes. These gene products facilitate grain production and may promote early flowering, a common drought escape mechanism that influences the transition into reproduction before stress becomes too severe. Physiologically, *S. bicolor* alleles increased leaf temperature while *Sorghum propinquum* alleles increased relative water content; these species-specific strategies reflect their variable belowground growth and impact of domestication on drought-responsive phenotypes. The QTL detected for relative water content and leaf temperature contained genes involved in auxin and abscisic acid (ABA) synthesis and signaling. In addition to playing roles in root development and water uptake, phytohormones can also affect aboveground responses, such as growth and stomatal closure. Therefore, our findings highlight the contribution of plant hormones to root-to-shoot communication and water uptake and loss through both above- and belowground strategies. The relationship between above- and belowground responses and hormone signaling was explored further in Chapter 5. Using the same *Sorghum* RIL population, five QTL for belowground responses to drought exposure were identified. Three of these QTL co-localized on chromosome four and with a root biomass QTL detected in this same population evaluated under salinity

architecture is reorganized under osmotic stress by the domesticated parent to favor vertical growth while also increasing root biomass, suggesting a main goal of enhanced water uptake in the osmotic stress response. Candidate genes within these QTL were associated with root development and hormone synthesis/recognition, contributing additional support to the allelic effects described in this work, as well as to the role of water acquisition described in Chapter 4. Genes within the two remaining QTL detected in the drought population were also involved in plant hormone responses, specifically abscisic acid (ABA). Genes encoding pentatricopeptide repeat (PPR)-containing proteins and Late Embryogenesis Abundant- like (LEA) proteins were identified in these regions. PPR's have established roles in ABA signaling in *Arabidopsis* and were also shown to be up-regulated in response to heat and drought stress in *Sorghum*. Further, LEA proteins are induced upon ABA and osmotic stress exposure, and function as molecular chaperones. Altogether, these findings further highlight the contribution of phytohormones in drought resistance, particularly through intricate signal cascades that influence plant functioning under drought, at the morphological, physiological, and molecular levels.

TABLE OF CONTENTS

LIST OF FIGURES

LIST OF TABLES

CHAPTER 1: OVERVIEW AND OBJECTIVES

The repercussions of climate change, namely changes in temperature and precipitation, are directly contributing to extreme weather events that affect plant growth and development (USGCRP, 2014, Pareek et al., 2020). Specifically, drought and heat waves impact water availability by reducing rainfall and increasing evaporation, negatively affecting crop yield (USGCRP, 2014, Lesk et al., 2021). As global agriculture depends on consistent plant responses to maintain yield during the growing season (Kukal and Irmak, 2018), it is crucial to adjust our knowledge of plant responses to a changing climate to ensure future food availability. However, maintaining and enhancing the producibility of grain-based products in the face of climate change is becoming more challenging due to population growth, which is expected to increase to nearly 10 billion by 2050 (Population Reference Bureau, 2018). In order to mitigate the effects of drought on plant growth and yield while also securing future food requirements, it is critical to refine our current understanding of plant responses to and consequences of drought exposure over developmental time.

The purpose of my dissertation work is to quantify the drought response at the whole plant (morphological, physiological, and histological) and genetic levels. I have researched three specific aims to evaluate plant responses to short-term and long-term drought exposure, using *Sorghum* as a model system.

***Specific Aim 1 – Determine the morphological, histological, and physiological strategies employed in response to repeated and prolonged drought exposure in sensitive and tolerant genotypes of* Sorghum bicolor.** Although numerous studies have described the short-term impacts of drought stress on *S. bicolor*, less is known about the drought response over the long term. In this study, I identified changes to morphological, histological, and physiological traits in response to repeated and prolonged drought exposure and determined if utilization of these mechanisms was mutually exclusive.

Specific Aims 2 and 3 – Identify genetic controls of drought-responsive shifts in aboveground morphology and physiology (Aim 2) and root system architecture (Aim 3) in a* Sorghum *recombinant inbred line (RIL) population via quantitative trait loci (QTL) mapping. Using a RIL population, generated via a cross between wild and weedy *Sorghum propinquum* and domesticated *Sorghum bicolor*, several QTL corresponding with drought-responsive shifts in above- and belowground phenotypes were identified. Further, allelic control of these traits and putative genes within these regions, which may play a role in drought tolerance, were uncovered.

The findings of my dissertation work will build upon the current definition of drought tolerance in grain crops by uncovering the involvement of accession- and species-specific strategies in drought resistance. Once elucidated, this knowledge can be used to ensure the future quality, affordability, and availability of grain-based products in the face of climate change and population growth.

References:

Kukal MS, Irmak S. 2018. Climate-Driven Crop Yield and Yield Variability and Climate Change Impacts on the U.S. Great Plains Agricultural Production. Scientific Reports 8, 3450.

Lesk C, Coffel E, Winter J, Ray D, Zscheischler J, Seneviratne S, Horton R. 2021. Stronger temperature–moisture couplings exacerbate the impact of climate warming on global crop yields. Nature Food 2, 683-691.

Pareek A, Dhankher OP, Foyer CH. 2020. Mitigating the impact of climate change on plant productivity and ecosystem sustainability. Journal of Experimental Botany 71, 451-456.

Population Reference Bureau. 2018 World Population Data.

USGCRP. 2014. Hatfield, J., G. Takle, R. Grotjahn, P. Holden, R. C. Izaurralde, T. Mader, E. Marshall, and D. Liverman, 2014: Ch. 6: Agriculture. Climate Change Impacts in the United States: The Third National Climate Assessment, J. M. Melillo, Terese (T.C.) Richmond, and G. W. Yohe, Eds., U.S. Global Change Research Program, 150-174.

CHAPTER 2: INTRODUCTION

Causes of Drought and its Impacts on Resource Availability

Drought conditions have both climatic and anthropogenic origins (Dai, 2011, NRDC, 2018). Regardless of the source, drought negatively impacts plant productivity and can reduce crop yield by 20-70% (Gupta et al., 2020). A natural source of drought includes changes in weather patterns, such as fluctuations in temperature and rainfall (NRDC, 2018). Increases in surface temperature are influenced by the accumulation of greenhouse gasses in the atmosphere, which induce evaporation of moisture from the environment. Greenhouse gas accumulation also results in increased evapotranspiration in plants, leading to excess water loss (Dai, 2011, NRDC, 2018). Increases in temperature can also impact the distribution of rainfall. These temperature fluctuations can alter air circulation and disturb global rainfall patterns (NRDC, 2018). Such climatic perturbations severely impact plant growth, development, and overall yield, especially when crops are rainfed (Turral et al., 2011, Gupta et al., 2020). Human-induced drought is a direct result of practices like irrigation and water extraction from groundwater and lakes, which is then stored in reservoirs. Although thought to combat drought, these practices diminish available water from natural sources; further, the water stored in reservoirs is susceptible to evaporation due to increased global temperatures (Van Loon et al., 2016, USGCRP, 2017).

The intensity and duration of drought has major effects on agricultural production (Datta, 2004; Dai, 2011; Fracasso *et al.,* 2016a). Indeed, it has been shown that inconsistent growing conditions impede plant growth and development (Xu et al., 2010). Given that the major cereal crops maize, wheat, rice, barley, and sorghum provide approximately 50% of the globally consumed protein, it is imperative to identify drought tolerant genotypes that can maintain growth parameters, and consequently grain yield, under arid conditions (Daryanto *et al.,* 2016, Gupta *et al.,* 2020). Moreover, the global population is expected to increase to 10 billion by 2050. Thus, securing future grain-based food needs in the face of climate change will be an additional obstacle but a crucial need (Yordanov *et al.,* 2000, Barnabas *et al.,* 2008, Qadir *et al.,* 2015, Zhu, 2016, Population Reference Bureau, 2018, Gupta *et al.,* 2020).

Phenotypic and Molecular Responses to Drought

Morphological Responses

Belowground, plant root system architecture (RSA) can undergo morphological changes to enhance water uptake (Ndlovu et al., 2021). Changes in root length, diameter, and angle all impact the efficiency of water uptake. Longer root systems with narrow angles are more effective at capturing moisture from deep soil layers, while root systems with wider angles are preferred for collecting moisture from the soil's surface (Ali *et al.,* 2009, Redillas *et al.,* 2012,

Borrell *et al.,* 2014, Singh *et al.,* 2014, Uga *et al.,* 2013, Uga *et al.,* 2015, Liang et al., 2017, Dinneny, 2019, Ndlovu et al., 2021). Further, *Sorghum* genotypes with long and thin roots displayed improved water uptake compared to those with short and wide root systems (Blum, 2005; Prasad et al., 2021). These findings suggest that drought-responsive adjustments to root length and biomass are negatively correlated, further demonstrating the crucial role of enhanced root length instead of root biomass under drought conditions.

While vertical belowground growth is favored in drought conditions, aboveground growth is often diminished. Reductions in height, leaf area and length, and aboveground biomass are associated with the drought response (Johnson *et al.,* 2014). Leaf-related strategies, such as curling/rolling and wilting, aid in reducing water loss via transpiration, but can decrease photosynthetic capacity (Johnson *et al.,* 2014, Liu *et al.,* 2014, Zhang *et al.,* 2015, Ndlovu et al., 2021). Drought-responsive reductions in aboveground growth can have impacts on fertilization and grain yield, a likely result of decreases in photosynthetic traits (Clauw *et al.,* 2015, Goche et al., 2020). Further, assimilate partitioning belowground, which enhances root traits and water acquisition, can also negatively impact aboveground growth due to resource allocation to the roots (Ali *et al.,* 2009).

Physiological Responses

Plants initiate a variety of physiological and biochemical pathways in response to drought, such as phytohormone signaling, osmotic adjustment, and transpirational/photosynthetic alterations. Overall, these responses work to restrict plant growth, maintain cell turgor, and adjust transpirational water loss. An example is the biosynthesis of abscisic acid (ABA), a major player in the drought response. The intricate signal cascades initiated through ABA's biosynthesis can reduce leaf growth, trigger stomatal closure, and induce the expression of drought-responsive genes (Kalladan *et al.,* 2017, Kundu and Gantait, 2017, McAdam and Brodribb, 2018, Goche et al., 2020). Altogether, these mechanisms work to partition assimilates belowground to assist in root elongation and aid in diminishing transpirational water loss (Tuberosa, 2012, Kundu and Gantait, 2017).

An additional example of a physiological response to drought is osmotic adjustment (OA). This process increases cellular solutes, which lowers osmotic potential and works to maintain cell turgor (Girma and Krieg, 1992, Tuberosa, 2012). These solutes, called osmolytes, can amass in both the roots and shoots, but their accumulation in these tissues serves different purposes (Ndlovu et al., 2021). As described in Blum (2005) and Ogawa and Yamauchi (2006), OA was found to be strongly related to deep root systems in *Sorghum*. These findings indicate that OA in the roots maintains turgor to encourage root growth, allowing for the exploration of moisture in deeper soil layers (Ogawa and Yamauchi, 2006). OA in the shoots acts to prevent wilting and maintain relative water content and stomatal conductance (Turner and Jones, 1980, Blum, 2017).

Although the accumulation of compatible solutes/osmolytes is advantageous, some plants tend to show decreased growth due to the metabolic requirements needed to maintain osmotic potential (Palta et al., 2007, Tuberosa, 2012).

Alterations in photosynthetic and water management strategies are also associated with the drought response, and include stomatal closure (Marcinska *et al.,* 2012, Buckley, 2019). Stomata are more likely to close at midday, when the vapor pressure deficit (VPD) is highest (Chaves *et al.,* 2016). In drought stressed plants, stomata may open only in the early morning, when temperatures are cooler, before VPD becomes too high (Chaves *et al.,* 2016). This action protects the tissue water status of the plant, ultimately preventing major water loss via transpiration; this action can also be measured via changes in leaf temperature. Although stomatal closure prevents transpirational water loss, this mechanism diminishes CO_2 availability, impacting photosynthesis, plant growth, and grain yield (Marcinska *et al.,* 2012, Rodrigues *et al.,* 2019). Non-stomatal changes that reduce photosynthetic rate include decreased chlorophyll content, which reduces the capacity for light harvesting and disrupts assimilate synthesis and transport (Marcinska *et al.,* 2012, Fracasso *et al.,* 2016b).

In addition, modifications to the vasculature can impact a plant's water status. Focusing specifically on the xylem, alterations to vessel size can influence water uptake and flow throughout the transpiration stream (Tyree and Ewers, 1991, Loviloso and Schubert, 1998). For example, as observed in Loviloso and Schubert (1998), xylem vessel diameter of grapevine was reduced in response to drought, and this corresponded with reductions in xylem hydraulic conductivity (Loviloso and Schubert, 1998). Similar responses have been observed in maize (Klein et al., 2020). In addition to reduced hydraulic conductivity, decreased vessel size lowers the risk of xylem cavitation/embolism and conserves water, both of which are advantageous under drought conditions (Reeger et al., 2021). In combination with xylem size/area, changes to vessel number can also impact water uptake (Tyree and Ewers, 1991).

Genomic and Genetic Responses

Water stress and ABA are both involved in inducing the expression of drought-responsive genes (Krupa et al., 2017). Although these are the main factors driving gene expression, other work has acknowledged that both ABA-dependent and ABA-independent signal transduction pathways exist (Krupa et al., 2017). These pathways ultimately influence the relationship between drought stress signaling and the expression of drought-responsive genes (Krupa et al., 2017). Further, as observed by Shinozaki et al. (2007), the timing surrounding the expression of drought-responsive genes can vary. As such, drought-induced genes are categorized into two main groups: 1) genes that code for stress tolerance proteins, and 2) those involved in signal transduction and the expression of drought-responsive genes (Shinozaki et al., 2007).

Quantitative trait loci (QTL) for known drought-responsive phenotypes have been identified in *Sorghum*, allowing for the discovery of putative genes involved in drought tolerance. As summarized in Abreha et al., (2022), QTL for staygreen chlorophyll content, leaf number and area, grain yield, transpiration, root traits, etc. have been identified in various *Sorghum* populations. As the drought response, particularly at the molecular level, is quite intricate, it is to be expected that some of these traits are controlled by multiple genes (Abreha et al., 2022). For example, some of the staygreen QTL, of which there are four (*Stg1-4*), contain genes coding for heat shock proteins and ABA, both of which are integral to the drought (and heat) stress response (Xu et al., 2000). The staygreen trait in *Sorghum* is associated with maintained leaf greenness during grain filling, particularly under water limitation (Borrell et al., 2014). Therefore, it is logical that the three chlorophyll content loci (*Chl1-3*) mapped by Xu et al. (2000) coincide with the map positions of *Stg1-4* (Krupa et al., 2017).

Using RNA-Seq, Abdel-Ghany et al. (2020) exposed drought resistant and susceptible *Sorghum* genotypes to PEG-induced drought stress and identified changes in gene expression in response to short term (1 hour post treatment) and long term (6 hours post treatment) exposure. The functional categories for the up- and down-regulated genes were provided for all genotypes and treatments. Enriched functional categories for the up-regulated genes for the drought resistant genotypes included: stress (biotic), protein degradation, transcription factor, development, stress/abiotic, and hormone metabolism (Abdel-Ghany et al., 2020). Similarly, Johnson et al. (2014) identified the enrichment of gene ontology terms relating to stress, specifically water deprivation. Up-regulated genes included those encoding the biosynthesis of ABA, Late Embryogenesis Abundant (LEA) proteins, which fall under the "development" category described in Abdel-Ghany et al., (2020), and P5CS2, which is involved in the metabolism of proline and plays a role in osmotic adjustment (Johnson et al., 2014).

Sorghum **as a Model**

Sorghum bicolor, a C4 grain crop grown for food, feed, and biofuel, is considered to be tolerant to a variety of environmental stressors, including drought (Bibi *et al.,* 2012, Abdel-Ghany *et al.,* 2020). *Sorghum* is one of the top five grain crops cultivated worldwide and is used as a primary food source in developing countries, many of which are most affected by climate change (Fracasso *et al.,* 2016a). Since *Sorghum* was domesticated in Africa approximately 8000 years ago, its adaptation to arid environments suggests that drought tolerance was acquired during domestication (Fracasso *et al.,* 2016b, Winchell et al., 2017, Henderson et al., 2020). Therefore, *Sorghum* is an excellent model system for elucidating the mechanisms underlying drought tolerance (Fracasso *et al.,* 2016b). Further, the genetic variability among *Sorghum* genotypes/accessions, its small diploid genome, and close relationship to *Zea mays* make it an ideal model to identify and more clearly define the genetic mechanisms of drought tolerance in related grasses (Swigonova *et al.,* 2004, Qadir *et al.,* 2015, Fracasso *et al.,* 2016b). Deepening

our knowledge on the phenotypic and molecular underpinnings of the drought response will aid in improving crop cultivation under climate change. Therefore, expanding upon and refining this foundational understanding will secure future food needs, both for *Sorghum* as well as other grain-based products.

References:

Abdel-Ghany S, Ullah F, Ben-Hur A, Reddy A. 2020. Transcriptome Analysis of Drought-Resistant and Drought-Sensitive Sorghum (*Sorghum bicolor*) Genotypes in Response to PEG-Induced Drought Stress. International Journal of Molecular Sciences **27(772)**.

Abreha KB, Enyew M, Carlsson AS, Vetukuri RR, Feyissa T, Motlhaodi T, Ng'uni D, Geleta M. 2022. Sorghum in dryland: morphological, physiological, and molecular responses of sorghum under drought stress. Planta **255**, 20.

Ali MA, Abbas A, Niaz S, Zulkiffal S, Ali S. 2009. Morpho-physiological criteria for drought tolerance in sorghum (*Sorghum bicolor*) at seedling and post-anthesis stages. International Journal of Agricultural Biology **11**, 674-680.

Barnabas B, Jager K, Feher A. 2008. The effect of drought and heat stress on reproductive processes in cereals. Plant, Cell, & Environment **31(1),** 11-39.

Bibi A, Sadaqat HA, Tahir MHN, Akram HM. 2012. Screening of Sorghum (*Sorghum bicolor* Var Moench) for Drought Tolerance at Seedling Stage in Polyethylene Glycol. Journal of Animal and Plant Sciences, 22(3): 671-678.

Blum A. 2005. Drought resistance, water-use efficiency, and yield potential—are they compatible, dissonant, or mutually exclusive? Australian Journal of Agricultural Research **56**, 1159.

Blum A. 2017. Osmotic adjustment is a prime drought stress adaptive engine in support of plant production: Osmotic adjustment and plant production. Plant, Cell & Environment **40**, 4-10.

Borrell A, Mullett J, George-Jaeggli B, van Oosterom E, Hammer G, Klein P, Jordan D. 2014. Drought adaptation of stay-green sorghum is associated with canopy development, leaf anatomy, root growth, and water uptake. Journal of Experimental Botany **64(21)**, 6251-6263.

Buckley T. 2019. How do stomata respond to water status? New Phytologist **224**, 21-36

Chaves M, Costa J, Zarrouk O, Pinheiro O, Lopes C, Pereira J. 2016. Controlling stomatal aperture in semi-arid regions – The dilemma of saving water or being cool. Plant Science **251**, 54-64.

Clauw P, Coppens F, De Beuf K, Dhondt S, Van Daele T, Maluex K, Storme V, Clement L, Gonzalez N, Inze D. 2015. Leaf Responses to Mild Drought in Natural Variants of Arabidopsis. Plant Physiology **167**, 800-816.

Dai A. 2011. Drought under global warming: a review. WIREs Climate Change **2**, 45-65.

Daryanto S, Wang L, Jacinthe PA. 2016. Global Synthesis of Drought Effects on Maize and Wheat Production. PLOS One **11(5)**.

Datta S. 2004. Rice biotechnology: A need for developing countries. The Journal of Agrobiotechnology Management and Economics **7**, 31-35.

Dinneny J. 2019. Developmental Responses to Water and Salinity in Root Systems. Annual Review of Cell and Developmental Biology **35**, 239-257.

Fracasso A, Trindade L, Amaducci S. 2016a. Drought stress tolerance strategies revealed by RNA-Seq in two sorghum genotypes with contrasting WUE. BMC Plant Biology, 16:115.

Fracasso A, Trindade L, Amaducci S. 2016b. Drought tolerance strategies highlighted by two *Sorghum bicolor* races in a dry-down experiment. Journal of Plant Physiology **190**, 1-14.

Girma S, Krieg D. 1992. Osmotic Adjustment in Sorghum. Plant Physiology. **99**, 577-582.

Goche T, Shargie NG, Cummins I, Brown AP, Chivasa S, Ngara R. 2020. Comparative physiological and root proteome analyses of two sorghum varieties responding to water limitation. Scientific Reports **10**, 11835.

Gupta A, Rico-Medina A, Cano-Delgado A. 2020. The physiology of plant response to drought. Science **368(6488)**, 266-269.

Henderson AN, Crim PM, Cumming JR, Hawkins JS. 2020. Phenotypic and physiological responses to salt exposure in *Sorghum* reveal diversity among domesticated landraces. American Journal of Botany **107**, 983-992.

Johnson S, Lim F, Finkler A, Fromm H, Slabas A, Knight M. 2014. Transcriptomic analysis of *Sorghum bicolor* responding to combined heat and drought stress. BMC Genomics **15(45)**.

Kalladan R, Lasky J, Chang T, Sharma S, Juenger T, Verslues P. 2017. Natural variation identifies genes affecting drought-induced abscisic acid accumulation in *Arabidopsis thaliana*. Proceedings of the National Academy of Sciences of the United States of America **114**, 11536-11541.

Klein SP, Schneider HM, Perkins AC, Brown KM, Lynch JP. 2020. Multiple Integrated Root Phenotypes Are Associated with Improved Drought Tolerance. Plant Physiology **183**, 1011–1025.

Krupa KN, Dalawai N, Shashidhar HE, Harinikumar KM., Manojkumar HB, Bharani S, Turaidar V. 2017. Mechanisms of Drought Tolerance in Sorghum: A Review. International Journal of Pure & Applied Bioscience. **5**, 221-237.

Kundu S, Gantait S. 2017. Abscisic acid crosstalk during abiotic stress response. Plant Gene.

Liang X, Erickson JE, Vermerris W, Rowland DL, Sollenberger LE, Silveira ML. 2017. Root architecture of sorghum genotypes differing in root angles under different water regimes. Journal of Crop Improvement **31**, 39-55.

Liu P, Yin L, Deng X, Wang S, Tanaka K, Zhang S. 2014. Aquaporin-mediated increase in root hydraulic conductance is involved in silicone-induced improved water uptake under osmotic stress in *Sorghum bicolor* L. Journal of Experimental Botany **65(17)**, 4747-4756.

Lovisolo C, Schubert A. 1998. Effects of water stress on vessel size and xylem hydraulic conductivity in Vitis vinifera L. Journal of Experimental Botany **49**, 693-700.

Marcinska I, Czyczylo-Mysza I, Skrzypek E, Filek M, Grzesiak S, Grzesiak M, Janowiak F, Hura T, Dziurka M, Dziurka K, Nowakowska A, Quarrie S. 2012. Impact of osmotic stress on physiological and biochemical characteristics in drought-susceptible and drought-resistant wheat genotypes. Acta Physiologiae Plantarum **35**, 451-461.

Mcadam A, Brodribb T. 2018. Mesophyll Cells Are the Main Site of Abscisic Acid Biosynthesis in Water-Stressed Leaves. Plant Physiology **117**, 911-917.

Ndlovu E, van Staden J, Maphosa M. 2021. Morpho-physiological effects of moisture, heat and combined stresses on Sorghum bicolor [Moench (L.)] and its acclimation mechanisms. Plant Stress **2**, 100018.

National Resources Defense Council (NRDC), Denchak M. 2018. Drought: Everything You Need to Know.

Ogawa A, Yamauchi A. 2006. Root Osmotic Adjustment under Osmotic Stress in Maize Seedlings 1. Transient Change of Growth and Water Relations in Roots in Response to Osmotic Stress. Plant Production Science **9**, 27-38.

Palta JA, Turner NC, French RJ, Buirchell BJ. 2007. Physiological responses of lupin genotypes to terminal drought in a Mediterranean-type environment. Annals of Applied Biology 150, 269-279.

Population Reference Bureau. 2018 World Population Data.

Prasad VBR, Govindaraj M, Djanaguiraman M, Djalovic I, Shailani A, Rawat N, Singla-Pareek SL, Pareek A, Prasad PVV. 2021. Drought and High Temperature Stress in Sorghum: Physiological, Genetic, and Molecular Insights and Breeding Approaches. International Journal of Molecular Sciences **22**, 9826.

Qadir M, Bibi A, Tahir MHN, Saleem M, Sadaqat H. 2015. Screening of sorghum (*Sorghum bicolor* L) genotypes under various levels of drought stress. Maydica **60**.

Redillas M, Jeong H, Kim Y, Jung H, Bang S, Choi Y, Ha S, Reuzeau C, Kim J. 2012. The overexpression of *OSNAC9* alters the root architecture of rice plants enhancing drought resistance and grain yield under field conditions. Plant Biotechnology Journal **10**, 792-805.

Reeger JE, Wheatley M, Yang Y, Brown KM. 2021. Targeted mutation of transcription factor genes alters metaxylem vessel size and number in rice roots. Plant Direct **5**.

Rodrigues J, Inze D, Nelissen N, Saibo J. 2019. Source-Sink Regulation in Crops Under Water Deficit. Trends in Plant Science **24**, 652-663.

Shinozaki K, Yamaguchi-Shinozaki K. 2007. Gene networks involved in drought stress response and tolerance. Journal of Experimental Botany 58, 221-227.

Singh V, van Oosterom E, Jordan D, Messina D, Cooper M, Hammer G. 2010. Morphological and architectural development of root systems in sorghum and maize. Plant and Soil **333**, 287-299.

Swigonova Z, Lai J, Ma J, Ramakrishna W, Llaca V, Bennetzen J, Messing J. 2004. Close split of sorghum and maize genome progenitors. Genome Research., 1916-1923.

Tuberosa R. 2012. Phenotyping for drought tolerance of crops in the genomic era. Frontiers in Physiology **3(47)**, 1-2.

Turner NC, Jones MM. 1980. Turgor Maintenance by Osmotic Adjustment: A Review and Evaluation. In: Turner, N.C. and Kramer, P.J., Eds., Adaptation of Plants to Water and High Temperature Stress, Willey & Sons, New York, 87-103.

Turral H, Burke JJ, Faurès J-M. 2011. *Climate change, water and food security*. Rome: Food and Agriculture Organization of the United Nations.

Tyree MT, Ewers FW. 1991. The hydraulic architecture of trees and other woody plants. New Phytologist **119**, 345-360.

Uga Y, Sugimoto K, Ogawa S, *et al.* 2013. Control of root system architecture by DEEPER ROOTING 1 increases rice yield under drought conditions. Nature Genetics **45**, 1097-1102.

Uga Y, Kitomi J, Ishikawa S, Yano M. 2015. Genetic improvements for root growth angle to enhance crop production. Breeding Science **65(2)**, 111-119.

U.S. Global Change Research Program (USGCRP), Wuebbles DJ, Fahey DW, Hibbard KA, Dokken DJ, Stewart BC, Maycock TK. 2017. *Climate Science Special Report: Fourth National Climate Assessment, Volume I*. U.S. Global Change Research Program.

Van Loon A. 2016. Drought in the Anthropocene. Nature Geoscience **9**, 89-91.

Winchell F, Stevens CJ, Murphy C, Champion L, Fuller Dorian Q. 2017. Evidence for Sorghum Domestication in Fourth Millennium BC Eastern Sudan: Spikelet Morphology from Ceramic Impressions of the Butana Group. Current Anthropology **58**, 673-683.

Xu W, Subudhi PK, Crasta OR, Rosenow DT, Mullet JE, Nguyen HT. 2000. Molecular mapping of QTLs conferring stay-green in grain sorghum (Sorghum bicolor L. Moench). Genome **43**, 461-469.

Yordanov I, Velikova V, Tsonev T. 2000. Plant Responses to Drought, Acclimation, and Stress Tolerance. Photosynthetica **38**, 171-186.

Zhang F, Zhang K, Du C, Li J, Xing Y, Tang L, Li Y. 2015. Effect of Drought Stress on Anatomical Structure and Chloroplast Ultrastructure in Leaves of Sugarcane. Sugar Tech **17(1)**, 41-48.

Zhu J. 2016. Abiotic stress signaling and responses in plants. Cell **167**, 313-32.

CHAPTER 3: REPEATED AND PROLONGED DROUGHT EXPOSURE REVEALS CONTRASTING WATER MANAGEMENT STRATEGIES USED BY TOLERANT AND SENSITIVE GENOTYPES OF *SORGHUM BICOLOR*

An original research article in preparation for submission to *Plant, Cell, and Environment*

Melissa A. Lehrer and Jennifer S. Hawkins

Abstract

Climate change-induced variations in temperature and precipitation negatively impact plant growth and development. To ensure future food quality and availability, a critical need exists to identify morphological, histological, and physiological responses that confer drought tolerance, especially in agronomically important grain crops. In this study, two *Sorghum bicolor* accessions that differ in their pre-flowering responses to drought were exposed to cycles of drought and rewatering. Morphological, histological, and physiological traits were measured across both juvenile and adult developmental stages. Our findings suggest that the induction of stomatal closure works to prevent hydraulic damage under drought conditions, particularly when growth-related and metaxylem adjustments are unable to compensate for this hydraulic risk. Our results demonstrate that morphological, histological, and physiological traits may work independently over developmental stages to achieve a similar goal of regulating transpirational water loss and reducing xylem embolism risk. This work enhances our understanding of drought-responsive water management strategies in grain crops.

Keywords: *Sorghum bicolor*, drought, plant morphology, water regulation, xylem embolism, stomatal closure, hydraulic damage

Introduction

Drought is one of the main environmental constraints limiting crop yield, resulting in a 20-70% decrease in agricultural production (Datta, 2004, Dai, 2011, Fracasso *et al.,* 2016). Due to its unpredictability and overall impact on plant growth and development, drought is a major threat to global food quality, availability, and affordability (Yordanov *et al.,* 2000, Barnabas *et al.,* 2007, Qadir *et al.,* 2015, Zhu, 2016). As climate change-induced drought is predicted to become more frequent, in conjunction with rising temperatures, it is imperative to identify the mechanisms that enhance plant resistance to water-limited conditions (Pachauri, 2015, Daryanto *et al.,* 2016).

The morphological and physiological responses to drought stress in plants have been well characterized (Flower et al., 1990, Blum, 1996, Tunistra et al., 1997, Chaves and Oliveira, 2004, Moussa and Abdel-Aziz, 2008, Ochieng et al., 2021). Drought-responsive shifts include reductions in height, leaf area, and aboveground biomass, which collectively work to partition assimilates belowground, minimize water loss via transpiration, and/or impact hydraulic conductance (Johnson *et al.,* 2014, Liu *et al.,* 2014, Zhang *et al.,* 2015, Olson et al., 2018). Belowground, changes in root length and/or angle enhance water acquisition from deeper soil layers (Ali *et al.,* 2009, Singh *et al.,* 2010, Redillas *et al.,* 2012, Borrell *et al.,* 2014).

Much of the published work in agriculturally important crop plants focuses on plants exposed to short periods of drought in greenhouse settings (Machado and Paulsen, 2001, Munamava and Riddock, 2001, Moussa and Abdel-Aziz, 2008, Aslam et al., 2015, Akman et al., 2020, Drobnitch et al., 2021). In practice, however, individual plants can experience short periods of drought and intermittent rainfall and/or prolonged periods of drought throughout an entire growing season (Godwin and Farrona, 2020). In order to more holistically define drought tolerance, the responses to and consequences of long-term drought exposure over developmental time require elucidation.

The major cereal crops maize, wheat, rice, barley, and sorghum provide between 25-50% of the global food energy derived from plants, and more than 50% of the calories consumed worldwide come directly from cereal grains (International Development Research Center, 2010, Awika, 2011). *Sorghum* is a staple C4 grain crop grown for food, animal feed, and biofuel. Due to its domestication in arid environments, *Sorghum* is considered to be drought tolerant. Therefore, it is an ideal model organism to study the drought responsive mechanisms in an agriculturally and economically important grain crop. In this study, two *Sorghum bicolor* accessions that vary in their pre- and post-flowering responses to drought were exposed to repeated and prolonged drought exposure throughout early and late vegetative stages (Premachandra et al., 1993). Morphological and physiological traits were measured during the drought and recovery phases, while vasculature traits were measured at the end of the study. We hypothesized that

maintenance of morphological, histological, and physiological traits near control levels would be observed in the pre-flowering, drought tolerant accession, TX7078. Conversely, reductions in morphological and histological traits and significant fluctuations of physiological features were expected to occur in the pre-flowering, drought sensitive accession, BTx642.

Methods and Materials

Experimental Design

Two accessions of *Sorghum bicolor*, TX7078 (PI 655990) and BTx642 (formerly B35, PI 656029), described as pre- and post-flowering drought tolerant, respectively (Premachandra et al., 1993) were obtained from the USDA Germplasm Resources Information Network (GRIN). Seventy-two replicates of each accession were germinated in 5 cm x 5 cm x 5 cm planting plugs in Premier Pro-Mix BX MYCO soil (Premier Tech Horticulture, Quakertown, PA, USA). Conditions during germination were as follows: 21°C, 75% humidity, and 4.5 vapor pressure deficit; seedlings were misted with tap water during germination. Once all plants reached the two-leaf stage (twenty-three days post sowing), seedlings were transplanted into 5 cm x 5 cm x 25 cm tree pots (Stuewe and Sons, Tangent, OR, USA) in a 3:1 combination of #4 silica sand and Premier Pro-Mix BX MYCO soil. Conditions of the greenhouse room were: 27°C/23°C (day/night), 16 hours of natural and/or supplemental light, and 25% humidity. Following transplant, seedlings were watered with tap water every day for one week. Plants were treated once during this establishment period with 80 ppm of 20-20-20 N-P-K (Jack's Classic Water Soluble Fertilizer, Allentown, PA, USA).

Following the establishment period, all seedlings were watered to 100% water content (WC), as measured with a pre-calibrated SM150 Soil Moisture Sensor (Dynamax, Houston, TX, USA). Controls were watered every day to every other day throughout the study. Drought stressed (DS) plants were allowed to dry to 0% WC and remained at this level for two days; water content was assessed every other day until 0% was reached. Upon completion of the treatment, DS plants were watered to 100% WC; this watering regime was repeated one, two, four, and six times (referred to henceforth as cycles) to mimic periods of drought with intermittent rainfall. Following rewatering, all plants were fertilized with 80 ppm of 20-20-20 N-P-K (Jack's Classic Water Soluble Fertilizer, Allentown, PA, USA).

Phenotypic Measurements

The following measurements were recorded at the end of each collection cycle, on all replicates, prior to rewatering: height (cm), culm diameter (mm), and width (at the widest point) and length of the third newest fully expanded leaf (mm). Temperature of the third newest fully expanded leaf (°C) was measured on the replicates collected for destructive harvest (**Table 1**). Height was measured from the base of the plant to the tip of the tallest leaf. Culm diameter was measured with calipers between the base of the plant and first internode. Leaf temperature, a proxy for

transpirational cooling, was measured in the center of each leaf immediately before watering (i.e. pre-watering) and five minutes, thirty minutes, and six hours post-watering using the FLIR TG165 Imaging Infrared Thermometer and Thermal Camera with an emissivity setting of 0.95 (Pandya *et al.,* 2013). Twelve replicates per treatment group for each accession were harvested at the end of each cycle to measure total aboveground biomass (g) and root biomass (g) (**Table 1**). All biomass measurements were performed on plant tissue that was dried at 65°C for a minimum of 72 hours.

Histological Analysis

Stem tissue between the base of the plant and first internode was collected from both accessions and treatment groups at 318 days post sowing and stored in 50% ethanol at 4°C. The day of imaging, stems were hand cut with a razor blade, submerged in dH_2O for three minutes, and stained with 0.025% toluidine blue (Carolina Biological Supply Company, Burlington, NC, USA) for five minutes. Cross sections were de-stained with dH_2O until the water ran clear. Cross sections were mounted in 50% glycerol and imaged at 10X on a compound Zeiss Observer.Z1 microscope with an Axiocam 503 Color Camera. Metaxylem diameter was measured in both the vertical (major) and horizontal (minor) axes in ImageJ; these values were used to calculate area of the metaxylem, using the following formula:

$$\text{Metaxylem Area } (\mu m^2) = \pi * \left(\frac{1}{2}A\right) * \left(\frac{1}{2}B\right)$$

where ***A*** is the diameter of the major axis of the metaxylem, and ***B*** is the diameter of the minor axis of the metaxylem.

In order to determine vascular bundle number per culm area, the number of vascular bundles were counted from each collected image (i.e. number of bundles per 0.6 mm^2, a minimum of 10 images per biological replicate). Next, the diameter of each stem cross section was determined; this value was used to calculate the area of the stem cross section (Area = πr^2, where r is equal to the radius). Lastly, the following formula was used to calculate the number of vascular bundles per culm:

No. of Vascular Bundles Per Culm = ((No. of Vascular Bundles Per Image) * (Culm Area, mm^2)/(0.6 mm^2))

Statistical Analysis

Non-metric multidimensional scaling (NMDS) using Bray-Curtis dissimilarity and analysis of similarity (ANOSIM) were performed in R (Version 2.5-6, *vegan* package, Oksanen *et al.,* 2019) to identify overall treatment effects (parameters: R statistics close to 1, significance value < 0.05, stress value < 0.2, k = 2) after each cycle for both accessions.

Normality of the data was assessed in SAS JMP (version 14.3) via a Shapiro-Wilk Test ($p > 0.05$, W close to 1). Data that were not normally distributed were transformed as necessary, and these transformed values were used in downstream analyses. If data could not be normalized, a non-parametric analysis (Kruskal-Wallis Test by Ranks) was used to identify treatment effects (*stats* package; R Version 4.1.0, R Core Team, 2013). Otherwise, one-way analysis of variance (ANOVA) was performed on normalized data in SAS JMP to identify treatment effects (version 14.3). Significance was assessed at alpha = 0.05.

To identify and compare accession-specific effects for each phenotype (i.e. accession effects), the percent change from control for each phenotypic measurement was determined for both accessions, using the following formula:

$$\text{Percent Change} = ((\text{DS Value} - \text{Control Average})/(\text{Control Average})) \times 100$$

where ***Control Average*** refers to the average of all control values for a particular phenotypic measurement, and ***DS Value*** refers to an individual value from each drought stressed replicate for a particular phenotype. These percent change values were evaluated via one-way ANOVA or Kruskal-Wallis Test by Ranks, with the same parameters as described above, to uncover accession-specific responses for each phenotype across cycles. All boxplots (**Supplementary Figures S6A-E)** were generated using *ggplot2* (version 3.3.5, Wickham, 2016).

Results

Clustering of morphological and physiological traits in the NMDS ordination, for both accessions and across all cycles, indicate a reduction in plant performance over developmental time in response to drought conditions (**Supplementary Figures S1 and S2**).

Morphological and Physiological Parameters

Plant Height

Plant height was reduced in response to drought in both accessions (**Figure 1, Supplementary Figures 3A and 3B**). These reductions were significantly greater in BTx642 compared to TX7078 after one ($p < 0.0001$), four ($p = 0.0006$), and six ($p < 0.0001$) cycles; there was an equal decrease in height between accessions after two cycles ($p = 0.6209$). Overall, TX7078 maintained a height more similar to controls compared to BTx642 across nearly all measured time points.

Culm Diameter

Reductions in culm diameter (**Supplementary Figures 4A and 4B)** were observed in both accessions after all cycles. Relative to controls, culm diameter was reduced in TX7078 by 4.9%, 23.2%, 35.6% and 16.2% and in BTx642 by 14.1%, 17.5%, 47.3%, and 31.48% after one, two,

four, and six cycles of drought, respectively. Culm diameter of TX7078 was maintained nearer to control levels compared to BTx642 after one ($p = 0.0010$), four ($p = 0.0008$), and six ($p < 0.0001$) cycles of drought; however, this trait was more greatly reduced in TX7078 compared to BTx642 after two cycles ($p = 0.0231$) (**Figure 2**).

Leaf Temperature

After one cycle of drought, leaf temperature increases were observed in both TX7078 (**Figure 3A)** and BTx642 (**Figure 4A)** prior to watering, at the peak of drought stress ($p = 0.0066$; $p = 0.0430$). At all post-watering timepoints, there were no significant differences in leaf temperature between control and treatment groups for TX7078 ($p > 0.05$, **Figure 3A**). Maintenance of leaf temperature at control levels was observed at both five minutes and thirty minutes post-watering in BTx642; however, leaf temperature in this accession was significantly higher than control plants after six hours post-watering ($p = 0.0107$, **Figure 4A**).

After two cycles of drought, there were no significant differences in leaf temperature between control and treatment groups at any time point for TX7078 ($p > 0.05$) (**Figure 3B**). However, leaf temperature of BTx642 was elevated in treatment plants prior to watering ($p = 0.0016$) and thirty minutes post-watering ($p = 0.0121$). There were no significant differences in leaf temperature five minutes and six hours post-watering ($p > 0.05$) (**Figure 4B**).

After four cycles of drought, maintenance of leaf temperature at control levels was observed in TX7078 at all time points except for six hours post-watering ($p = 0.0140$, **Figure 3C**). An elevated leaf temperature was observed for BTx642 only at the pre-watering measurement ($p = 0.0026$); leaf temperature was then maintained at control levels at five minutes, thirty minutes, and six hours post-watering ($p > 0.05$; **Figure 4C**).

After six cycles of drought, increases in leaf temperature at pre-watering ($p < 0.0001$), as well as at thirty minutes ($p = 0.0018$) and six hours ($p = 0.0234$) post-watering were observed in TX7078; leaf temperature was only maintained at control levels at the five minutes post-watering time point in this accession ($p > 0.05$) (**Figure 3D**). Leaf temperature trends were the same for BTx642 (pre-watering: $p = 0.0007$; five minutes post-watering: $p > 0.05$; thirty minutes post-watering: $p = 0.0232$; six hours post-watering: $p = 0.0051$, **Figure 4D**).

Metaxylem Area and Vascular Bundle Number

Metaxylem area was reduced in both accessions in response to repeated and prolonged drought exposure (**Supplementary Figures 5A and 5B);** however, there were no accession-specific differences in this trait (**Figure 5A,** $p = 0.696$). In contrast, the number of vascular bundles per culm decreased by 29% in TX7078 in response to drought, while this trait was unchanged in response to drought in BTx642 (**Supplementary Figures 6A and 6B**, **Figure 5B**).

Biomass-Related Parameters

Measured Leaf Area

After one cycle, measured leaf area was reduced by 8.9% and 30.8% in TX7078 and BTx642, respectively ($p < 0.0001$). A similar trend was observed after six cycles, where the reduction in measured leaf area was greater in BTx642 at 41.3% compared to TX7078 at 21.4% ($p = 0.0046$). There was an equal decrease in measured leaf area between accessions after two ($p = 0.4448$) and four ($p = 0.2696$) cycles (**Figure 6**). Overall, TX7078 was better able to maintain this trait nearer to control levels compared to BTx642 (**Supplementary Figures 7A and 7B**).

Aboveground Biomass

Aboveground biomass was reduced in response to drought in both accessions after all cycles (treatment, $p < 0.05$; **Supplementary Figures 8A and 8B**), and there was an equal change in this trait from control between accessions across all cycles (accession, $p > 0.05$; **Figure 7**).

Belowground Biomass

After one and two cycles of drought, maintenance of belowground biomass at control levels was observed in TX7078 and BTx642; however, after six cycles, belowground biomass was significantly reduced in both accessions (**Supplementary Figures 9A and 9B**). Overall, there was an equal change from control in belowground biomass between accessions across all cycles ($p > 0.05$; **Figure 8**)

Root-to-Shoot Ratio

Increases in the root-to-shoot ratio (**Supplementary Figure 10A**) were observed in TX7078 after one ($p = 0.0004$) and two cycles ($p = 0.0405$); however, this trait was reduced following six cycles of drought ($p < 0.0001$). The same trend was observed in BTx642 (one cycle, $p = 0.0003$, two cycles, $p=0.0500$, six cycles, $p<0.0001$) (**Supplementary Figure 10B**). Given these identical trends, there was an equal change from control between accessions after one ($p = 0.0698$), two ($p = 0.6438$), and six cycles ($p=0.7037$) (**Figure 9**).

Discussion

Aboveground and Belowground Biomass are Unreliable Indicators of Drought Tolerance

Despite the greater drought-responsive reductions in height and culm diameter in BTx642 (**Figure 1**), there was an equal change in aboveground biomass between accessions across all cycles (**Figure 7**). When merging these findings with measured leaf area (**Figure 6**), measured leaf area was reduced in BTx642 to a greater extent after one and six cycles compared to TX7078. The findings for measured leaf area provide a potential explanation: although this trait was not reduced in TX7078 after one and six cycles, the smaller stature of TX7078 resulted in

comparable overall reductions in aboveground biomass in response to drought. This suggests that aboveground biomass is a poor indicator of drought tolerance relative to leaf-specific/growth-specific traits. Similar results were found in Drobnitch et al., 2021, where the final shoot biomass of drought tolerant and susceptible genotypes of *Sorghum* was not genotype specific. In addition, belowground biomass (**Figure 8**) and root:shoot ratio (**Figure 9**) were comparably reduced in both accessions across all cycles. As a result, these parameters are also unreliable indicators of drought tolerance.

Stomatal Closure Reduces the Risk of Xylem Embolism

Although height and culm diameter were reduced in both accessions in response to drought (**Figures 1-2**), these traits were more consistently maintained near control levels in TX7078. Further, this accession displayed a shorter stature across nearly all cycles compared to BTx642 under both drought and control conditions (**Figure S3**). Although plant height and culm diameter have been found to be major predictors of xylem vessel diameter in tree species, as described in Olson et al. (2018), we did not find this to be the case for *Sorghum*. Despite the variability in stem traits observed here, there were no accession-specific changes to metaxylem area (**Figure 5A**, **Figures S5A, S5C**), suggesting that, although stress responsive, this trait is fixed in these *Sorghum* accessions. Stress-responsive decreases in metaxylem area are advantageous under drought, particularly when balancing water uptake with transpirational water loss (Lovisolo and Schubert, 1998). These vasculature modifications increase hydraulic resistance within the xylem, impeding water flow within the transpiration stream and acting as a water saving mechanism in both accessions (Boehm, 1893, Hargrave et al., 1994).

When looking further into transpirational water regulation, changes in transpiration rate prior to and following watering was more consistently observed in BTx642 (**Figure 4**) compared to TX7078 (**Figure 3**). Alteration of transpiration rate in BTx642 was detected either at the peak of water scarcity (pre-watering) and/or during hotter times of the day (thirty minutes post-watering, approximately 12 pm and/or six hours post-watering, approximately 4 pm) in response to drought, likely to minimize stomatal water loss (Tang and Boyer, 2008). Similar control of stomatal opening in response to drought has been observed in maize (Cochard, 2002). This tight control of stomatal aperture, coupled with reductions in metaxylem area, is critical for BTx642. This accession's taller stature, and subsequently longer hydraulic path, are associated with greater tension on water within the xylem, raising the susceptibility to cavitation events (Domec et al., 2008, Tang and Boyer, 2008, Liu et al., 2019, Lechthaler et al., 2020). Given that wider vessels are more susceptible to embolism, the observed reductions in metaxylem area would ordinarily function to reduce this risk; however, this trait was equally reduced in both accessions (Haworth et al., 2017). Thus, it is unlikely that metaxylem modifications alone were sufficient to prevent embolism occurrence in BTx642. When this vasculature modification is coupled with stomatal closure, embolism resistance is improved through the interruption of conductance

between the roots and the shoots (Tang and Boyer, 2008). However, the maintenance of vascular bundle number at control levels in BTx642 (**Figure 5B, Figure S5D)** ensures the availability of usable xylem in the event that embolism formation renders some vessels non-functional (Tang and Boyer, 2008). In contrast to these mechanisms, the morphological and histological features of TX7078 do not require physiological adjustment and facilitate hydraulic safety. Therefore, the maintenance of leaf temperature at control levels (**Figure 3**) and reduction of vascular bundle number (**Figure 5B, Figure S5B**) indicate that the shorter stature and hydraulic path make TX7078 inherently less prone to hydraulic damage compared to BTx642. Our findings highlight the critical role of stomatal closure to both reduce transpirational water loss and the risk of xylem embolism. This is particularly crucial when morphological and histological adjustments alone are unable to compensate for the physiological consequences of long-term drought exposure.

Conclusions

This study demonstrated how pre-flowering drought tolerant and pre-flowering drought sensitive *Sorghum bicolor* accessions use morphological and physiological mechanisms, respectively and independently, to manage water uptake and loss over developmental time. The variable utilization of these strategies also had major impacts on hydraulic safety. Further, our findings illustrated how aboveground and belowground biomass alone are unreliable measures of drought tolerance. Traits that are often inferred through aboveground biomass measurements, like plant height, culm diameter, and leaf area, may be more reflective of drought tolerance. Further, root system architecture may be a more informative indicator of drought tolerance as it relates to belowground traits, such as root positioning, diameter, and angle (Liang et al., 2017, Girma et al., 2020). Overall, the work described here delineates the morphological and physiological contributions to hydraulic safety in response to long term drought exposure. As such, our findings redefine drought tolerance and further specify traits to be used for crop improvement.

References

Akman H, Zhang C, Ejeta G. 2020. Physio-morphological, biochemical, and anatomical traits of drought-tolerant and susceptible sorghum cultivars under pre- and post-anthesis drought. Physiologia Plantarum **172**, 912-921.

Ali M, Abbas A, Niaz S, Zulkiffal M, Ali S. 2009. Morpho-physiological Criteria for Drought Tolerance in Sorghum (Sorghum bicolor) at Seedling and Post-anthesis Stages. International Journal of Agriculture and Biology **11**, 674-680.

Aslam M, Zamir MSI, Anjum SA, Khan I, Tanveer M. 2015. An investigation into morphological and physiological approaches to screen maize (*Zea mays* L.) hybrids for drought tolerance. Cereal Research Communications **43**, 41-51.

Awika JM. 2011. Major Cereal Grains Production and Use around the World. In: Awika JM,, In: Piironen V,, In: Bean S, eds. ACS Symposium Series. Washington, DC: American Chemical Society, 1-13.

Barnabás B, Jäger K, Fehér A. 2007. The effect of drought and heat stress on reproductive processes in cereals. Plant, Cell & Environment.

Boehm H. 1893. Capillarität und Saftsteigen**.** Berichte der Deutschen Botanischen Gesellschaft **11**, 202-212.

Blum A. 1996. Crop responses to drought and the interpretation of adaptation. Plant Growth Regulation **20**, 135-148.

Borrell AK, Mullet JE, George-Jaeggli B, van Oosterom EJ, Hammer GL, Klein PE, Jordan DR. 2014. Drought adaptation of stay-green sorghum is associated with canopy development, leaf anatomy, root growth, and water uptake. Journal of Experimental Botany **65**, 6251-6263.

Chaves MM, Oliveira, MM. 2004. Mechanisms underlying plant resilience to water deficits: prospects for water-saving agriculture. Journal of Experimental Botany **55**, 2365-2384.

Cochard H. 2002. Xylem embolism and drought-induced stomatal closure in maize. Planta **215**, 466-471.

Dai A. 2011. Drought under global warming: A Review. Climate Change - Wiley Online Library.

Daryanto S, Wang L, Jacinthe P-A. 2016. Global Synthesis of Drought Effects on Maize and Wheat Production (D Hui, Ed.). PLOS ONE **11**, e0156362.

Datta S. 2004. Rice Biotechnology: A Need for Developing Countries. AgBioForum **7(1&2)**, 31-35.

Drobnitch ST, Comas LH, Flynn N, Ibarra Caballero J, Barton RW, Wenz J, Person T, Bushey J, Jahn CE, Gleason SM. 2021. Drought-Induced Root Pressure in Sorghum bicolor. Frontiers in Plant Science **12**, 571072.

Domec J-C, Lachenbruch B, Meinzer FC, Woodruff DR, Warren JM, McCulloh KA. 2008. Maximum height in a conifer is associated with conflicting requirements for xylem design. Proceedings of the National Academy of Sciences **105**, 12069-12074.

Flower DJ, Rani AU, Peacock M. 1990. Influence of Osmotic Adjustment on the Growth, Stomatal Conductance and Light Interception of Contrasting Sorghum Lines in a Harsh Environment. Australian Journal of Plant Physiology **17**, 91-105.

Fracasso A, Trindade L, Amaducci S. 2016. Drought tolerance strategies highlighted by two Sorghum bicolor races in a dry-down experiment. Journal of Plant Physiology **190**, 1-14.

Girma F, Mekbib F, Tadesse T, Menamo T, Bantte K. 2020. Phenotyping sorghum [Sorghum bicolor (L.) Moench] for drought tolerance with special emphasis to root angle. African Journal of Agricultural Research **16**, 1213-1222.

Godwin J, Farrona S. 2020. Plant Epigenetic Stress Memory Induced by Drought: A Physiological and Molecular Perspective. In: Spillane C,, In: McKeown P, eds. Methods in Molecular Biology. Plant Epigenetics and Epigenomics. New York, NY: Springer US, 243-259.

Hargrave KR, Kolb KJ, Ewers FW, Davis SD. 1994. Conduit diameter and drought-induced embolism in *Salvia mellifera* Greene (Labiatae). New Phytologist **126**, 695-705.

Haworth M, Centritto M, Giovannelli A, Marino G, Proietti N, Capitani D, De Carlo A, Loreto F. 2017**.** Xylem morphology determines the drought response of two *Arundo donax* ecotypes from contrasting habitats. GCB Bioenergy **9**, 119-131.

International Development Research Center. 2010. Facts and Figures on Food and Biodiversity. Canada: IDRC Communications, International Development Research Centre. Available online at: https://www.idrc.ca/en/research-in-action/facts-figures-food-and-biodiversity.

Johnson SM, Lim F-L, Finkler A, Fromm H, Slabas AR, Knight MR. 2014. Transcriptomic analysis of Sorghum bicolor responding to combined heat and drought stress. BMC Genomics **15**, 456.

Lechthaler S, Kiorapostolou N, Pitacco A, Anfodillo T, Petit G. 2020. The total path length hydraulic resistance according to known anatomical patterns: What is the shape of the root-to-

leaf tension gradient along the plant longitudinal axis? Journal of Theoretical Biology **502**, 110369.

Liang X, Erickson JE, Vermerris W, Rowland DL, Sollenberger LE, Silveira ML. 2017. Root architecture of sorghum genotypes differing in root angles under different water regimes. Journal of Crop Improvement **31**, 39-55.

Liu H, Gleason SM, Hao G, Hua L, He P, Goldstein G, Ye Q. 2019. Hydraulic traits are coordinated with maximum plant height at the global scale. Science Advances **5(2)**.

Liu P, Yin L, Deng X, Wang S, Tanaka K, Zhang S. 2014. Aquaporin-mediated increase in root hydraulic conductance is involved in silicon-induced improved root water uptake under osmotic stress in Sorghum bicolor L. Journal of Experimental Botany **65**, 4747-4756.

Lovisolo C, Schubert A. 1998. Effects of water stress on vessel size and xylem hydraulic conductivity in Vitis vinifera L. Journal of Experimental Botany **49(321)**, 693-700.

Machado S, Paulsen GM. 2001. Combined effects of drought and high temperature on water relations of wheat and sorghum. Plant and Soil **233**, 179-187.

Moussa HR, Abdel-Aziz SM. 2008. Comparative response of drought tolerant and drought sensitive maize genotypes to water stress. Australian Journal of Crop Science **1(1)**, 31-36.

Munamava M, Riddoch I. 2001. Response of three sorghum (*Sorghum bicolor* L. Moench) varieties to soil moisture stress at different developmental stages. South African Journal of Plant and Soil **18**, 75-79.

Ochieng G, Ngugi K, Wamalwa LN, Manyasa E, Muchira N, Nyamongo D, Odeny DA. 2021. Novel sources of drought tolerance from landraces and wild sorghum relatives. Crop Science **61**, 104-118.

Oksanen J, Blanchet FG, Friendly M, Kindt R, Legendre P, McGlinn D, Minchin PR, O'Hara RB, Simpson GL, Soylmos P, *et al.* 2019. *vegan: Community Ecology Package*.

Olson ME, Soriano D, Rosell JA, *et al.* 2018. Plant height and hydraulic vulnerability to drought and cold. Proceedings of the National Academy of Sciences **115**, 7551-7556.

Pachauri RK, Mayer L, Intergovernmental Panel on Climate Change (Eds.). 2015. *Climate change 2014: synthesis report*. Geneva, Switzerland: Intergovernmental Panel on Climate Change.

Pandya MR, Shah DB, Trivedi HJ, Lunagaria MM, Pandey V, Panigrahy S, Parihar JS. 2013. Field Measurements of Plant Emissivity Spectra: An Experimental Study on Remote

Sensing of Vegetation in the Thermal Infrared Region. Journal of the Indian Society of Remote Sensing **41**, 787-796.

Premachandra GS, Hahn DT, Joly RJ. 1994. Leaf Water Relations and Gas Exchange in Two Grain Sorghum Genotypes Differing in Their Pre- and Post-Flowering Drought Tolerance. Journal of Plant Physiology **143**, 96-101.

Qadir M, Bibi A, Tahir MHN, Saleem MF, Sadaqat HA. 2015. Screening of sorghum (Sorghum bicolor L) genotypes under various levels of drought stress. Maydica **60**.

Redillas MCFR, Jeong JS, Kim YS, Jung H, Bang SW, Choi YD, Ha S-H, Reuzeau C, Kim J-K. 2012. The overexpression of *OsNAC9* alters the root architecture of rice plants enhancing drought resistance and grain yield under field conditions: *OsNAC9* improves drought resistance and grain yield in rice. Plant Biotechnology Journal **10**, 792-805.

R Core Team. 2013. *R: A language and environment for statistical computing.* Vienna, Austria: R Foundation for Statistical Computing.

Singh V, van Osterom E, Jordan D, Messina C, Cooper M, Hammer G. 2010. Morphological and architectural development of root systems in sorghum and maize. Plant Soil **333**, 287-299.

Tang AC, Boyer JS. 2008. Xylem tension affects growth-induced water potential and daily elongation of maize leaves. Journal of Experimental Botany **59**, 753-764.

Tuinstra MR, Grote EM, Goldsbrough PB, Ejeta G. 1997. Genetic analysis of post-flowering drought tolerance and components of grain development in Sorghum bicolor (L.) Moench. Molecular Breeding **3**, 439-448.

Wickham H. **2016**. *ggplot2: Elegant Graphics for Data Analysis*. Verlag, New York: R Foundation for Statistical Computing.

Yordanov I, Velikova V, Tsonev T. 2000. Plant Responses to Drought, Acclimation, and Stress Tolerance. Photosynthetica **38**, 171-186.

Zhang F, Zhang K, Du C, Li J, Xing Y, Tang L, Li Y. 2015. Effect of Drought Stress on Anatomical Structure and Chloroplast Ultrastructure in Leaves of Sugarcane. Sugar Tech **17(1)**, 41-48.

Zhu J-K. 2016. Abiotic Stress Signaling and Responses in Plants. Cell **167**, 313-324.

Table 1: Days post sowing and leaf stage for each of the five collection cycles. Biological replication for each destructive harvest is provided for each accession and treatment group.

Collection Cycle	Days Post Sowing	Leaf Stage (Main Stem)	Sample Size for Destructive Harvest
1 Cycle	46	4-5	TX7078 = 12 per treatment group BTx642 = 12 per treatment group
2 Cycles	62	6-7	TX7078 = 12 per treatment group BTx642 = 12 per treatment group
4 Cycles	87	8-9	N/A
6 Cycles	108	11-13	TX7078 = 12 per treatment group BTx642 = 7-12 per treatment group
Stem Collection	318	13-17	TX7078 = 3per treatment group BTx642 = 2-3 per treatment group

Figure 1: Plant height is maintained nearer to control levels in TX7078 compared to BTx642. Following one, four, and six cycles of drought and rewatering, height is maintained closer to control levels in TX7078 (teal) compared to BTx642 (black). After two cycles, there is an equal change in height from controls. The black dashed line at y=0 reflects a 0% change from average control height. Black asterisks indicate a significant difference between accessions ($p < 0.05$).

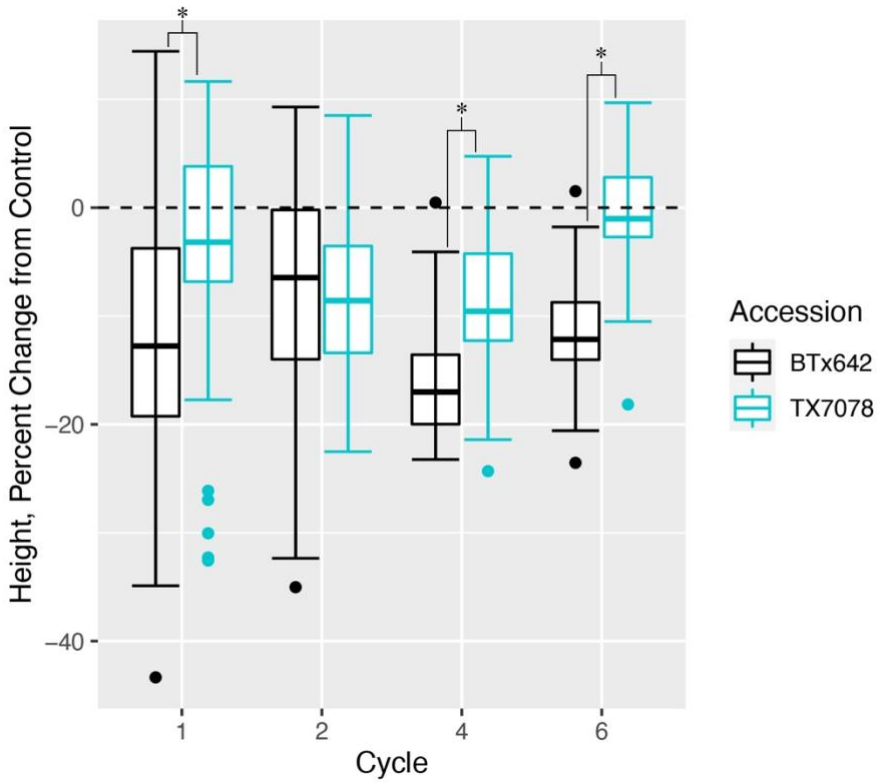

Figure 2: Culm diameter is more greatly reduced in BTx642 compared to TX7078. Following one, four, and six cycles of drought and rewatering, culm diameter is maintained nearer to controls in TX7078 (teal) compared to BTx642 (black), as indicated by the black asterisk ($p < 0.05$). However, after two cycles, the culm diameter of BTx642 is more similar to their respective controls compared to TX7078 (indicated by the red asterisk, $p < 0.05$). The black dashed line at y=0 reflects a 0% change from average control culm diameter.

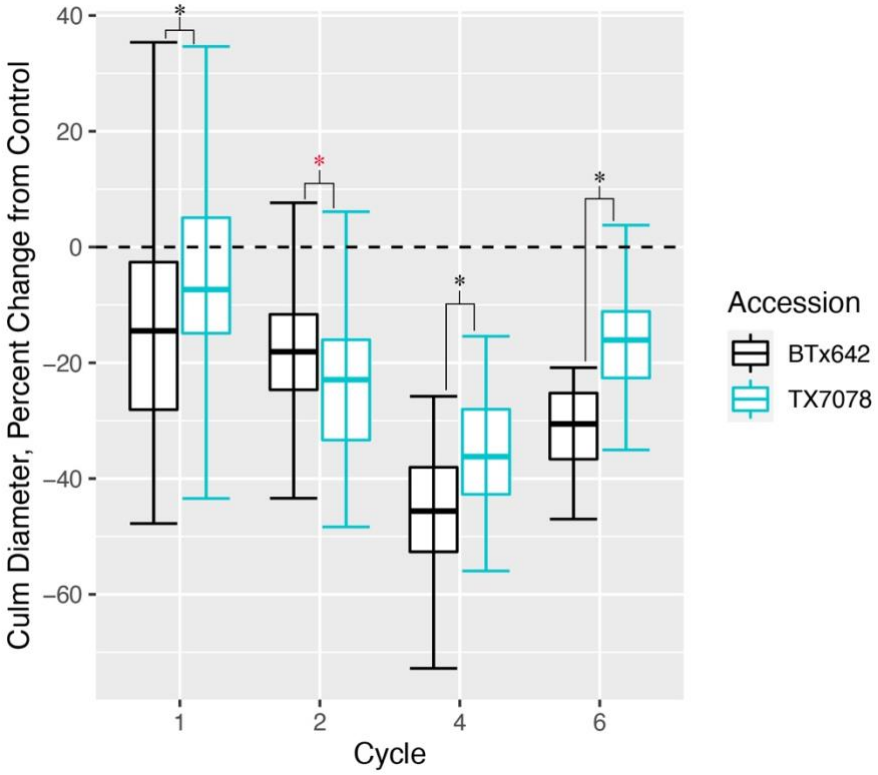

Figure 3: Leaf temperature is more often maintained at control levels following pre-flowering drought exposure in TX7078. Leaf temperature of the third newest fully expanded leaf was recorded pre-rewatering, and five minutes post-watering, thirty minutes post-watering, and six hours post-watering following one (**A**), two (**B**), four (**C**), and six (**D**) cycles of drought. Prior to the sixth cycle, when the reproductive stage of development was initiated, leaf temperature was frequently maintained at control levels. Black asterisks indicate significant differences between control and treatment groups ($p < 0.05$).

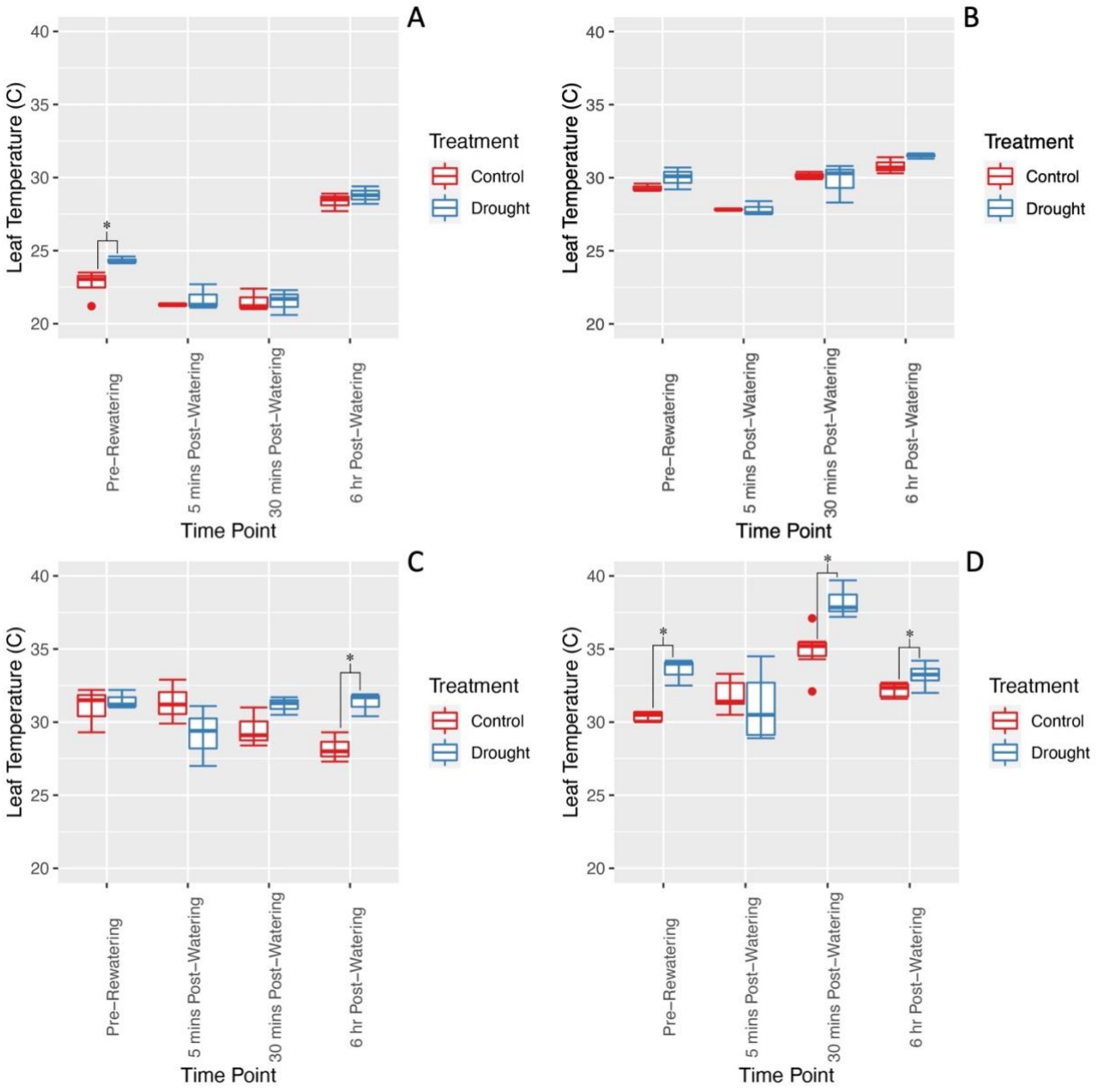

Figure 4: Leaf temperature is increased at the peak of drought stress and/or during the hottest time(s) of the day in BTx642. Leaf temperature of the third newest fully expanded leaf was recorded pre-rewatering, and five minutes post-watering, thirty minutes post-watering, and six hours post-watering following one (**A**), two (**B**), four (**C**), and six (**D**) cycles of drought and rewatering. Black asterisks indicate significant differences between control and treatment groups ($p < 0.05$).

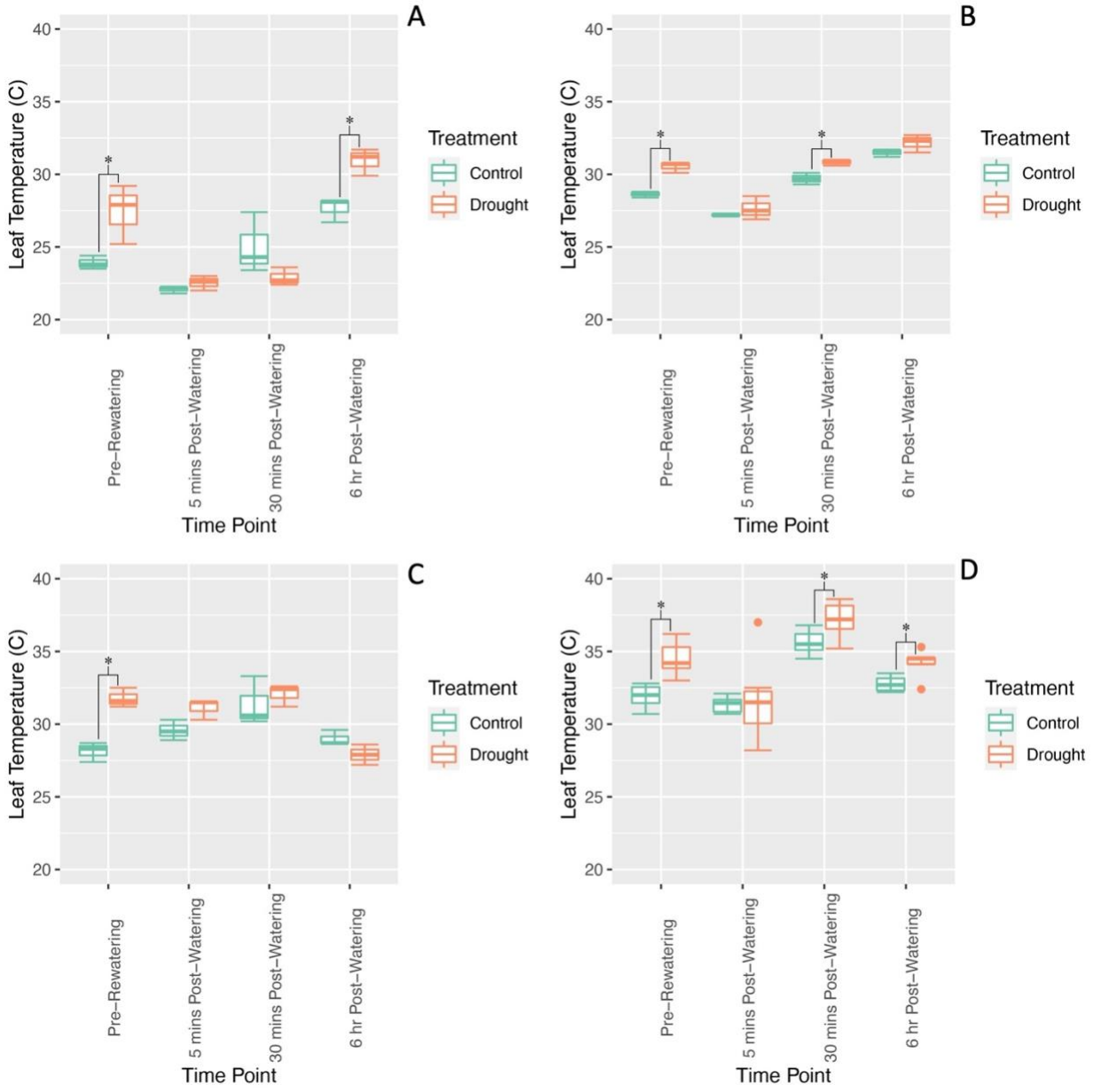

Figure 5: Metaxylem area is reduced in response to drought in both TX7078 and BTx642; vascular bundle number is more variable. Metaxylem area (**A**) was equally reduced from controls in response to drought in both *S. bicolor* accessions. Number of vascular bundles per culm (**B**) is maintained at control levels in BTx642, but significantly reduced in TX7078 following prolonged drought exposure ($p < 0.05$). BTx642 = black, TX7078 = teal.

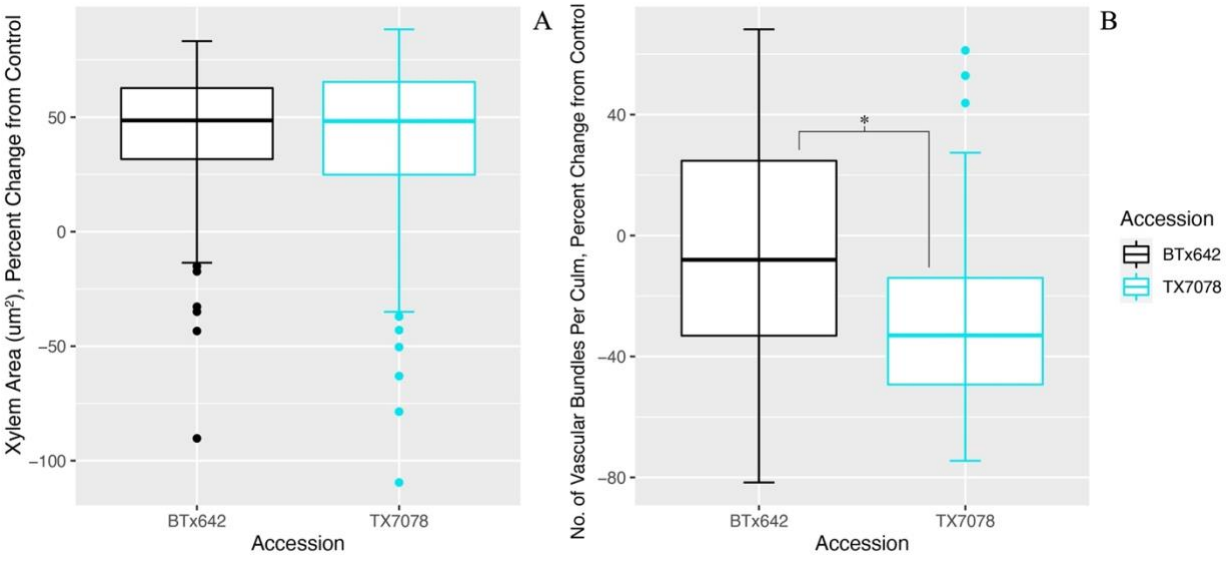

Figure 6: Measured leaf area is more consistently maintained nearer to control levels in TX7078 compared to BTx642. Following one and six cycles of drought and rewatering, maintenance of measured leaf area closer to control levels is detected in TX7078 (teal) compared to BTx642 (black). There is an equal change in this trait between accessions after two and four cycles. The black dashed line at y=0 reflects a 0% change from average control measured leaf area.

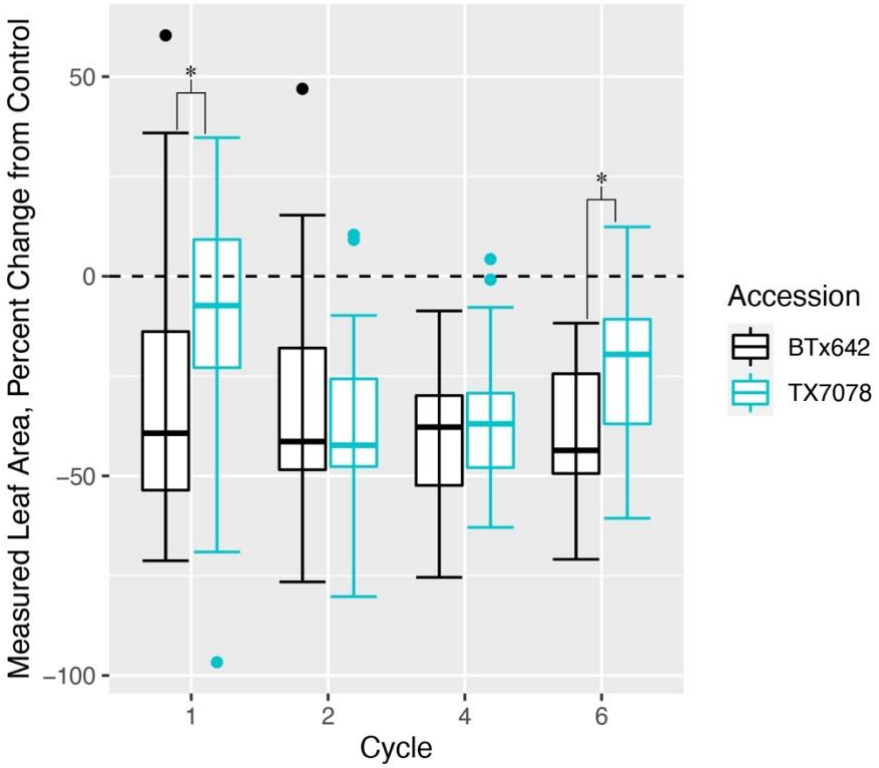

Figure 7: Aboveground biomass is similarly reduced in TX7078 and BTx642 following prolonged drought exposure. Following one, two, and six cycles of drought and rewatering, there are no accession-specific differences in aboveground biomass between TX7078 (teal) and BTx642 (black). The black dashed line at y=0 reflects a 0% change from average control aboveground biomass.

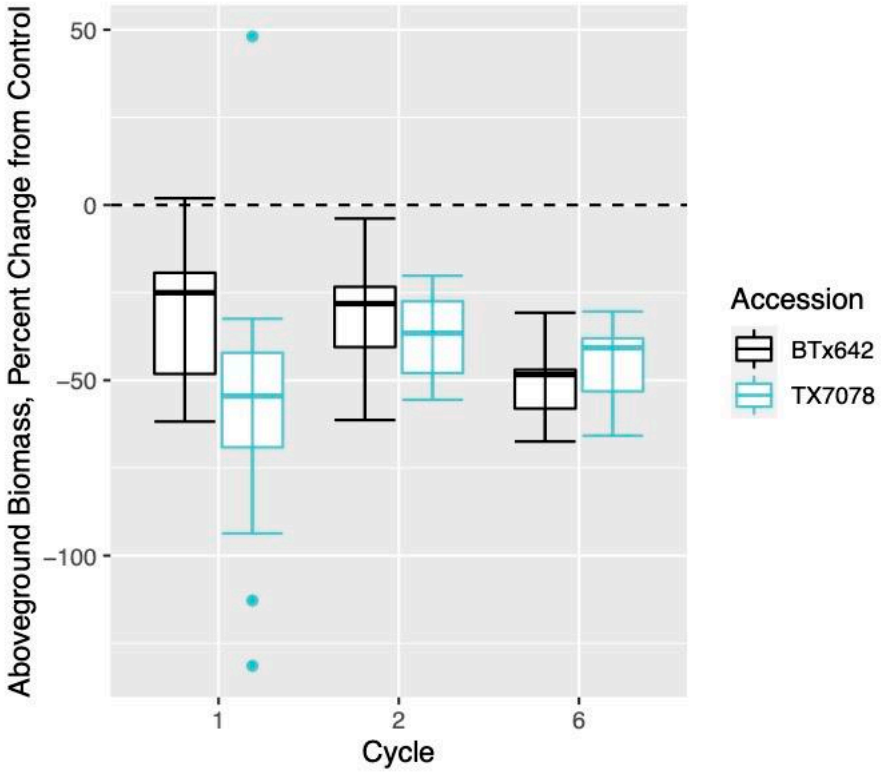

Figure 8: There are no accession-specific changes identified for belowground biomass associated with drought exposure over developmental time. Following one, two, and six cycles of drought and rewatering, belowground biomass is equally modified in both accessions. The black dashed line at y=0 reflects a 0% change from average control belowground biomass. BTx642 = black, TX7078 = teal.

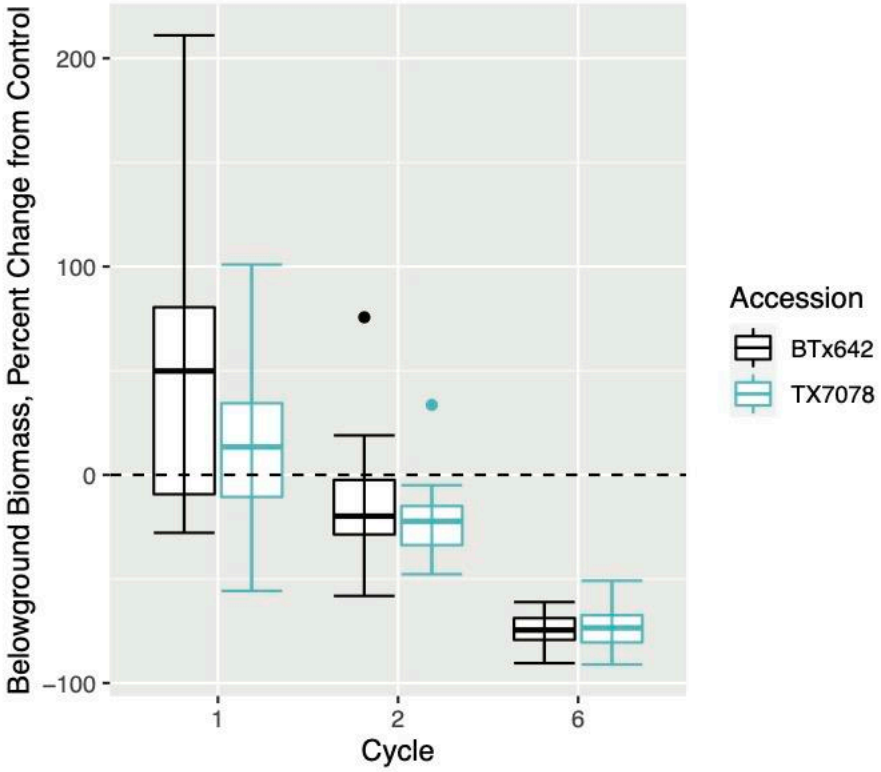

Figure 9: Root-to-shoot ratio is similarly modified following prolonged drought exposure. Following one, two, and six cycles of drought and rewatering, there are no significant accession-specific differences in the root-to-shoot ratio between TX7078 (teal) and BTx642 (black). The black dashed line at y=0 reflects a 0% change from the average control root-to-shoot ratio.

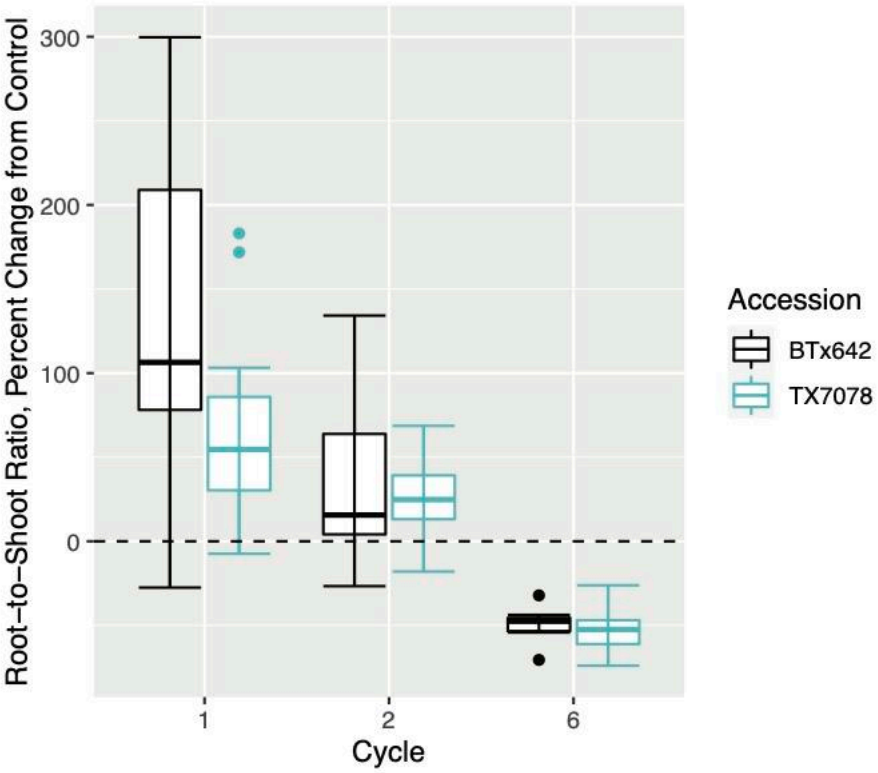

Figure S1: Non-metric multidimensional scaling across two dimensions highlights the response of TX7078 to prolonged drought exposure. After one cycle of drought and rewatering (**A**), an overall treatment effect was not observed (R=0.00432, p=0.2197). After two (**B**; R=0.2609, p = 0.0001), four (**C**; R=0.5231, p=0.0001) and six (**D**; R=0.1264, p=0.0029) cycles of drought and rewatering, treatment effects are detected in the pre-flowering drought tolerant *S. bicolor* accession, TX7078.

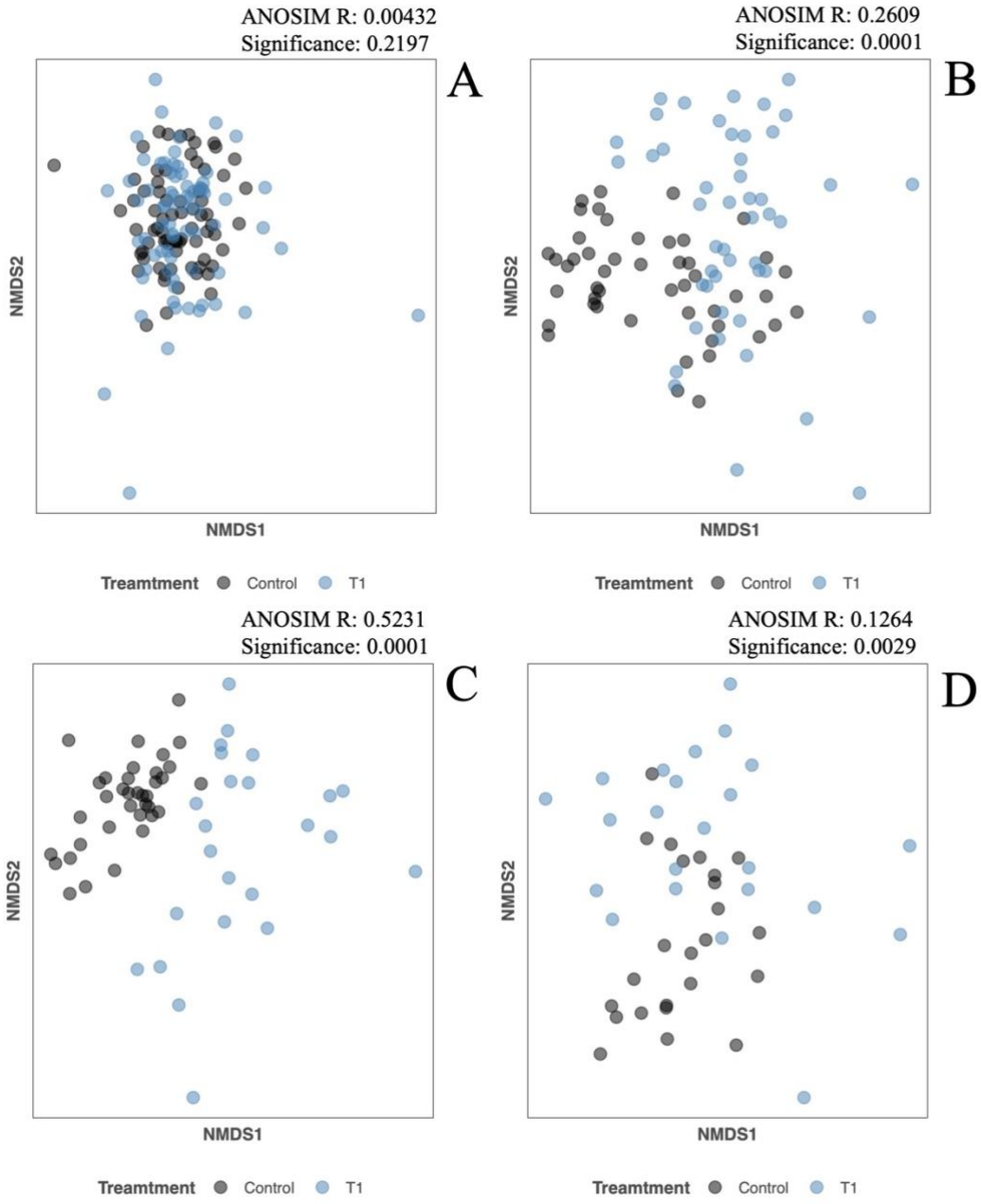

Figure S2: Treatment effects are detected in BTx642 via non-metric multidimensional scaling across two dimensions. Following one (**A**; R=0.1573, p=0.0001), two (**B**; R=0.2086, p=0.0001), four (**C**; R=0.5655, p=0.0001) and six (**D**; R=0.6099, p=0.0001) cycles of drought and rewatering, treatment effects are observed in the pre-flowering drought sensitive *S. bicolor* accession, BTx642.

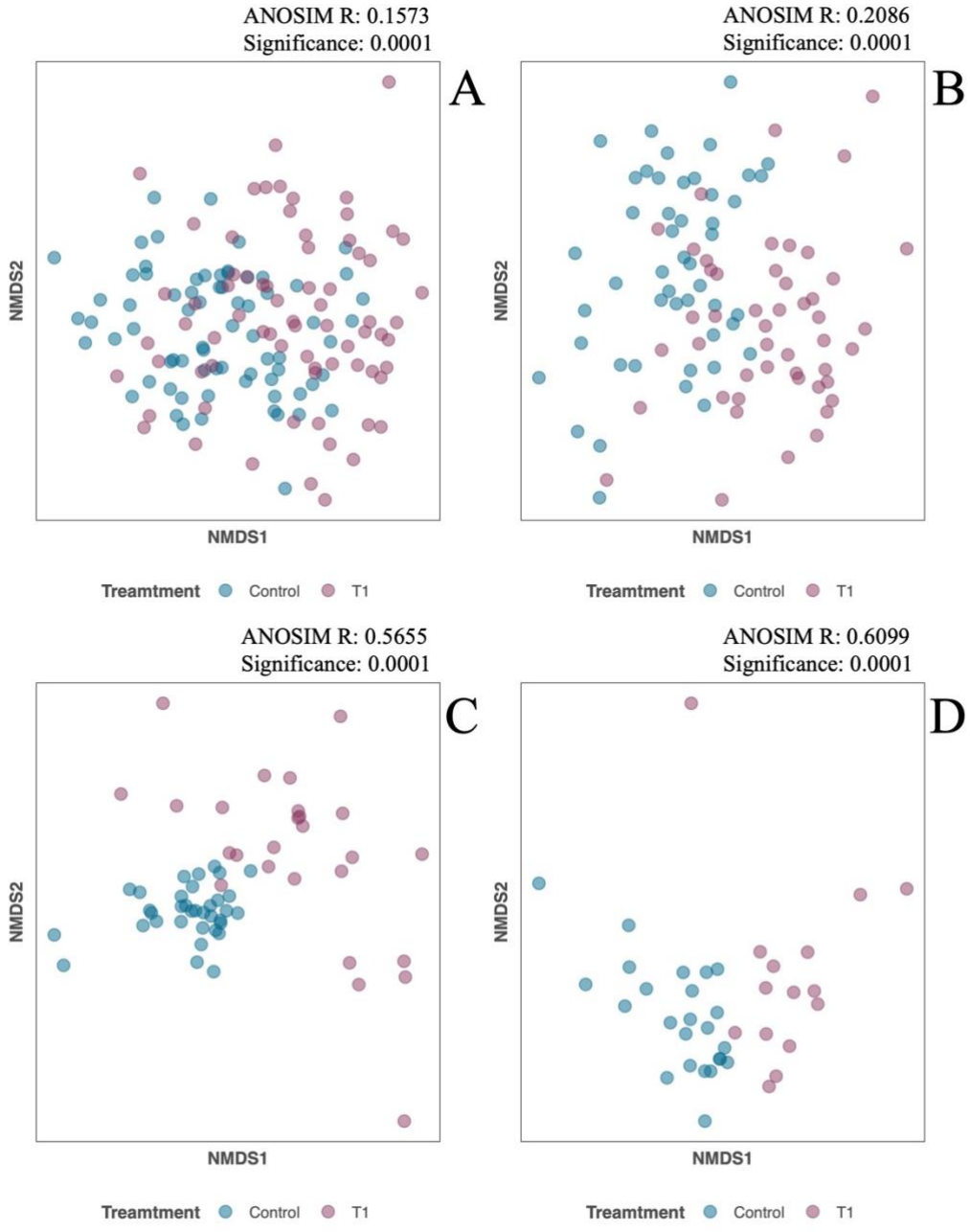

Figure S3: Plant height is reduced in both TX7078 and BTx642 following cyclical drought exposure. After one, two, and four cycles of drought and rewatering, height was reduced in TX7078 (**A**); however, height was significantly reduced after all cycles in BTx642 (**B**).

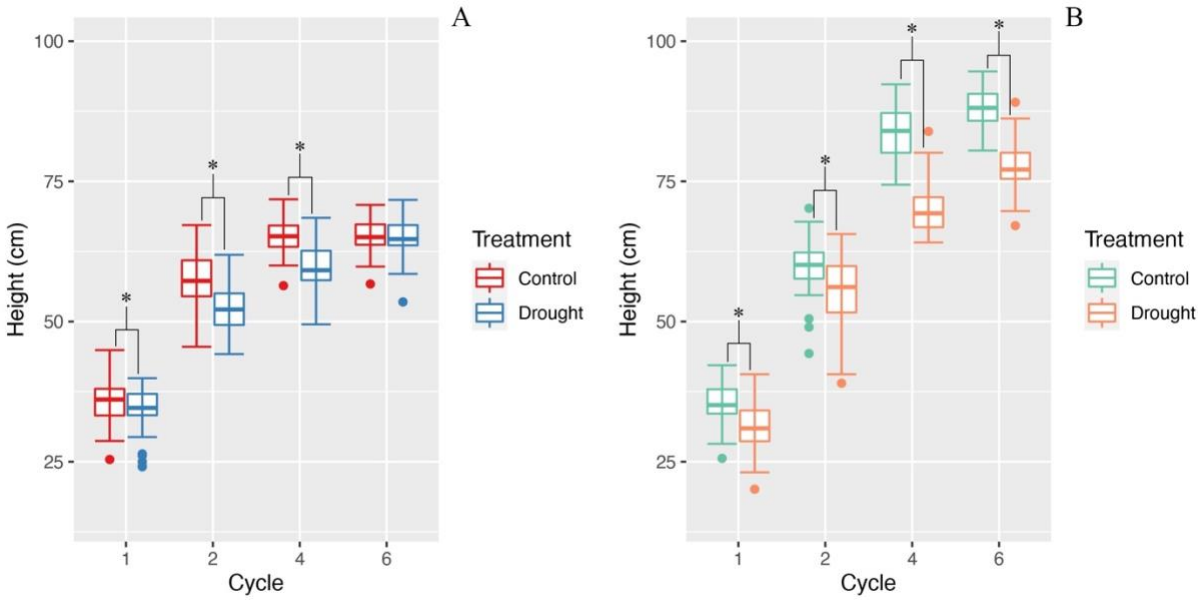

Figure S4: Repeated and prolonged drought exposure reduces culm diameter in both TX7078 and BTx642. After two, four, and six cycles of drought and rewatering, culm diameter was reduced in TX7078; there was no significant reduction in culm diameter after one cycle (**A**). Culm diameter was reduced in BTx642 after all cycles (**B**).

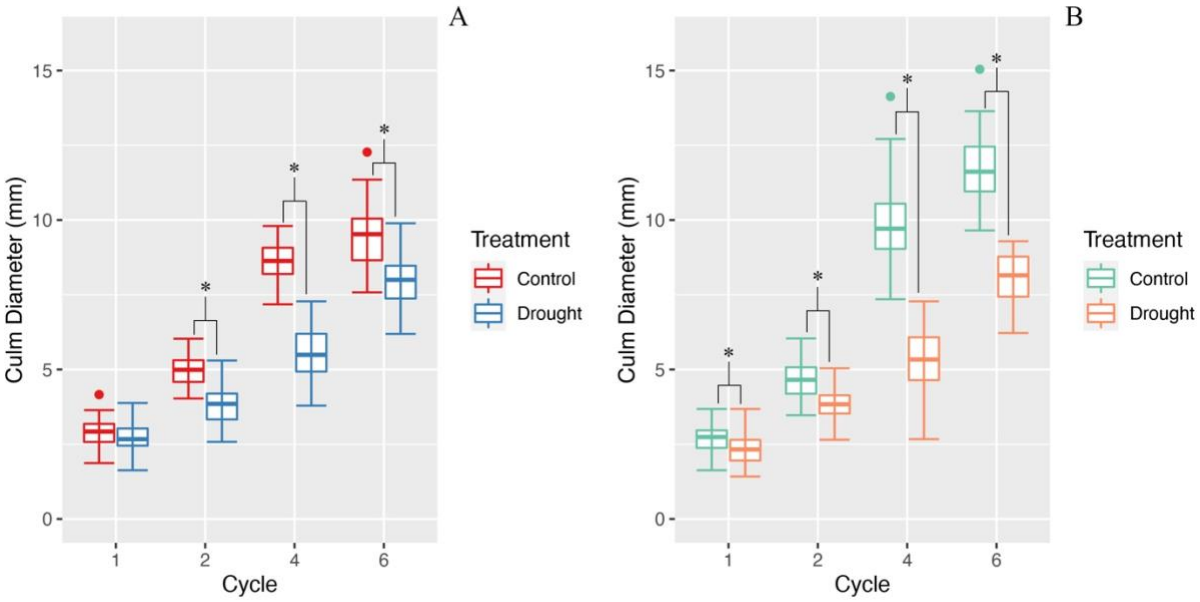

Figure S5: Prolonged drought exposure reduces metaxylem area in TX7078 and BTx642 but variably impacts vascular bundle number. Following cyclical drought exposure, reductions in metaxyelm area were detected in both TX7078 (**A**) and BTx642 (**C**). However, reductions in vascular bundle number per culm area were observed in TX7078 (**C**) following drought exposure; this trait was maintained at control levels in BTx642 (**D**), as there was no detected treatment effect. These parameters were measured at the end of the study, 318 days post sowing.

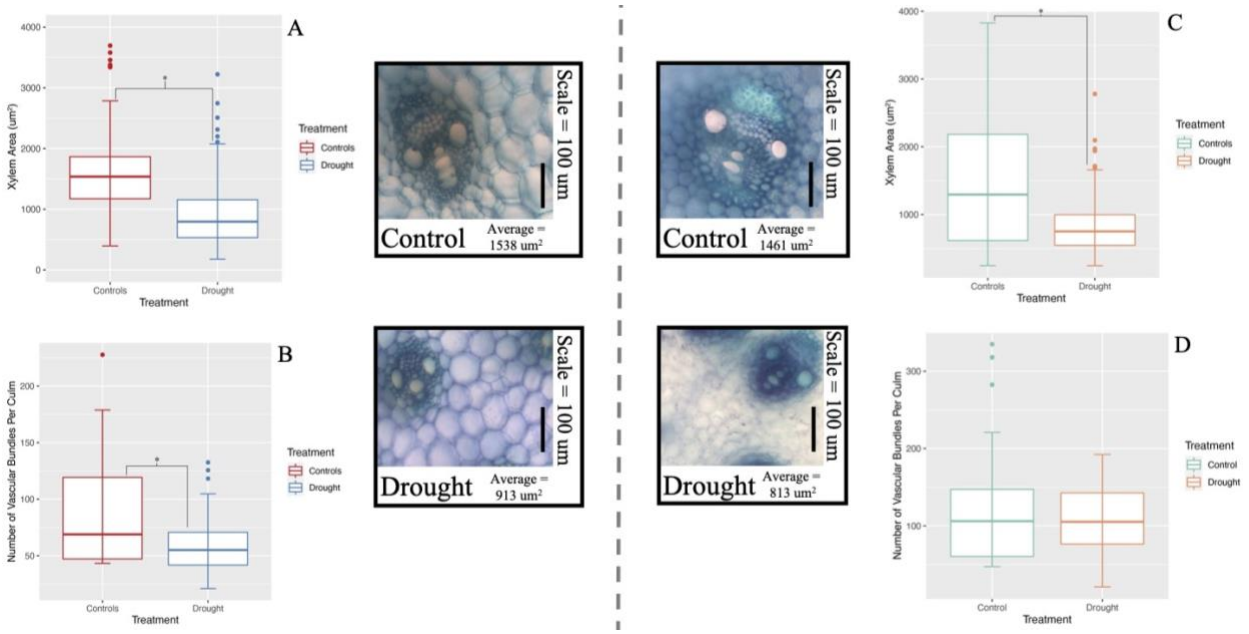

Figure S6: Prolonged drought exposure reduces measured leaf area in both TX7078 and BTx642. After two, four, and six cycles of drought and rewatering, measured leaf area was reduced in TX7078; there was no significant reduction after one cycle (**A**). Measured leaf area was reduced in BTx642 after all cycles (**B**).

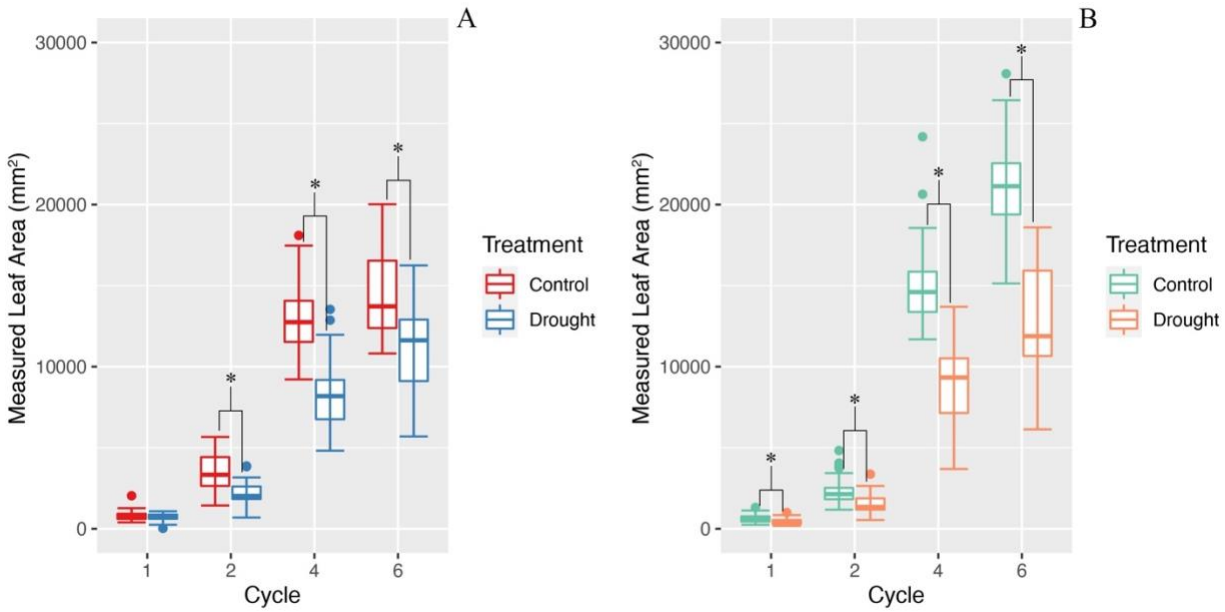

Figure S7: Prolonged drought exposure reduces aboveground biomass in both TX7078 and BTx642. After all cycles of drought and rewatering, reductions in aboveground biomass were observed in both accessions; TX7078, **A** and BTx642, **B**.

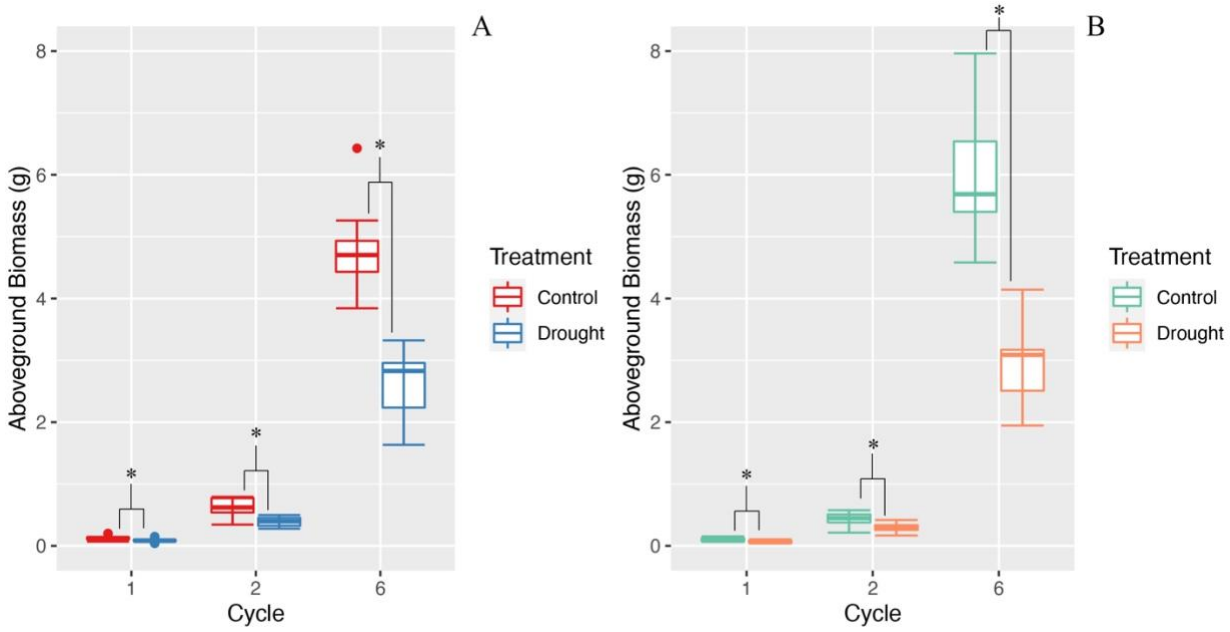

Figure S8: Belowground biomass is minimally impacted during early drought exposure in both accessions. Belowground biomass was maintained at control levels in both accessions following one and two cycles of drought and rewatering. However, after six cycles, this trait was significantly reduced in both accessions. TX7078, **A** and BTx642, **B**.

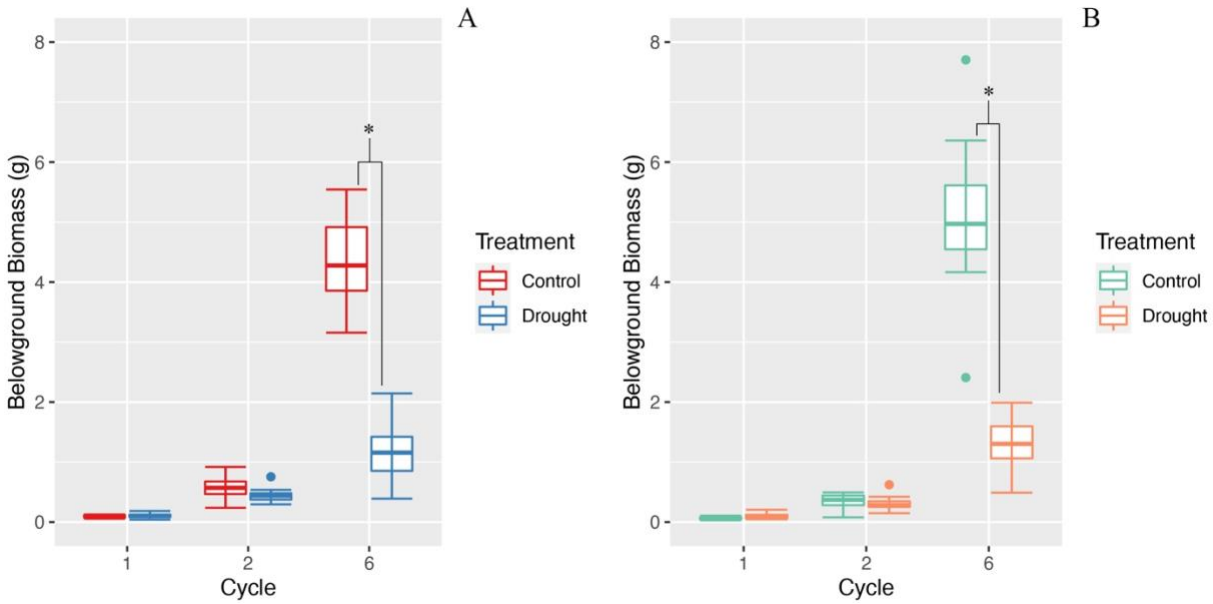

Figure S9: Root-to-Shoot ratio is enhanced and then reduced in response to prolonged drought exposure in TX7078 and BTx642. After one and two cycles of drought and rewatering, root-to-shoot ratio increased in response to drought in both TX708 (**A**) and BTx642 (**B**); after six cycles this parameter is reduced in both accessions.

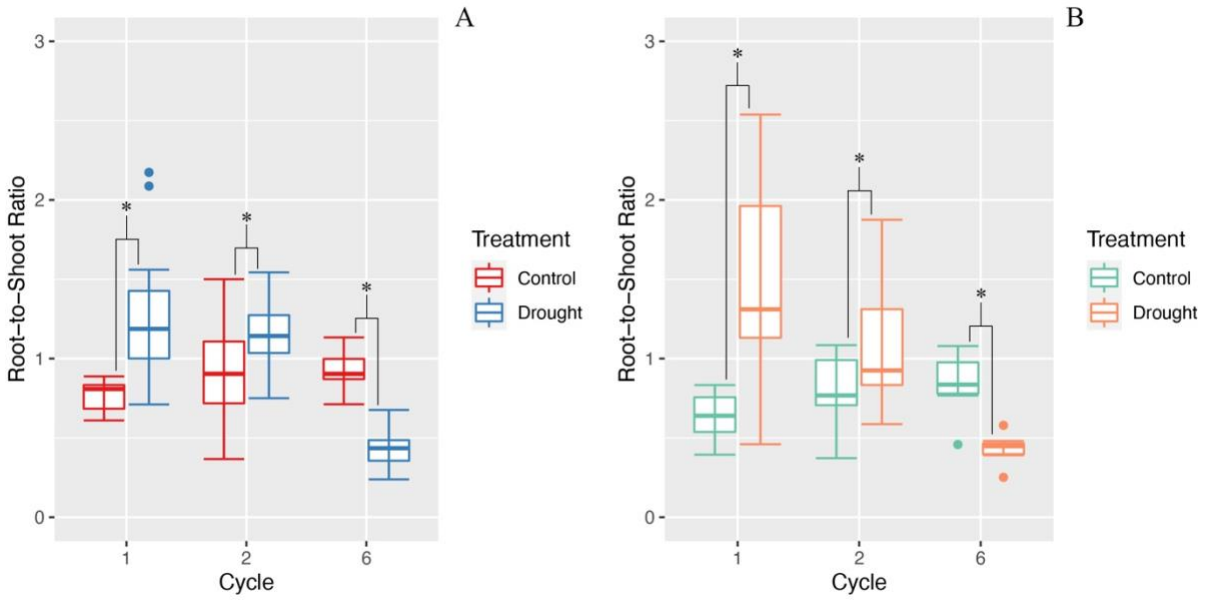

CHAPTER 4: ALLELIC CONTROLS OF THE DROUGHT RESPONSE REVEALED VIA QTL MAPPING IN A *SORGHUM* RECOMBINANT INBRED LINE POPULATION

Melissa A. Lehrer, Rajanikanth Govindarajulu, Farren Smith, and Jennifer S. Hawkins

Abstract

Drought stress severely impedes plant growth, development, and yield. Therefore, it is critical to uncover the genetic mechanisms underlying morphological and physiological drought tolerance strategies to ensure future food security. To identify these genetic controls in *Sorghum*, an agriculturally and economically important grain crop, an interspecific recombinant inbred line (RIL) population was established by crossing a drought-tolerant inbred line of *Sorghum bicolor* (TX7000) with its wild, weedy, and drought-sensitive relative, *Sorghum propinquum*. This RIL population was evaluated under drought conditions, allowing for the identification of quantitative trait loci (QTL) contributing to drought resistance. We detected eight QTL specific to the drought population. The genes within these regions emphasized the role of: 1) hormone synthesis and signaling in above- and belowground tissues, and 2) the impact of grain *Sorghum* varieties on drought-responsive phenotypes, such as short stature and maintenance of aboveground biomass. Overall, the genetic controls uncovered in this work shed light on the interconnected roles of above- and belowground responses in drought resistance as it relates to the balance of water uptake and loss. Further, the detected allelic effects demonstrate how, under drought, the economically important component of cereals (i.e. the grain) is preferentially preserved.

Keywords: *Sorghum*, recombinant inbred line, domestication, grain sorghum, early flowering, water management, hormone signaling

Introduction

Climate change combined with population growth threaten global food quality, availability, and affordability (Lesk et al., 2016). In order to ensure future food security, it is imperative to identify genotypes of grain crops that can withstand the abiotic stresses that limit crop production (Fahad et al., 2017). Drought impacts crop yield by impeding growth and developmental at both the morphological and physiological levels (Yardanov et al., 2000, Barnabas et al., 2007, Rakshit et al., 2020). Although roots play a crucial role in regulating water acquisition and uptake under drought conditions, aboveground strategies, such as stomatal closure and leaf curling/wilting, work to minimize transpirational water loss (Gewin, 2010, Fahad et al., 2017, Chen et al., 2020, Rakshit et al., 2020). Identification of the genetic mechanisms that facilitate drought tolerance will enable the development of crop varieties that can maintain agronomically important traits under unfavorable conditions.

Morphological and physiological responses to drought are well documented in cereals. For example, decreases in cell elongation and differentiation, a direct result of reduced turgor pressure, lead to reductions in aboveground growth (Fahad et al., 2017, Rakshit et al., 2020). These vegetative consequences can lead to a reduced time to anthesis, which has a significant negative impact on grain yield (Fahad et al., 2017, Rakshit et al., 2020). Physiologically, decreases in leaf water potential correspond with reductions in transpiration rate (Fahad et al., 2017). These responses are a result of stomatal closure, which minimizes water loss via transpiration while also decreasing evapotranspiration. Thus, leaf temperatures increase due to reduced evaporative cooling (Fahad et al., 2017). Physiological responses include hormone biosynthesis and signaling, which can influence plant growth and stomatal aperture through intricate signal cascades (Hasanuzzaman and Tanveer, 2020).

Prior research indicates that drought tolerance in *Sorghum* was acquired via domestication (Henderson et al., 2020). Further, *Sorghum* accessions from the durra landrace were found to be the most tolerant (Henderson et al., 2020). Therefore, the *Sorghum* recombinant inbred line (RIL) population used in this work, generated from a cross between *Sorghum propinquum* (female parent) and *Sorghum bicolor* (TX7000 inbred, durra landrace, male parent), provides the opportunity to explore the evolutionary origins of drought tolerance (Govindarajulu *et al*., 2021). TX7000, an elite grain-producing line of *S. bicolor*, displays pre-anthesis drought tolerance, while *S. propinquum* is drought sensitive and displays phenotypes associated with wild grasses, such as small seeds, narrow leaves, and tillering (Evans *et al.,* 2013, Govindarajulu *et al*., 2021). Evaluation of this population under salinity stress has successfully identified the allelic and genetic controls of the osmotic and ionic components of salinity stress (Hostetler et al., 2021). As drought also has an osmotic component, this *Sorghum* population provides the opportunity to identify loci unique to the drought response, as influenced by domestication and improvement. We identified eight drought-specific QTL relating to both morphological and physiological traits.

These QTL were associated with alterations to aboveground growth and traits relating to transpiration/water management. Further, seven of these QTL explained greater than 10% of the phenotypic variation.

Methods and Materials

Plant Material:
A recombinant inbred line (RIL) population, generated from an interspecific cross between *Sorghum propinquum* (courtesy William Rooney, Texas A&M University, College Station, TX, USA) and *Sorghum bicolor* (TX7000 inbred), was used to explore the genetic controls associated with the drought response. The RIL population consists of 168 $F_{3:6}$ lines, with 5.4% being F_3, 11.4% being F_4, 82.1% being F_5, and 1.1% being F_6. Each line was derived via the single seed descent method (Brim, 1966, Snape and Riggs, 1975).

Experimental Design and Conditions:
In a controlled greenhouse room, between two and four seeds of each RIL were organized into two treatment groups (control and drought stressed) and randomly sown in 5 cm x 5 cm x 25 cm pots (Stuewe and Sons, Tangent, OR, USA). Each pot was filled with #4 silica sand with approximately one inch of Premier Pro-Mix BX MYCO soil (Premier Tech Horticulture, Quakertown, PA, USA) on top in which the seeds were germinated. Conditions during germination were as follows: 27 °C day/23 °C night, 75% humidity, and approximately fifteen hours of natural light. During germination, and up to seventeen days post-sowing, all seedlings were watered once daily with tap water and fertilized once weekly with 80 PPM 20-20-20 NPK (Jack's Classic Water Soluble Fertilizer, Allentown, PA, USA). Between twelve and thirteen days post-sowing, all but one seedling was harvested from the pot, leaving five RILs per treatment group (1680 total plants). At seventeen days post-sowing, half of the replicates (drought stressed) were left unwatered for the remainder of the study (until twenty-six days post-sowing).

Phenotypic Measurements:
Prior to the initiation of drought stress (17 days post sowing), the newest fully expanded leaf on each plant was marked, and this leaf was used to collect measurements of relative water content, leaf greenness, and leaf temperature. Between twenty-six and twenty-nine days post-sowing, the following measurements were recorded: height (cm), leaf greenness (nmol/cm), leaf temperature (°C), total aboveground biomass (g), and relative water content (RWC, %). Height was measured from the base of the plant to the top of the stalk. Leaf greenness was measured across the length of the leaf using a Minolta SPAD-502 Chlorophyll Meter and averaged. Leaf temperature was measured using the FLIR T-165 Imaging IR Thermometer with an emissivity setting of 0.95 (Pandya *et al.,* 2013). Total aboveground biomass was collected by drying the entire aboveground part of the plant at 65°C for a minimum of 72 hours. Relative water content was

measured as follows: leaf tips were removed with scissors and weighed with an analytical balance (fresh weight). Leaf tips were placed into 500 uL of ddH_2O and stored at 4°C for approximately one week. Turgid leaf tips were then weighed again with an analytical balance (referred to as the turgid weight). The leaf tips were then dried at 65°C for a minimum of 72 hours. Following, dried leaf tips were weighed to obtain the dry weight. Relative water content for each leaf tip was calculated using the following formula:

$$\text{RWC}\ (\%) = \ (\text{Fresh Weight} - \text{Dry Weight})/(\text{Turgid Weight} - \text{Dry Weight})\ \text{x}\ 100$$

Statistical Analysis

All statistical analyses were performed on both control and drought stressed (DS) populations. Four biological replicates of each RIL under control and drought conditions were considered for QTL analysis (only two replicates per treatment group were used for leaf temperature). All statistical analyses and graphing were performed in R version 1.4.1717 (R Core Team, 2013).

Least square means for each phenotype in each treatment group were calculated for each RIL. Normality of these data was assessed using both a Shapiro-Wilk test and Q-Q plots using the *stats* package in R (Version 4.1.0, R Core Team, 2013). Data that were not normally distributed were transformed as appropriate (**Supplementary Table S1**) and used in subsequent statistical analyses and in the QTL analysis. Correlations of phenotypes (on both the raw phenotype data and the LSM data) in each treatment group were assessed via a Pearson's Correlation analysis using the *PerformanceAnalytics* package in R (version 2.0.4, Peterson and Carl, 2020) (**Supplementary Figures S1A-D**).

Non-metric multidimensional scaling (NMDS) was performed to identify any treatment effects on the raw phenotype data. Clustering of the NMDS used Bray-Curtis dissimilarity when all phenotypes (excluding leaf temperature) were included in the analysis. The NMDS, which was performed using the *vegan* packing in R (Version 2.5-7, Oksanen *et al.,* 2020), was coupled with an analysis of similarity (ANOSIM, significance assessed at alpha = 0.05), which adds statistical significance to the NMDS. Further, one-way analysis of variance (ANOVA) was performed using the *stats* package in R (Version 4.1.0, R Core Team, 2013) to identify treatment effects for individual phenotypes across the population; significance was assessed at α= 0.05. If the raw phenotype data could not be normalized, a Kruskal-Wallis test was performed instead (*stats* package; R Version 4.1.0, R Core Team, 2013). Boxplots (**Supplementary Figures S2A-E)** were generated using *ggplot2* (version 3.3.5, Wickham, 2016)

Genetic Map Construction and QTL Analysis

The *Sorghum* RIL population used in this study was generated as previously described in Govindarajulu et al. (2021). This population has successfully led to the identification of candidate genes involved in the regulation of tiller elongation (Govindarajulu et al., 2021) and salinity tolerance (Hostetler et al., 2021) in *Sorghum*. However, as advanced lines were used in

this study, an updated genetic map was required. In brief, high-quality nuclear DNA was isolated from each advanced RIL (20), which were then sequenced at 2x depth. Following alignment of the RIL sequence reads to the masked *S. bicolor* reference, ver 3.1 (Paterson, 2008), SNPs were analyzed with GenosToABHPlugin in Tassel ver. 5.0 (Bradbury et al., 2007). SNPs derived from each parent were called as follows: *S. propinquum* (A), *S. bicolor* (B), or heterozygous (H). Using SNPbinner, breakpoints were calculated from the ABH formatted SNP data file, allowing for the construction of genotype bins (Gonda et al., 2019). Upon removal of heterozygous bin markers, duplicate bin markers, and markers indicative of double crossovers, the kosambi map function in R/qtl (Broman and Sen, 2011; Broman et al., 2003) was used to construct a high-density genetic map (Govindarajulu et al., 2021).

QTL analysis was performed in R using the *qtl* package (version 1.5.0, Broman et al., 2003). Interval mapping (IM) was used to identify QTL with logarithm of the odds (LOD) peak scores that passed the significance threshold ($\propto = 0.05$) after a 1000 permutation test (Churchill and Doerge, 1994). Next, a multiple QTL model (MQM) was used to identify additional additive QTL, refine QTL positions, and test for interactions between QTL for each phenotype and treatment group. The MQM was assessed via Type III ANOVA, allowing for the proportion of variance explained and the additive effect for each QTL to be determined. QTL with a negative additive value indicates that the trait was negatively influenced by *S. bicolor* alleles, while a positive additive value indicates that the trait was positively influenced by *S. bicolor* alleles. Putative genes found within a 1.0 LOD confidence intervals were extracted and inspected for each QTL (*Sorghum bicolor* ver. 3.1).

Results

Genetic Map Construction

Following inclusion of the advanced lines in the bin map construction, there were a total of 4254 markers. Upon removal of duplicate and heterozygous markers, 2170 markers remained. These markers covered all 10 *Sorghum* chromosomes, with a total length of 899.4 cM (**Supplementary Figure S3, Supplementary Table S2)**.

Drought Exposure Impacts Plant Performance

Height, aboveground biomass, and leaf greenness significantly decreased in the drought stressed RILs compared to the controls (**Table 1, Supplementary Figures S2A-E**). Additionally, relative water content (RWC) was also reduced in response to drought. Further, leaf temperature significantly increased upon drought exposure, suggesting induction of stomatal closure and reduced transpiration rate (**Table 1, Supplementary Figures 2A-E**). Clustering of morphological traits and RWC data in the NMDS ordination provides additional support for the reduction in plant performance under drought conditions (**Supplementary Figure S4**).

Phenotype and QTL Analysis

Height

Under control conditions, height ranged from 7.3 cm to 23.8 cm (average = 13.4 cm). In plants exposed to drought, Ht was reduced by 33.8%, to an average of 8.86 cm (range = 1.3 cm to 21.1 cm). Five significant QTL were identified for this trait, three in the control population and two in the drought population. In the controls, the QTL on chromosomes seven, eight, and nine explained 12.7% of the phenotypic variation, and had an average additive effect of −0.018. In the drought population, the QTL on chromosomes one and nine explained 14.3% of the phenotypic variation and had an average additive effect of −0.061. These negative additive effects indicate that *S. bicolor* alleles negatively influenced height under both control and drought conditions. Despite both being on chromosome nine, the QTL in the control and drought populations do not fall in the same location. The QTL in the control population ranges between 2.74 Mb – 3.09 Mb, with the peak at 2.99 Mb, while the QTL in the drought population ranges between 55.5 Mb – 57.0 Mb, with the peak at 56.7 Mb. Of the 310 genes located within the two QTL in the drought population, candidate genes involved in the drought response were associated with plant hormone responses, signal transduction, responses to water deprivation, osmotic stress, salinity stress, and heat stress, root development, regulation of development and reproduction, cutin/wax biosynthesis, xylem development, protein folding/refolding, and photosynthetic regulation (**Table S3**).

Aboveground Biomass (AGB)

In the controls, the average aboveground biomass (AGB) was 0.596 g (range = 0.116 g to 1.263 g). In response to drought, AGB was reduced by 67.7%, to an average of 0.193 g (range = 0.0067 g to 0.378 g). Five significant QTL were identified for this trait, two in the control population and three in the drought population. In the controls, the QTL on chromosomes one and five explained 18.6% of the phenotypic variation and had an average additive effect of 0.019. In the drought population, the QTL on chromosomes one, four, and five explained 25.8% of the phenotypic variation, and had an average additive effect of 0.014. These positive additive effects indicate that *S. bicolor* alleles positively influenced this trait. The QTL detected in the drought population on chromosome 5 (qAGB_5.DS, peak = 66.5 Mb) overlaps completely with the QTL detected in the controls (qAGB_5.Ctrl, peak = 64.9 Mb). This suggests that the genes within this overlapping region play roles in plant growth, development, and/or architecture rather than in any specific drought-responsive mechanisms. However, of the 544 genes located within the two QTL unique to the drought population, candidate genes involved in the drought response were associated with responses to water deprivation, osmotic stress, salt stress, and heat stress, floral/reproductive development, vegetative regulation and development, plant hormone biosynthesis and responses, root development, regulation of stomatal movement, and cutin/wax biosynthesis (**Table S3**).

Relative Water Content (RWC)

In the controls, relative water content (RWC) averaged at 93.5% (range = 5.71% to 100%). In response to drought, RWC reduced by 45%, to an average of 51.4% (range = 2.04% to 100%). A single significant QTL, located on chromosome five, was identified in the drought population. This QTL explained 6.15% of the phenotypic variation and had an additive effect of −0.372. This negative additive effect indicates that *S. bicolor* alleles negatively influenced this trait. Of the 141 genes located within this QTL, candidate genes involved in the drought response were associated with developmental growth, root morphogenesis and development, responses to water deprivation and salt stress, plant hormone responses and signaling, and regulation of stomatal movement (**Table S3**).

Leaf Temperature (LT)

In the controls, leaf temperature (LT), acting as a proxy for transpiration/evaporative cooling, ranged from 24.7 °C to 35.4 °C (average = 30.3 °C). In response to drought, LT increased by 12.9%, to an average of 34.3 °C (range = 30.6 °C to 41.4 °C). Two significant QTL, located on chromosomes five and six, were identified in the drought population. These QTL explained 32.7% of the phenotypic variation and had an average positive additive effect of 0.463. These positive additive effects indicate that *S. bicolor* alleles positively influenced LT. Of the 136 genes located within these QTL, candidate genes involved in the drought response were associated with responses to heat and water deprivation, hormone signaling and responses, developmental and reproductive regulation, and cell morphogenesis/differentiation (**Table S3**).

Foliar Chlorophyll Content (SPAD)

Under well-watered conditions, foliar chlorophyll content ranged from 11.9 nmol/cm to 39.3 nmol/cm (average = 28.4 nmol/cm). In response to drought, leaf greenness was reduced by 23%, to an average of 21.9 nmol/cm (range = 3.2 nmol/cm − 49.2 nmol/cm). A single significant QTL, located on chromosome six, was identified in the control population. This QTL explained 8.11% of the phenotypic variation and had an additive effect of − 0.684. This negative additive effect indicates that *S. bicolor* alleles negatively influenced this trait. No significant QTL were identified for leaf greenness in the drought population.

Discussion

In grain and forage crops, maintenance of traits pertaining to grain yield and biomass is essential under abiotic stress in order to prevent major economic and agricultural outcomes (Fahad et al., 2017). Thus, identifying the genetic controls of drought tolerance as they relate to the preservation of these economically important features is crucial, particularly when ensuring future food security for the growing population (Fahad et al., 2017). Given the negative impact of drought on yield, much work has been done to characterize the drought-responsive impacts on growth, grain yield, and water management strategies in cereal crops (Gupta et al., 2020, Ndlovu et al., 2021). At the morphological level, reductions in plant growth are due to impaired cell

elongation (Fahad et al., 2017). As growth is a byproduct of cell division and differentiation, the loss of cell turgor in response to drought negatively impacts these processes (Fahad et al., 2017). As a result, plants can have a shorter stature, as well as smaller and/or a reduced number of leaves (Fahad et al., 2017). In addition to these vegetative consequences, drought can also impact grain yield; however, this can depend on the timing and/or severity of the exposure (Fahad et al., 2017). For example, drought during the vegetative phase can shorten time to anthesis, a common drought escape mechanism, while post-anthesis drought exposure can reduce the grain filling period (Hadebe et al., 2017, Fahad et al., 2017).

The *S. bicolor* variety used as the male parent in this recombinant inbred population, TX7000, is a grain sorghum, and has physical attributes that differ from forage sorghum varieties (Undersander et al., 1990, Roth and Harper, 1995, Evans et al., 2013, Sick, 2020). As such, it was predicted that *S. bicolor* alleles would negatively influence height, as vertical growth is less desirable for grain-related traits compared to the stem biomass accumulation associated with forage varieties (Evans et al., 2013). Further, although forage varieties of *Sorghum* tend to be both taller and leafier, the correlation between aboveground biomass (AGB) and grain yield would likely result in a positive effect of *S. bicolor* alleles on AGB (Casari et al., 2019). Both predictions were supported by our findings: *S. bicolor* alleles decreased height and increased AGB in drought conditions (**Table 2**). These results are further strengthened by the findings of Hostetler et al. (2021), where this same *Sorghum* population was evaluated under salinity stress. The salt-specific QTL detected by Hostetler et al. 2021 on chromosome four for aboveground biomass-related traits, as well as the QTL detected for height on chromosomes one and nine, overlap with the following QTL detected in the present study: qAGB_4.DS, qHt_1.DS, and qHt_9.DS (**Table 2**). Further, aboveground biomass and height were similarly controlled by *S. bicolor* in response to salinity stress as they were under drought (Hostetler et al., 2021). Therefore, when under osmotic stress, traits favoring grain varieties, such as reduced height and enhanced biomass, are preferentially maintained in this *Sorghum* population.

The genes located within the drought-specific QTL detected for height and AGB (**Table 2, Table S3**) are involved in reproductive processes, root development, and plant hormone responses. Those associated with reproductive processes fell into the following categories: regulation of photoperiodism, floral development, vegetative phase change, and regulation of reproduction. Given how *S. bicolor* alleles influenced height and AGB, the identification of these gene products highlights the impact of grain varieties on growth phenotypes under drought. Therefore, the identification of gene products within these functional categories is logical for two reasons: 1) early flowering is a known response associated with drought escape, which aids the transition into reproduction before stress becomes too severe (Hadebe et al., 2017, Fahad et al., 2017, Ndlovu et al., 2021), and 2) these genes facilitate reproductive processes (i.e. grain production) and ultimately favor traits associated with grain sorghum varieties (Evans et al., 2013).

In addition to morphological mechanisms, physiological strategies are also employed to combat drought conditions. For example, maintaining cellular moisture is fundamental for plant growth and development, and is often accomplished through osmotic adjustment, i.e. the cellular accumulation of solutes in response to low water potential (Tuberosa, 2012, Ndlovu et al., 2021). This process serves to maintain cellular moisture levels, and ultimately turgidity. As a result, osmotic adjustment can be linked with high relative water content (RWC) (Boyer et al., 2008). In a similar vein, modifications to stomatal aperture can minimize transpirational water loss under drought conditions; however, this can also increase internal leaf temperature and have photosynthetic consequences (Verslues et al., 2006, Casari et al., 2019).

Given the crucial yet sensitive role of balancing plant water status under drought conditions, it was predicted that the alleles of the drought tolerant domesticated parent, *S. bicolor*, would positively influence traits relating to water management (Henderson et al., 2020). For instance, the average positive additive effect for the two QTL detected for leaf temperature (qLT_5.DS and qLT_6.DS) reflects the induction of stomatal closure (i.e. reduced transpiration rate) as influenced by *S. bicolor* alleles (**Table 2**). Interestingly, the negative additive effect for the QTL detected for RWC in the drought population (qRWC_5.DS) indicates that *S. bicolor* alleles reduced this trait. This relationship between RWC and *S. bicolor* alleles does not correspond well with the findings for leaf temperature. Given their roles in water uptake and water loss prevention, it was expected that these traits would be positively controlled by *S. bicolor* alleles. However, one mechanism contributing to high RWC gives these findings more context. As summarized in Ndlovu et al. (2021), a main factor contributing to high water content in *Sorghum* is a deep and extensive root system. In conjunction with the aboveground variability between *S. bicolor* and *S. propinquum*, these two species also differ in their root system architecture: *S. propinquum* has a much more substantial root system compared to *S. bicolor* (Cox et al., 2018, Govindarajulu et al., 2021). Therefore, *S. propinquum* alleles positively influence RWC due to enhanced moisture acquisition that facilitates high RWC, whereas the tight stomatal control seen in *S. bicolor* was derived following domestication.

Genes within the QTL detected for RWC (qRWC_5.DS) were involved in biological functions relating to belowground growth, such as root morphogenesis/development and responses to auxin. Further, two of these genes (Sobic.005G218000, Sobic.005G218100) encode s-adenosyl-l-methionine-dependent (SAM) methyltransferases. SAM methyltransferases are involved in a variety of pathways, such as hormone and lignin biosynthesis (Heidari et al., 2020). Additionally, SAM is used as a methyl donor in the biosynthesis of ethylene and polyamines (Hedari et al., 2020). In combination with regulating aboveground growth, ethylene also regulates the transcription of many components involved in auxin transport (Růžička et al., 2007, Dubois et al., 2018). Therefore, ethylene modulates root growth through its impact on auxin signaling and transport (Růžička et al., 2007). Moreover, the main polyamines synthesized via SAM methyl donation (i.e. putrescine, spermidine, and spermine) can regulate stomatal aperture through modifying the size of the potassium channels in the plasma membrane of guard cells (Chen et al.,

2019). Thus, polyamines play a role in controlling transpirational water loss and maintaining cellular moisture levels (Chen et al., 2019). SAM methyltransferases may play a major role in the drought stress response by impacting root growth and water management (Heidari et al., 2020).

Within the two drought-specific QTL detected for leaf temperature (qLT_5.DS and qLT_6.DS), many genes were involved in hormone mediated signaling and response to abscisic acid (ABA). Two of these genes (Sobic.006G218400, Sobic.006G218600) encode kelch repeats, which are F-box protein functional domains (Jain et al., 2007). These kelch repeats are located on the C-terminus of F-box proteins and bind to different substrates via protein-protein interactions (Jain et al., 2007, Hong et al., 2020). F-box proteins themselves are a part of the ubiquitin protease system, which is responsible for protein degradation (Schumann et al., 2011). In addition to this association, F-box proteins also play roles in hormone signaling (Small and Vierstra, 2004, Rao and Virupapuram, 2021). For example, an *Arabidopsis thaliana* F-box protein called Drought Tolerance Repressor 1 (DOR1) plays a role in the ABA-mediated drought response by inducing stomatal closure (Zhang et al., 2008, Rao and Virupapuram, 2021). Additional genes within qLT_6.DS (Sobic.006G215400, Sobic.006G215600) encode serine-threonine protein kinases. There are a variety of members in the serine-threonine protein kinase family, and one of these members, sucrose non-fermenting 1-related protein kinases (SnRKs), has been shown to be involved in plant stress responses (Diédhiou, et al., 2008). For example, two SnRK type kinases in *Arabidopsis*, SnRK2 and SnRK3, were found to be involved in ABA signaling and stomatal closure (Mustilli et al., 2002, Kobayashi et al., 2004, Diédhiou, et al., 2008). The genes encoding kelch repeats and protein kinases identified in this study may play similar roles in *Sorghum*, highlighting the importance of intricate ABA signaling and control of stomatal water loss in drought resistance.

Conclusions

The species-specific control of the traits described in this work highlight the role of domestication and selection on grain yield and water management mechanisms under drought. For example, the identified increases in AGB and reductions in height, as influenced by *S. bicolor*, demonstrate the impact of grain *Sorghum* varieties, such as TX7000, on drought-responsive phenotypes. Further indication of this allelic control is suggested by prospective candidate genes within the QTL detected for height and AGB. These gene products were found to be involved in reproductive processes, which may facilitate early flowering, and ultimately grain production, under drought. Physiologically, leaf temperature and relative water content (RWC) were increased by *S. bicolor* and *S. propinquum*, respectively, emphasizing the impact of species-specific belowground growth variability on these traits. The putative genetic controls within the QTL detected for RWC and leaf temperature highlight the potential contribution of hormone synthesis and signaling in drought resistance. These hormonal controls are important from two perspectives: 1) through the impact on root growth, water uptake, and the maintenance of cell turgidity, and 2) via the prevention of transpirational water loss as induced by ABA-

influencing stomatal closure. Overall, this work provides additional support for *Sorghum* accessions of the durra landrace, such as *S. bicolor*, serving as resources for crop improvement due to their drought resistant phenotypes that were acquired via domestication.

References

Barnabás B, Jäger K, Fehér A. 2007. The effect of drought and heat stress on reproductive processes in cereals. Plant, Cell & Environment.

Boyer JS, James RA, Munns R, Condon T (A. G), Passioura JB. 2008. Osmotic adjustment leads to anomalously low estimates of relative water content in wheat and barley. Functional Plant Biology **35**, 1172.

Bradbury PJ, Zhang Z, Kroon DE, Casstevens TM, Ramdoss Y, Buckler ES. 2007. TASSEL: software for association mapping of complex traits in diverse samples. Bioinformatics **23**, 2633-2635.

Brim CA. 1966. A Modified Pedigree Method of Selection in Soybeans ¹. Crop Science **6**, 220-220.

Broman KW, Sen Ś. 2011. *A guide to QTL mapping with R/qtl*. Dordrecht: Springer.

Broman KW, Wu H, Sen S, Churchill GA. 2003. R/qtl: QTL mapping in experimental crosses. Bioinformatics **19**, 889-890.

Casari R, Paiva D, Silva V, *et al.* 2019. Using Thermography to Confirm Genotypic Variation for Drought Response in Maize. International Journal of Molecular Sciences **20**, 2273.

Chen D, Shao Q, Yin L, Younis A, Zheng B. 2019. Polyamine Function in Plants: Metabolism, Regulation on Development, and Roles in Abiotic Stress Responses. Frontiers in Plant Science **9**, 1945.

Chen X, Wu Q, Gao Y, Zhang J, Wang Y, Zhang R, Zhou Y, Xiao M, Xu W, Huang R. 2020. The Role of Deep Roots in Sorghum Yield Production under Drought Conditions. Agronomy **10**, 611.

Churchill GA, Doerge RW. 1994. Empirical threshold values for quantitative trait mapping. Genetics **138**, 963-971.

Cox S, Nabukalu P, Paterson A, Kong W, Nakasagga S. 2018. Development of Perennial Grain Sorghum. Sustainability **10**, 172.

Diédhiou CJ, Popova OV, Dietz K-J, Golldack D. 2008. The SNF1-type serine-threonine protein kinase SAPK4regulates stress-responsive gene expression in rice. BMC Plant Biology **8**, 49.

Dubois M, Van den Broeck L, Inzé D. 2018. The Pivotal Role of Ethylene in Plant Growth. Trends in Plant Science **23**, 311-323.

Evans J, McCormick RF, Morishige D, Olson SN, Weers B, Hilley J, Klein P, Rooney W, Mullet J. 2013. Extensive variation in the density and distribution of DNA polymorphism in sorghum genomes. PloS One **8**, e79192.

Fahad S, Bajwa AA, Nazir U, *et al.* 2017. Crop Production under Drought and Heat Stress: Plant Responses and Management Options. Frontiers in Plant Science **8**, 1147.

Gewin V. 2010. Food: An underground revolution. Nature **466**, 552-553.

Gonda I, Ashrafi H, Lyon DA, *et al.* 2019. Sequencing-Based Bin Map Construction of a Tomato Mapping Population, Facilitating High-Resolution Quantitative Trait Loci Detection. The Plant Genome **12**, 180010.

Govindarajulu R, Hostetler AN, Xiao Y, *et al.* 2021. Integration of high-density genetic mapping with transcriptome analysis uncovers numerous agronomic QTL and reveals candidate genes for the control of tillering in sorghum (M Hufford, Ed.). G3 Genes|Genomes|Genetics **11**, jkab024.

Gupta A, Rico-Medina A, Caño-Delgado AI. 2020. The physiology of plant responses to drought. Science **368**, 266-269.

Hadebe ST, Modi AT, Mabhaudhi T. 2017. Drought Tolerance and Water Use of Cereal Crops: A Focus on Sorghum as a Food Security Crop in Sub-Saharan Africa. Journal of Agronomy and Crop Science **203**, 177-191.

Hasanuzzaman M, Tanveer M (Eds.). 2020. *Salt and drought stress tolerance in plants: signaling networks and adaptive mechanisms*. Cham: Springer.

Heidari P, Mazloomi F, Nussbaumer T, Barcaccia G. 2020. Insights into the SAM Synthetase Gene Family and Its Roles in Tomato Seedlings under Abiotic Stresses and Hormone Treatments. Plants **9**, 586.

Henderson AN, Crim PM, Cumming JR, Hawkins JS. 2020. Phenotypic and physiological responses to salt exposure in *Sorghum* reveal diversity among domesticated landraces. American Journal of Botany **107**, 983-992.

Hong MJ, Kim DY, Choi H-I, Seo YW, Kim J-B. 2020. Isolation and characterization of kelch repeat-containing F-box proteins from colored wheat. Molecular Biology Reports **47**, 1129-1141.

Hostetler AN, Govindarajulu R, Hawkins JS. 2021. QTL mapping in an interspecific sorghum population uncovers candidate regulators of salinity tolerance. Plant Stress **2**, 100024.

Jain M, Nijhawan A, Arora R, Agarwal P, Ray S, Sharma P, Kapoor S, Tyagi AK, Khurana JP. 2007. F-box proteins in rice. Genome-wide analysis, classification, temporal and

spatial gene expression during panicle and seed development, and regulation by light and abiotic stress. Plant Physiology **143**, 1467-1483.

Kobayashi Y, Yamamoto S, Minami H, Kagaya Y, Hattori T. 2004. Differential activation of the rice sucrose nonfermenting1-related protein kinase2 family by hyperosmotic stress and abscisic acid. The Plant Cell **16**, 1163-1177.

Lesk C, Rowhani P, Ramankutty N. 2016. Influence of extreme weather disasters on global crop production. Nature **529**, 84-87.

Mustilli A-C, Merlot S, Vavasseur A, Fenzi F, Giraudat J. 2002. Arabidopsis OST1 protein kinase mediates the regulation of stomatal aperture by abscisic acid and acts upstream of reactive oxygen species production. The Plant Cell **14**, 3089-3099.

Ndlovu E, van Staden J, Maphosa M. 2021. Morpho-physiological effects of moisture, heat and combined stresses on Sorghum bicolor [Moench (L.)] and its acclimation mechanisms. Plant Stress **2**, 100018.

Oksanen J, Blanchet FG, Friendly M, Kindt R, Legendre P, McGlinn D, Minchin PR, O'Hara RB, Simpson GL, Soylmos P, *et al.* 2019. *vegan: Community Ecology Package*.

Pandya MR, Shah DB, Trivedi HJ, Lunagaria MM, Pandey V, Panigrahy S, Parihar JS. 2013. Field Measurements of Plant Emissivity Spectra: An Experimental Study on Remote Sensing of Vegetation in the Thermal Infrared Region. Journal of the Indian Society of Remote Sensing **41**, 787-796.

Paterson AH. 2008. Genomics of Sorghum. International Journal of Plant Genomics **2008**, 1-6.

Peterson B, Carl P. 2020. PerformanceAnalytics: Econometric Tools for Performance and Risk Analysis.

Rakshit A, Singh HB, Singh AK, Singh US, Fraceto L (Eds.). 2020. *New Frontiers in Stress Management for Durable Agriculture*. Singapore: Springer Singapore.

Rao V, Virupapuram V. 2021. Arabidopsis F-box protein At1g08710 interacts with transcriptional protein ADA2b and imparts drought stress tolerance by negatively regulating seedling growth. Biochemical and Biophysical Research Communications **536**, 45-51.

R Core Team. 2013. *R: A language and environment for statistical computing.* Vienna, Austria: R Foundation for Statistical Computing.

Roth G, Harper J. 1995. Forage Sorghum. Penn State Extension.

Růzicka K, Ljung K, Vanneste S, Podhorská R, Beeckman T, Friml J, Benková E. 2007. Ethylene regulates root growth through effects on auxin biosynthesis and transport-dependent auxin distribution. The Plant Cell **19**, 2197-2212.

Schumann N, Navarro-Quezada A, Ullrich K, Kuhl C, Quint M. 2011. Molecular Evolution and Selection Patterns of Plant F-Box Proteins with C-Terminal Kelch Repeats. Plant Physiology **155**, 835-850.

Sick S. 2020. Forage Sorghum and Sudangrass: Two Alternatives for Livestock and More. Farmers Business Network.

Smalle J, Vierstra RD. 2004. THE UBIQUITIN 26S PROTEASOME PROTEOLYTIC PATHWAY. Annual Review of Plant Biology **55**, 555-590.

Snape JW, Riggs TJ. 1975. Genetical consequences of single seed descent in the breeding of self-pollinating crops. Heredity **35**, 211-219.

Tuberosa R. 2012. Phenotyping for drought tolerance of crops in the genomics era. Frontiers in Physiology **3**.

Undersander D, Smith L, Kaminski A, Kelling K, Doll J. 1995. Sorghum - Forage. Alternative Field Crops Manual.

Verslues PE, Agarwal M, Katiyar-Agarwal S, Zhu J, Zhu J-K. 2006. Methods and concepts in quantifying resistance to drought, salt and freezing, abiotic stresses that affect plant water status. The Plant Journal **45**, 523-539.

Wickham H. **2016**. *ggplot2: Elegant Graphics for Data Analysis*. Verlag, New York: R Foundation for Statistical Computing.

Yordanov I, Velikova V, Tsonev T. 2000. Plant Responses to Drought, Acclimation, and Stress Tolerance. Photosynthetica **38**, 171-186.

Zhang Y, Xu W, Li Z, Deng XW, Wu W, Xue Y. 2008. F-Box Protein DOR Functions As a Novel Inhibitory Factor for Abscisic Acid-Induced Stomatal Closure under Drought Stress in Arabidopsis. Plant Physiology **148**, 2121-2133.

Table 1: Summary statistics for phenotypic values for control and drought stressed populations. Statistical significance was assessed via one-way analysis of variance and/or Kruskal-Wallis test. S.D. = standard deviation.

Ht = Height, **SPAD** = Leaf Greenness/Chlorophyll Content, **RWC** = Relative Water Content, **AGB** = Aboveground Biomass, **LT** = Leaf Temperature

Trait	Control	S.D.	Drought Stressed	S.D.	Percent Change from Control (%)	Statistical Significance
Ht (cm)	13.37	2.35	8.86	1.75	-33.77	***
SPAD (nmol/cm)	28.39	3.70	21.87	7.42	-22.97	***
RWC (%)	93.46	9.77	51.37	34.31	-45.03	***
AGB (g)	0.60	0.18	0.19	0.056	-67.65	***
LT (°C)	30.34	2.067	34.25	1.82	+12.90	***

Table 2: Summary of QTL identified in *Sorghum* RIL population under control and drought conditions, using transformed least square means. QTL were detected via Multiple QTL Mapping (MQM) in control and drought conditions. QTL are named using the following structure: q[Trait]_[Chr].[Trtmt]. PVE = percent variation explained.

AGB = Aboveground Biomass, **Ht** = Height, **LT** = Leaf Temperature, **RWC** = Relative Water Content, **SPAD** = Leaf Greenness/Chlorophyll Content, **Ctrl** = Control, **DS** = Drought Stressed

Trait	Trtmt	QTL Name	Chr	Position (cM)	Bin (Max LOD)	LOD Score	p-value	PVE (%)	Additive Effect	Start (Mb)	Peak (Mb)	End (Mb)
Ht	Ctrl	qHt_7.Ctrl	7	52.97	59.66	6.28	0.004	3.7	-0.043	59.51	59.66	59.94
Ht	Ctrl	qHt_8.Ctrl	8	5.81	0.20	3.51	0.023	3.6	-0.042	0.084	0.20	1.73
Ht	Ctrl	qHt_9.Ctrl	9	37.95	2.99	5.17	0.004	5.4	-0.053	2.75	2.99	3.1
Ht	DS	qHt_1.DS	1	121.17	79.95	3.26	0.033	5.4	-0.052	79.86	79.95	80.58
Ht	DS	qHt_9.DS	9	63.13	56.69	5.62	0.004	8.9	-0.071	55.49	56.69	57.032
RWC	DS	qRWC_5.DS	5	80.70	71.53	3.27	0.044	6.2	-0.372	70.34	71.53	71.74
SPAD	Ctrl	qSPAD_6.Ctrl	6	36.70	53.75	3.58	0.017	8.1	-0.684	52.69	53.75	55.31
AGB	Ctrl	qAGB_1.Ctrl	1	52.87	7.92	3.5	0.022	3.4	0.015	5.6	7.92	15.83
AGB	Ctrl	qAGB_5.Ctrl	5	48.39	64.9	4.77	0.002	7.1	0.023	54.9	64.9	66.76
AGB	DS	qAGB_1.DS	1	73.12	59.82	3.98	0.013	9.3	0.016	58.51	59.82	61.63
AGB	DS	qAGB_4.DS	4	66.94	66.05	3.78	0.016	10.7	0.017	64.17	66.05	66.24
AGB	DS	qAGB_5.DS	5	45.75	65.91	3.78	0.037	5.9	0.010	64.62	65.91	66.58
LT	DS	qLT_5.DS	5	3.79	0.55	3.53	0.021	18.7	0.501	0.46	0.55	0.801
LT	DS	qLT_6.DS	6	45.78	56.34	3.2	0.031	13.9	0.426	56.28	56.34	56.98

Figure 1: Genetic map with QTL locations from 168 $F_{3:6}$ *Sorghum* RILs. Colored vertical lines display the position of each QTL for each trait in control and drought conditions. Closed black circles within each colored vertical line represent the peak of the QTL (in centimorgans, cM). The open spaces on each chromosome reflect the removal of duplicate and/or heterozygous markers; horizontal lines represent bins used as markers. The genetic map positions (in cM) are shown in the y-axis, while the chromosome number is located across the x-axis.

AGB = Aboveground Biomass, **Ht** = Height, **LT** = Leaf Temperature, **RWC** = Relative Water Content, **SPAD** = Leaf Greenness/Chlorophyll Content, **Ctrl** = Control, **DS** = Drought Stressed

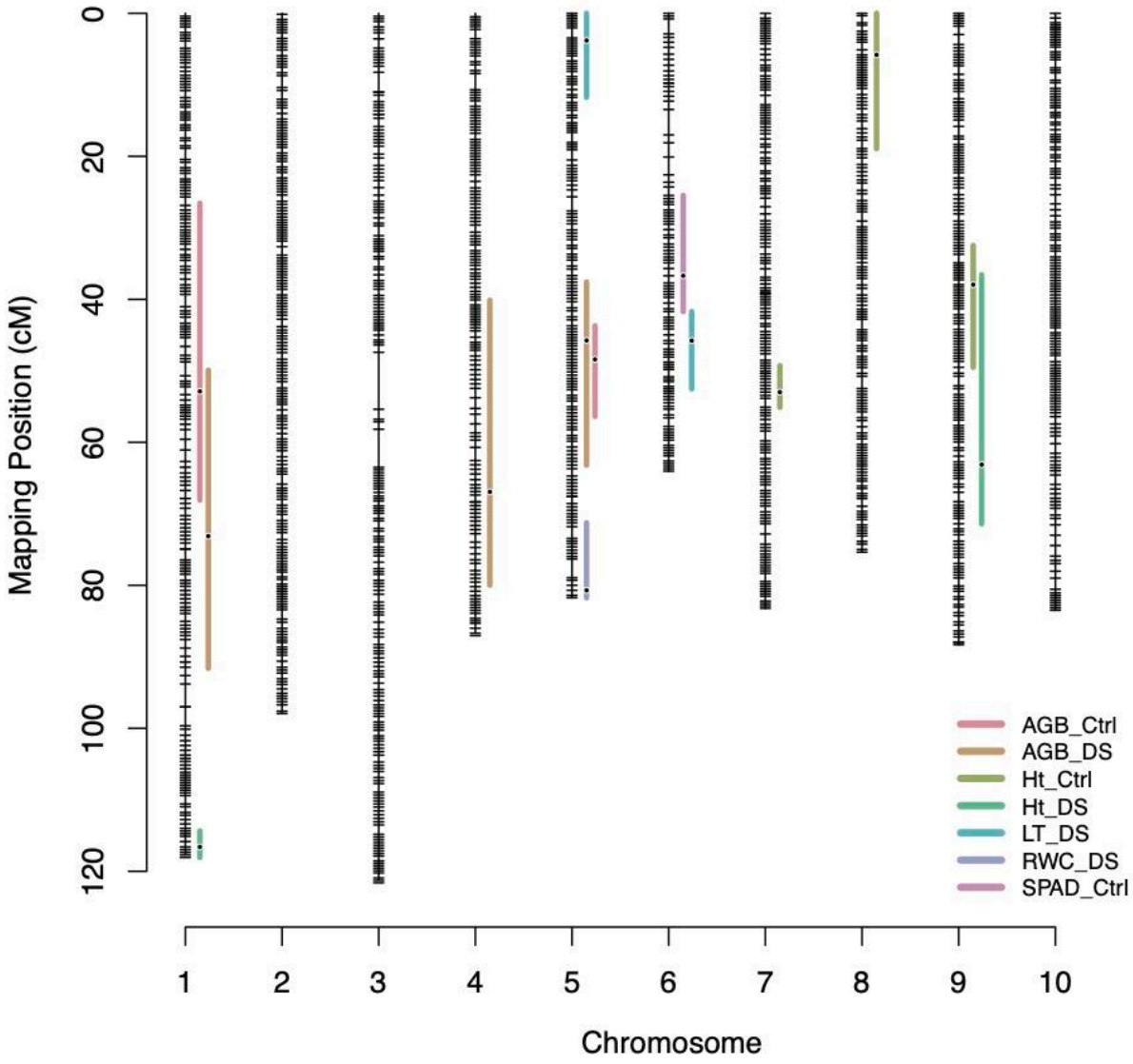

Table S1: Transformation of least square means values. Phenotypes were transformed to meet normality, and these values were used in the QTL analysis.

Ht = Height, **SPAD** = Leaf Greenness/Chlorophyll Content, **RWC** = Relative Water Content, **AGB** = Aboveground Biomass, **LT** = Leaf Temperature

Trait	Control Transformation	Shapiro-Wilk Test p-value	Drought Stressed Transformation	Shapiro-Wilk Test p-value
Ht (cm)	Cubed Root	0.07546	Square Root	0.1026
SPAD (nmol/cm)	None	0.2765	Twelve outliers removed	0.4826
RWC (%)	Removed values >100% + 6th power	0.1242	Removed values >100% or <0% + square root	0.08102
AGB (g)	Square root	0.363	None	0.05075
LT (°C)	Cubed	0.08179	Two outliers removed	0.8437

Table S2: Genetic map summary. The genetic map consists of 10 total chromosomes, and spans 899.4 cM with a total of 1991 bin markers. On average, markers are 0.4 cM apart with a maximum spacing of 8.0 cM.

Chromosome	Control Transformation	Shapiro-Wilk Test p-value	Drought Stressed Transformation	Shapiro-Wilk Test p-value
1	308	117.6	0.4	3.2
2	256	97.8	0.4	1.7
3	254	121.2	0.5	8.0
4	213	86.6	0.4	2.3
5	185	81.7	0.4	2.6
6	170	64.0	0.4	3.5
7	203	83.2	0.4	1.4
8	174	75.4	0.4	1.7
9	221	88.3	0.4	1.4
10	186	83.5	0.5	1.6
Overall	**2170**	**899.4**	**0.4**	**8.0**

Table S3. Candidate genes identified for each QTL. Genes were identified within 1 logarithm of the odds (LOD) confidence interval for each QTL. Genes are organized by trait.

	QTL	Gene_ID	Sorghum_Annotation	Arabidopsis_Annotation	Rice_Annotation
1	qAGB_1.DS	Sobic.001G302666		flavin–monooxygenase glucosinolate S–oxygenase 5	"flavin–containing monooxygenase family protein, putative, expressed"
2	qAGB_1.DS	Sobic.001G302800	"similar to Nitrate/chlorate transporter, putative, expressed"	nitrate transporter 1.1	"peptide transporter PTR2, putative, expressed"
3	qAGB_1.DS	Sobic.001G303200	"similar to Flavin–containing monooxygenase family protein, putative, expressed"	Flavin–binding monooxygenase family protein	"flavin–containing monooxygenase family protein, putative, expressed"
4	qAGB_1.DS	Sobic.001G303600	similar to RbohAp108	respiratory burst oxidase protein F; Riboflavin synthase–like superfamily protein	"respiratory burst oxidase protein B, putative, expressed"
5	qAGB_1.DS	Sobic.001G303750		Flavin–binding monooxygenase family protein	"flavin–containing monooxygenase family protein, putative, expressed"
6	qAGB_1.DS	Sobic.001G303900	similar to Putative uncharacterized protein	Haloacid dehalogenase–like hydrolase (HAD) superfamily protein	"CPuORF23 – conserved peptide uORF–containing transcript, expressed"
7	qAGB_1.DS	Sobic.001G304800	similar to Putative uncharacterized protein	Protein of unknown function (DUF3527)	expressed protein
8	qAGB_1.DS	Sobic.001G305000		hydroxyproline–rich glycoprotein family protein	"stress responsive protein, putative, expressed"
9	qAGB_1.DS	Sobic.001G306000	"weakly similar to U–box domain containing protein, expressed"	U–box domain–containing protein kinase family protein	"protein kinase, putative, expressed"
10	qAGB_1.DS	Sobic.001G306101		U–box domain–containing protein kinase family protein	"protein kinase, putative, expressed"
11	qAGB_1.DS	Sobic.001G306300		U–box domain–containing protein kinase family protein	"protein kinase, putative, expressed"
12	qAGB_1.DS	Sobic.001G307800	"similar to Harpin–induced protein 1 containing protein, expressed"	Late embryogenesis abundant (LEA) hydroxyproline–rich glycoprotein family	"harpin–induced protein 1 domain containing protein, expressed"
13	qAGB_1.DS	Sobic.001G309100		zinc knuckle (CCHC–type) family protein	"zinc knuckle domain containing protein, expressed"
14	qAGB_1.DS	Sobic.001G311800	similar to Expressed protein	EXORDIUM like 5	"phosphate–induced protein 1 conserved region domain containing protein, expressed"
15	qAGB_1.DS	Sobic.001G312500	PTHR13832:SF252 – PROTEIN PHOSPHATASE 2C 27–RELATED	Protein phosphatase 2C family protein	"protein phosphatase 2C, putative, expressed"
16	qAGB_1.DS	Sobic.001G312600	similar to Seven transmembrane protein Mlo2	Seven transmembrane MLO family protein	"MLO domain containing protein, putative, expressed"
17	qAGB_1.DS	Sobic.001G312900	similar to Hexose transporter	tonoplast monosaccharide transporter2	"transporter family protein, putative, expressed"
18	qAGB_1.DS	Sobic.001G313100	similar to Calcium–dependent protein kinase isoform 1	Calcium–dependent protein kinase family protein	"CAMK_CAMK_like.8 – CAMK includes calcium/calmodulin depedent protein kinases, expressed"
19	qAGB_1.DS	Sobic.001G313600	similar to Putative uncharacterized protein	Heavy metal transport/detoxification superfamily protein	"heavy metal–associated domain containing protein, expressed"
20	qAGB_1.DS	Sobic.001G313800	similar to Putative uncharacterized protein	AP2/B3–like transcriptional factor family protein	"B3 DNA binding domain containing protein, expressed"
21	qAGB_1.DS	Sobic.001G314400	similar to MADS–box transcription factor TaAGL7	AGAMOUS–like 19	"OsMADS56 – MADS–box family gene with MIKCc type–box, expressed"
22	qAGB_1.DS	Sobic.001G314500	similar to Ubiquitin carrier protein	sumo conjugation enzyme 1	"ubiquitin–conjugating enzyme, putative, expressed"
23	qAGB_1.DS	Sobic.001G314700	similar to Putative uncharacterized protein	PLAC8 family protein	"uncharacterized Cys–rich domain containing protein, putative, expressed"
24	qAGB_1.DS	Sobic.001G315700	similar to Mitogen–activated protein kinase 6	MAP kinase 4	"CGMC_MAPKCMGC_2_ERK.14 – CGMC includes CDA, MAPK, GSK3, and CLKC kinases, expressed"
25	qAGB_1.DS	Sobic.001G316200		NAD(P)–binding Rossmann–fold superfamily protein	"erythronate–4–phosphate dehydrogenase, putative, expressed"
26	qAGB_1.DS	Sobic.001G316500	similar to Putative uncharacterized protein	alpha/beta–Hydrolases superfamily protein	"hydrolase, alpha/beta fold family domain containing protein, expressed"
27	qAGB_1.DS	Sobic.001G319500	similar to Glutathione S–transferase GST 31	Glutathione S–transferase family protein	"glutathione S–transferase, putative, expressed"
28	qAGB_1.DS	Sobic.001G319600	similar to Glutathione S–transferase GSTU31	Glutathione S–transferase family protein (GSTU17)	"glutathione S–transferase, putative, expressed"
29	qAGB_1.DS	Sobic.001G320300	similar to Putative mandelonitrile lyase	Glucose–methanol–choline (GMC) oxidoreductase family protein	"HOTHEAD precursor, putative, expressed"
30	qAGB_1.DS	Sobic.001G321900	"similar to Chromosome chr15 scaffold_37, whole genome shotgun sequence"	shaggy–like protein kinase 32	"CGMC_GSK.9 – CGMC includes CDA, MAPK, GSK3, and CLKC kinases, expressed"
31	qAGB_1.DS	Sobic.001G323500	PF05623 – Protein of unknown function (DUF789) (DUF789)	Protein of unknown function (DUF789)	expressed protein
32	qAGB_1.DS	Sobic.001G323600	similar to Os07g0582400 protein	polyol/monosaccharide transporter 5	"transporter family protein, putative, expressed"
33	qAGB_1.DS	Sobic.001G323701	similar to Putative uncharacterized protein	CCCH–type zinc fingerfamily protein with RNA–binding domain	"zinc finger family protein, putative, expressed"
34	qAGB_1.DS	Sobic.001G324100		senescence–related gene 1	"leucoanthocyanidin dioxygenase, putative, expressed"
35	qAGB_1.DS	Sobic.001G326900	similar to Cytosolic pyruvate orthophosphate dikinase	pyruvate orthophosphate dikinase	"pyruvate, phosphate dikinase, chloroplast precursor, putative, expressed"
36	qAGB_1.DS	Sobic.001G327300	2.1.1.79 – Cyclopropane–fatty–acyl–phospholipid synthase / Unsaturated–phospholipid methyltransferase	Cyclopropane–fatty–acyl–phospholipid synthase	"Cyclopropane–fatty–acyl–phospholipid synthase, putative, expressed"
37	qAGB_1.DS	Sobic.001G327700	similar to Putative uncharacterized protein OJ1047_C01.5	Nucleotide–diphospho–sugar transferase family protein	expressed protein
38	qAGB_1.DS	Sobic.001G327900	similar to Putative uncharacterized protein	GRAS family transcription factor	"SHR, putative, expressed"
39	qAGB_1.DS	Sobic.001G328200	similar to Putative Interferon–related developmental regulator	interferon–related developmental regulator family protein / IFRD protein family	"interferon–related developmental regulator, putative, expressed"
40	qAGB_4.DS	Sobic.004G305600	"similar to Chromosome chr11 scaffold_13, whole genome shotgun sequence"	chromatin protein family (SKIP)	"SKIP/SNW domain containing protein, expressed"
41	qAGB_4.DS	Sobic.004G305900	similar to DNAJ heat shock N–terminal domain–containing protein–like	Chaperone DnaJ–domain superfamily protein	"heat shock protein DnaJ, putative, expressed"
42	qAGB_4.DS	Sobic.004G306200	similar to Peptidyl–prolyl cis–trans isomerase	FK506–binding protein 12	"peptidyl–prolyl cis–trans isomerase, FKBP–type, putative, expressed"

43	qAGB_4.DS	Sobic.004G306500	similar to Putative MADS−domain transcription factor	K−box region and MADS−box transcription factor family protein (SVP)	"OsMADS22 − MADS−box family gene with MIKCc type−box, expressed"
44	qAGB_4.DS	Sobic.004G306700	similar to Peptidyl−prolyl cis−trans isomerase	peptidyl−prolyl cis−trans isomerase / cyclophilin−40 (CYP40) / rotamase	"peptidyl−prolyl cis−trans isomerase CYP40, putative, expressed"
45	qAGB_4.DS	Sobic.004G307800	similar to Putative uncharacterized protein	serine/arginine repetitive matrix−like protein	expressed protein
46	qAGB_4.DS	Sobic.004G308700	similar to Putative light−harvesting chlorophyll−a/b protein of photosystem I	photosystem I light harvesting complex gene 5 (LHCA5)	"chlorophyll A−B binding protein, putative, expressed"
47	qAGB_4.DS	Sobic.004G308900		ethylene−responsive element binding protein (ERF13)	"AP2 domain containing protein, expressed"
48	qAGB_4.DS	Sobic.004G306700	similar to Alpha−amylase precursor	alpha−amylase−like (AMY1)	"alpha−amylase precursor, putative, expressed"
49	qAGB_4.DS	Sobic.004G309200	similar to Alpha−amylase precursor	alpha−amylase−like	"alpha−amylase precursor, putative, expressed"
50	qAGB_4.DS	Sobic.004G309500	similar to Putative uncharacterized protein	Protein of unknown function (DUF1685); spire, putative (DUF1685)	expressed protein
51	qAGB_4.DS	Sobic.004G309600	similar to Putative uncharacterized protein	abscisic acid responsive elements−binding factor 2 (ABF2)	"bZIP transcription factor, putative, expressed"
52	qAGB_4.DS	Sobic.004G309700	"similar to Putative mannan endo−1,4−beta−mannosidase 9 precursor"	Glycosyl hydrolase superfamily protein (MAN1)	"OsMan03 − Endo−Beta−Mannanase, expressed"
53	qAGB_4.DS	Sobic.004G310000	similar to Lipase class 3−like	alpha/beta−Hydrolases superfamily protein; triacylglycerol lipase−like 1	"lipase, putative, expressed"
54	qAGB_4.DS	Sobic.004G311900		MAPK/ERK kinase kinase 1; Protein kinase superfamily protein (YDA)	"STE_MEKK_ste11_MAP3K.12 − STE kinases include homologs to sterile 7, sterile 11 and sterile 20 from yeast, expressed"
55	qAGB_4.DS	Sobic.004G312200	similar to WRKY transcription factor 32	WRKY DNA−binding protein 9	"WRKY32, expressed"
56	qAGB_4.DS	Sobic.004G312300	similar to Putative uncharacterized protein	zinc finger/BTB domain protein, putative (DUF1644)	expressed protein
57	qAGB_4.DS	Sobic.004G312600	similar to CopI	Transducin/WD40 repeat−like superfamily protein (COP1)	"COP1, putative, expressed"
58	qAGB_4.DS	Sobic.004G313200	"similar to Beta−1,3−glucanase precursor"	O−Glycosyl hydrolases family 17 protein	"glucan endo−1,3−beta−glucosidase precursor, putative, expressed"
59	qAGB_4.DS	Sobic.004G316500		"nuclear factor Y, subunit A5"	"nuclear transcription factor Y subunit, putative, expressed"
60	qAGB_4.DS	Sobic.004G317000	similar to Putative growth−regulating factor 3	growth−regulating factor 5 (GRF5)	"growth regulating factor protein, putative, expressed"
61	qAGB_4.DS	Sobic.004G317200	PTHR27000:SF188 − LRR RECEPTOR−LIKE SERINE/THREONINE−PROTEIN KINASE ERECTA	Leucine−rich receptor−like protein kinase family protein (ERECTA)	"receptor−like protein kinase 5 precursor, putative, expressed"
62	qAGB_4.DS	Sobic.004G317300	similar to Putative myosin heavy chain	"myosin, putative"	"myosin, putative, expressed"
63	qAGB_4.DS	Sobic.004G317300	similar to Putative myosin heavy chain	"myosin, putative"	"XI−I, putative, expressed"
64	qAGB_4.DS	Sobic.004G318600		Subtilase family protein	"OsSub22 − Putative Subtilisin homologue, expressed"
65	qAGB_4.DS	Sobic.004G318700	similar to Putative subtilisin−like proteinase	Subtilase family protein (SASP)	"OsSub22 − Putative Subtilisin homologue, expressed"
66	qAGB_4.DS	Sobic.004G319000	similar to Putative subtilisin−like proteinase	Subtilase family protein	"OsSub22 − Putative Subtilisin homologue, expressed"
67	qAGB_4.DS	Sobic.004G321300	similar to Ethylene−responsive transcription factor 1	related to AP2 12	"AP2 domain containing protein, expressed"
68	qAGB_4.DS	Sobic.004G323000	similar to Putative uncharacterized protein	"CAP (Cysteine−rich secretory proteins, Antigen 5, and Pathogenesis−related 1 protein) superfamily protein"	"SCP−like extracellular protein, expressed"
69	qAGB_4.DS	Sobic.004G323100	similar to Putative Pathogenesis−related protein PR−1	"CAP (Cysteine−rich secretory proteins, Antigen 5, and Pathogenesis−related 1 protein) superfamily protein"	"SCP−like extracellular protein, expressed"
70	qAGB_4.DS	Sobic.004G323200	similar to Os02g0786900 protein	"CAP (Cysteine−rich secretory proteins, Antigen 5, and Pathogenesis−related 1 protein) superfamily protein"	"SCP−like extracellular protein, expressed"
71	qAGB_4.DS	Sobic.004G323300	similar to Putative uncharacterized protein	"CAP (Cysteine−rich secretory proteins, Antigen 5, and Pathogenesis−related 1 protein) superfamily protein"	"SCP−like extracellular protein, expressed"
72	qAGB_4.DS	Sobic.004G323600	similar to Os02g0787300 protein	mitogen−activated protein kinase kinase 4	"STE_MEK_ste7_MAP2K.5 − STE kinases include homologs to sterile 7, sterile 11 and sterile 20 from yeast, expressed"
73	qAGB_4.DS	Sobic.004G324100	similar to Diacylglycerol kinase−like	diacylglycerol kinase 7	"diacylglycerol kinase, putative, expressed"
74	qAGB_4.DS	Sobic.004G326400	similar to Putative receptor−like kinase Xa21−binding protein 3	XB3 ortholog 2 in Arabidopsis thaliana (XBAT32)	"ankyrin repeat−rich protein, putative, expressed"
75	qAGB_4.DS	Sobic.004G327000	similar to Putative MAP4K alpha1	Protein kinase superfamily protein	"STE_PAK_Ste20_STLK.2 − STE kinases include homologs to sterile 7, sterile 11 and sterile 20 from yeast, expressed"
76	qHt_1.DS	Sobic.001G535500		DHFS−FPGS homolog B (DFB)	"folylpolyglutamate synthase, mitochondrial precursor, putative, expressed"
77	qHt_1.DS	Sobic.001G535900	similar to Aquaporin TIP3−1	tonoplast intrinsic protein 3;1	"aquaporin protein, putative, expressed"
78	qHt_1.DS	Sobic.001G536000	similar to Putative uncharacterized protein	actin−related protein 4	"actin, putative, expressed"
79	qHt_1.DS	Sobic.001G536400	"similar to THO complex subunit 1, putative, expressed"	nuclear matrix protein−related	"THO complex subunit 1, putative, expressed"
80	qHt_1.DS	Sobic.001G537300	similar to Rolled leaf 2	Homeobox−leucine zipper family protein / lipid−binding START domain−containing protein (ATHB15)	"START domain containing protein, expressed"
81	qHt_1.DS	Sobic.001G539600	similar to Expansin−B11 precursor	expansin B2	"expansin precursor, putative, expressed"
82	qHt_1.DS	Sobic.001G539700	similar to Expansin−B11 precursor	expansin B2	"expansin precursor, putative, expressed"
83	qHt_1.DS	Sobic.001G539760	similar to Expansin−B11 precursor	expansin B2	"expansin precursor, putative, expressed"
84	qHt_1.DS	Sobic.001G539820	similar to Expansin−B11 precursor	expansin B2	"expansin precursor, putative, expressed"
85	qHt_1.DS	Sobic.001G539880	similar to Expansin−B11 precursor	expansin B2	"expansin precursor, putative, expressed"

86	qHt_1.DS	Sobic.001G539940	similar to Expansin–B11 precursor	expansin B2	"expansin precursor, putative, expressed"
87	qHt_1.DS	Sobic.001G540000		expansin B4	"expansin precursor, putative, expressed"
88	qHt_1.DS	Sobic.001G540400	similar to Putative uncharacterized protein	RNA polymerase II transcription mediators	expressed protein
89	qHt_1.DS	Sobic.001G540700	similar to Os03g0105800 protein	Protein of unknown function (DUF3527); hypothetical protein (DUF3527)	expressed protein
90	qHt_1.DS	Sobic.001G540800	"weakly similar to DNA–binding family protein, putative, expressed"	AT hook motif DNA–binding family protein (AHL12)	"DNA binding protein, putative, expressed"
91	qHt_1.DS	Sobic.001G541700	PTHR23023:SF94 – FLAVIN–CONTAINING MONOOXYGENASE FMO GS–OX–LIKE 1–RELATED	Flavin–binding monooxygenase family protein	"flavin–containing monooxygenase family protein, putative, expressed"
92	qHt_1.DS	Sobic.001G542100		expansin B4	"expansin precursor, putative, expressed"
93	qHt_1.DS	Sobic.001G542200	similar to Expansin–B4 precursor	expansin B4	"expansin precursor, putative, expressed"
94	qHt_9.DS	Sobic.009G208100	similar to OSK1	SNF1 kinase homolog 10 (KIN10)	"CAMK_KIN1/SNF1/Nim1_like_AMPKh.3 – CAMK includes calcium/calmodulin depedent protein kinases, expressed"
95	qHt_9.DS	Sobic.009G209100		Hyaluronan / mRNA binding family (ATRGGA)	"plasminogen activator inhibitor 1 RNA–binding protein, putative, expressed"
96	qHt_9.DS	Sobic.009G209200	similar to Os05g0533500 protein	serine acetyltransferase 1;1 (SAT5)	"serine acetyltransferase protein, putative, expressed"
97	qHt_9.DS	Sobic.009G210200	similar to Os05g0534100 protein	Acid phosphatase/vanadium–dependent haloperoxidase–related protein	"Divergent PAP2 family domain containing protein, expressed"
98	qHt_9.DS	Sobic.009G210300	PTHR23056:SF45 – CALCINEURIN B–LIKE PROTEIN	Calcium–binding EF–hand family protein (SOS3)	"calcineurin B, putative, expressed"
99	qHt_9.DS	Sobic.009G210500	similar to Putative uncharacterized protein OSJNBa0053E05.23	CASC3/Barentsz eIF4AIII binding (BTZ1)	expressed protein
100	qHt_9.DS	Sobic.009G211700	similar to Histone deacetylase HDT2	histone deacetylase 3	"ZOS5–12 – C2H2 zinc finger protein, expressed"
101	qHt_9.DS	Sobic.009G211800	similar to OSIGBa0138E08–OSIGBa0161L23.3 protein	UDP–Glycosyltransferase superfamily protein	"UDP–glucoronosyl and UDP–glucosyl transferase domain containing protein, expressed"
102	qHt_9.DS	Sobic.009G212100	similar to Putative uncharacterized protein OJ1741_B01.8	IQ–domain 31	"IQ calmodulin–binding motif family protein, putative, expressed"
103	qHt_9.DS	Sobic.009G212600	similar to Putative uncharacterized protein	aldehyde dehydrogenase 12A1	expressed protein
104	qHt_9.DS	Sobic.009G212700		RAB GTPase homolog G3B	"ras–related protein, putative, expressed"
105	qHt_9.DS	Sobic.009G213600	similar to Putative uncharacterized protein	Protein of unknown function (DUF778)	"green ripe–like, putative, expressed"
106	qHt_9.DS	Sobic.009G214100	similar to Putative uncharacterized protein	heat shock protein 60–3A	"T–complex protein, putative, expressed"
107	qHt_9.DS	Sobic.009G215700	"similar to Late embryogenesis abundant protein, group 3"	Late embryogenesis abundant protein (LEA) family protein	"late embryogenesis abundant protein, group 3, putative, expressed"
108	qHt_9.DS	Sobic.009G216700	similar to Putative uncharacterized protein OJ1288_A07.9	Transducin/WD40 repeat–like superfamily protein	"WD domain, G–beta repeat domain containing protein, expressed"
109	qHt_9.DS	Sobic.009G218800	similar to Putative uncharacterized protein	Acid phosphatase/vanadium–dependent haloperoxidase–related protein	"Divergent PAP2 family domain containing protein, expressed"
110	qHt_9.DS	Sobic.009G219500	similar to Putative NADPH–dependent retinol dehydrogenase/reductase	indole–3–butyric acid response 1	"dehydrogenase/reductase SDR family member 2, putative, expressed"
111	qHt_9.DS	Sobic.009G221400	similar to Putative uncharacterized protein	related to ABI3/VP1 1; AP2/B3–like transcriptional factor family protein	"B3 DNA binding domain containing protein, expressed"
112	qHt_9.DS	Sobic.009G221500	similar to Phosphatidic acid phosphatase beta–like	lipid phosphate phosphatase 2	"lipid phosphatase protein, putative, expressed"
113	qHt_9.DS	Sobic.009G223300	similar to Guanine nucleotide–binding protein subunit beta–like protein	Transducin/WD40 repeat–like superfamily protein (ATARCA)	"WD repeat–containing protein, putative, expressed"
114	qHt_9.DS	Sobic.009G224500	similar to Putative uncharacterized protein	myb domain protein 36	"MYB family transcription factor, putative, expressed"
115	qHt_9.DS	Sobic.009G226900	similar to Putative uncharacterized protein	Cytochrome b561/ferric reductase transmembrane with DOMON related domain	"auxin–responsive protein, putative, expressed"
116	qHt_9.DS	Sobic.009G228600	similar to Os02g0313500 protein	cytochrome c oxidase 19–2	"CHCH domain containing protein, expressed"
117	qHt_9.DS	Sobic.009G228700	similar to Putative uncharacterized protein	novel interactor of JAZ	expressed protein
118	qHt_9.DS	Sobic.009G229200	similar to Auxin–responsive protein IAA19	indoleacetic acid–induced protein 8	"OsIAA19 – Auxin–responsive Aux/IAA gene family member, expressed"
119	qHt_9.DS	Sobic.009G229600	similar to Putative uncharacterized protein OSJNBa0001A14.17	golgin candidate 5 (GC5)	"tRNA–binding arm, putative, expressed"
120	qLT_5.DS	Sobic.005G006100		NAC domain containing protein 1	hypothetical protein
121	qLT_5.DS	Sobic.005G007700	similar to Putative uncharacterized protein P0458H05.113	BRISC complex subunit Abro1–like protein	expressed protein
122	qLT_5.DS	Sobic.005G008600		dsRNA–binding domain–like superfamily protein	"double–stranded RNA binding motif containing protein, expressed"
123	qLT_6.DS	Sobic.006G215400	PF00069//PF11721 – Protein kinase domain (Pkinase) // Di–glucose binding within endoplasmic reticulum (Malectin)	Leucine–rich repeat transmembrane protein kinase	"SHR5–receptor–like kinase, putative, expressed"
124	qLT_6.DS	Sobic.006G215600	PF00069//PF11721//PF13855 – Protein kinase domain (Pkinase) // Di–glucose binding within endoplasmic reticulum (Malectin) // Leucine rich repeat (LRR_8)	Leucine–rich repeat transmembrane protein kinase	"SHR5–receptor–like kinase, putative, expressed"
125	qLT_6.DS	Sobic.006G218400	similar to H0313F03.20 protein	Galactose oxidase/kelch repeat superfamily protein	"OsFBK15 – F–box domain and kelch repeat containing protein, expressed"
126	qLT_6.DS	Sobic.006G218600	similar to H0313F03.20 protein	Galactose oxidase/kelch repeat superfamily protein	"OsFBK15 – F–box domain and kelch repeat containing protein, expressed"
127	qLT_6.DS	Sobic.006G218900	similar to H0714H04.1 protein	hercules receptor kinase 2 (HERK2)	"TKL_IRAK_CrRLK1L–1.9 – The CrRLK1L–1 subfamily has homology to the CrRLK1L homolog, expressed"
128	qLT_6.DS	Sobic.006G219500	similar to H0714H04.6 protein	Remorin family protein	"remorin family protein, putative, expressed"

129	qLT_6.DS	Sobic.006G219600	similar to H0714H04.7 protein	SIT4 phosphatase–associated family protein	"SIT4 phosphatase–associated protein domain containing protein, expressed"
130	qLT_6.DS	Sobic.006G222700	similar to Chloroplast lipocalin	chloroplastic lipocalin	"OsCHL Chloroplastic lipocalin, expressed"
131	qRWC_5.DS	Sobic.006G215400	PF00069//PF11721 – Protein kinase domain (Pkinase) // Di–glucose binding within endoplasmic reticulum (Malectin)	Leucine–rich repeat transmembrane protein kinase	"SHR5–receptor–like kinase, putative, expressed"
132	qRWC_5.DS	Sobic.006G215500			"OsFBX114 – F–box domain containing protein, expressed"
133	qRWC_5.DS	Sobic.006G215600	PF00069//PF11721//PF13855 – Protein kinase domain (Pkinase) // Di–glucose binding within endoplasmic reticulum (Malectin) // Leucine rich repeat (LRR_8)	Leucine–rich repeat transmembrane protein kinase	"SHR5–receptor–like kinase, putative, expressed"
134	qRWC_5.DS	Sobic.006G215650			
135	qRWC_5.DS	Sobic.006G215700	weakly similar to Putative uncharacterized protein OJ1362_G11.4	F–box family protein	"OsFBX172 – F–box domain containing protein, expressed"
136	qRWC_5.DS	Sobic.006G215750			
137	qRWC_5.DS	Sobic.006G215800	Predicted protein	Microtubule associated protein (MAP65/ASE1) family protein	
138	qRWC_5.DS	Sobic.006G215900	weakly similar to Putative uncharacterized protein OJ1362_G11.5	F–box family protein	"OsFBX172 – F–box domain containing protein, expressed"
139	qRWC_5.DS	Sobic.006G215950		F–box/RNI–like superfamily protein	"OsFBX452 – F–box domain containing protein, expressed"
140	qRWC_5.DS	Sobic.006G216400	similar to H0818E11.4 protein	SAUR–like auxin–responsive protein family (SAUR41)	"OsSAUR21 – Auxin–responsive SAUR gene family member, expressed"
141	qRWC_5.DS	Sobic.006G216500	weakly similar to H0818E11.7 protein	SAUR–like auxin–responsive protein family	expressed protein
142	qRWC_5.DS	Sobic.006G216700	similar to H0818E11.7 protein	SAUR–like auxin–responsive protein family	"OsSAUR2 – Auxin–responsive SAUR gene family member, expressed"
143	qRWC_5.DS	Sobic.006G216900			expressed protein
144	qRWC_5.DS	Sobic.006G217100	similar to OSJNBa0093O08.12 protein	RmlC–like cupins superfamily protein	"Cupin domain containing protein, expressed"
145	qRWC_5.DS	Sobic.006G217200	similar to H0313F03.9 protein	Pentatricopeptide repeat (PPR) superfamily protein	"PPR repeat domain containing protein, putative, expressed"
146	qRWC_5.DS	Sobic.006G217400			
147	qRWC_5.DS	Sobic.006G217700	"similar to Chromosome chr10 scaffold_76, whole genome shotgun sequence"	gamma–soluble NSF attachment protein	"gamma–soluble NSF attachment protein, putative, expressed"
148	qRWC_5.DS	Sobic.006G217800	similar to OSJNBa0058K23.6 protein	phytochrome interacting factor 3	"helix–loop–helix DNA–binding domain containing protein, expressed"
149	qRWC_5.DS	Sobic.006G217900	similar to H0313F03.16 protein	Leucine–rich receptor–like protein kinase family protein (FLS2)	"leucine–rich repeat receptor protein kinase EXS precursor, putative, expressed"
150	qRWC_5.DS	Sobic.006G217950			
151	qRWC_5.DS	Sobic.006G218000	similar to H0313F03.17 protein	serine/arginine repetitive matrix–like protein; TPRXL	expressed protein
152	qRWC_5.DS	Sobic.006G218100	weakly similar to Putative uncharacterized protein	RING/U–box superfamily protein	expressed protein
153	qRWC_5.DS	Sobic.006G218200	Predicted protein	RING/U–box superfamily protein	expressed protein
154	qRWC_5.DS	Sobic.006G218300		NAC (No Apical Meristem) domain transcriptional regulator superfamily protein	"no apical meristem protein, putative, expressed"
155	qRWC_5.DS	Sobic.006G218400	similar to H0313F03.20 protein	Galactose oxidase/kelch repeat superfamily protein	"OsFBK15 – F–box domain and kelch repeat containing protein, expressed"
156	qRWC_5.DS	Sobic.006G218600	similar to H0313F03.20 protein	Galactose oxidase/kelch repeat superfamily protein	"OsFBK15 – F–box domain and kelch repeat containing protein, expressed"
157	qRWC_5.DS	Sobic.006G218700	similar to H0313F03.21 protein	Protein kinase superfamily protein (CRPK1)	"tyrosine protein kinase domain containing protein, putative, expressed"
158	qRWC_5.DS	Sobic.006G218900	similar to H0714H04.1 protein	hercules receptor kinase 2 (HERK2)	"TKL_IRAK_CrRLK1L–1.9 – The CrRLK1L–1 subfamily has homology to the CrRLK1L homolog, expressed"
159	qRWC_5.DS	Sobic.006G218950			
160	qRWC_5.DS	Sobic.006G219000	similar to H0114G12.8 protein	F–box protein 2 (FBX2)	"OsFBW1 – F–box domain and WD40 repeat containing protein, expressed"
161	qRWC_5.DS	Sobic.006G219200	similar to H0714H04.4 protein	BCL–2–associated athanogene 1	"ATBAG1, putative, expressed"
162	qRWC_5.DS	Sobic.006G219300	similar to H0714H04.5 protein	multidrug resistance–associated protein 2 (ABCC2)	"ABC transporter family protein, putative, expressed"
163	qRWC_5.DS	Sobic.006G219500	similar to H0714H04.6 protein	Remorin family protein	"remorin family protein, putative, expressed"
164	qRWC_5.DS	Sobic.006G220200	similar to H0215F08.3 protein	polyamine oxidase 2	"CPuORF12 – conserved peptide uORF–containing transcript, expressed"
165	qRWC_5.DS	Sobic.006G221500	similar to OSIGBa0148A10.2 protein	Phospholipid/glycerol acyltransferase family protein	"acyltransferase, putative, expressed"
166	qRWC_5.DS	Sobic.006G221600	similar to OSIGBa0148A10.3 protein	nucleolar pre–ribosomal–associated protein	expressed protein
167	qRWC_5.DS	Sobic.006G222700	similar to Chloroplast lipocalin	chloroplastic lipocalin	"OsCHL Chloroplastic lipocalin, expressed"

Supplementary Figures 1A-D: Pearson correlations on raw phenotypes (**A, B**) and transformation least squared mean values (**C, D**) for the control (**A, C**) and drought (**B, D**) populations.

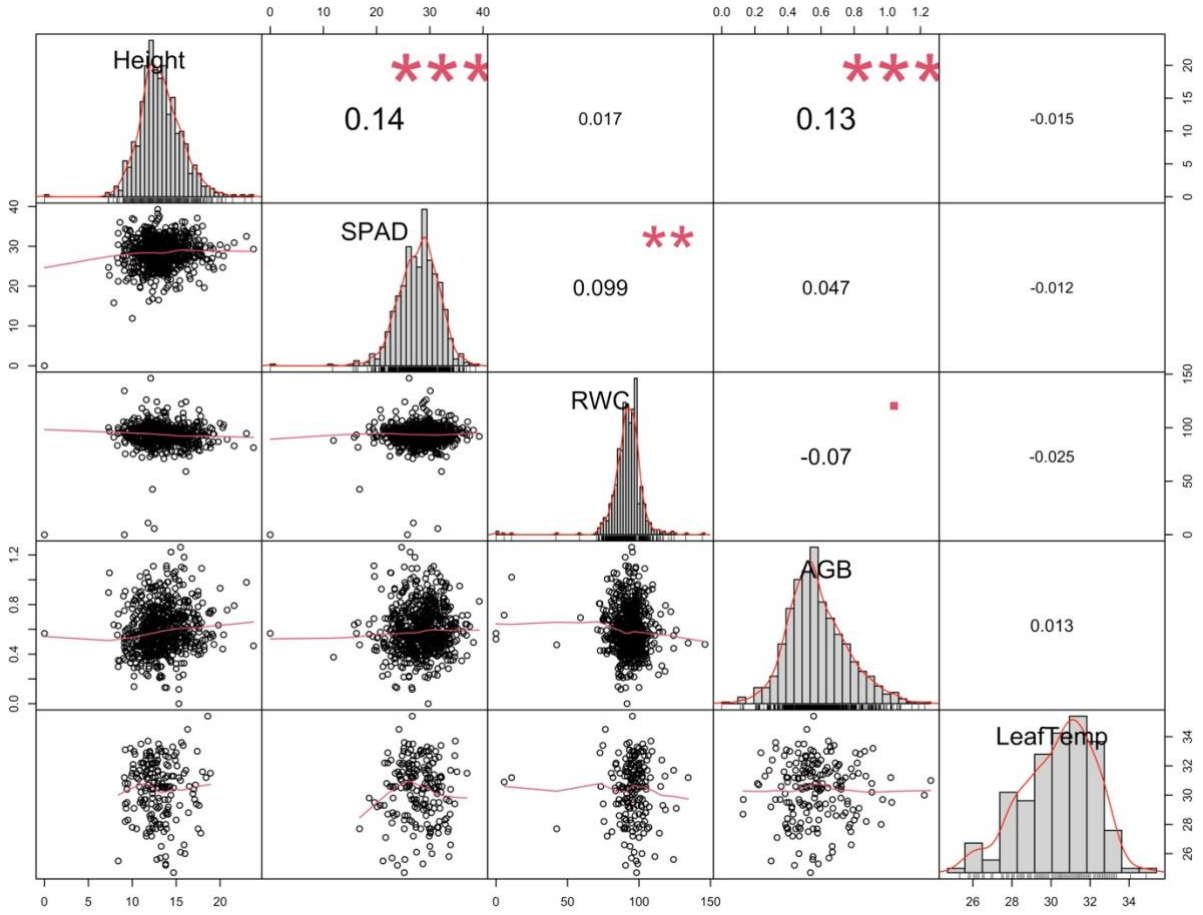

A

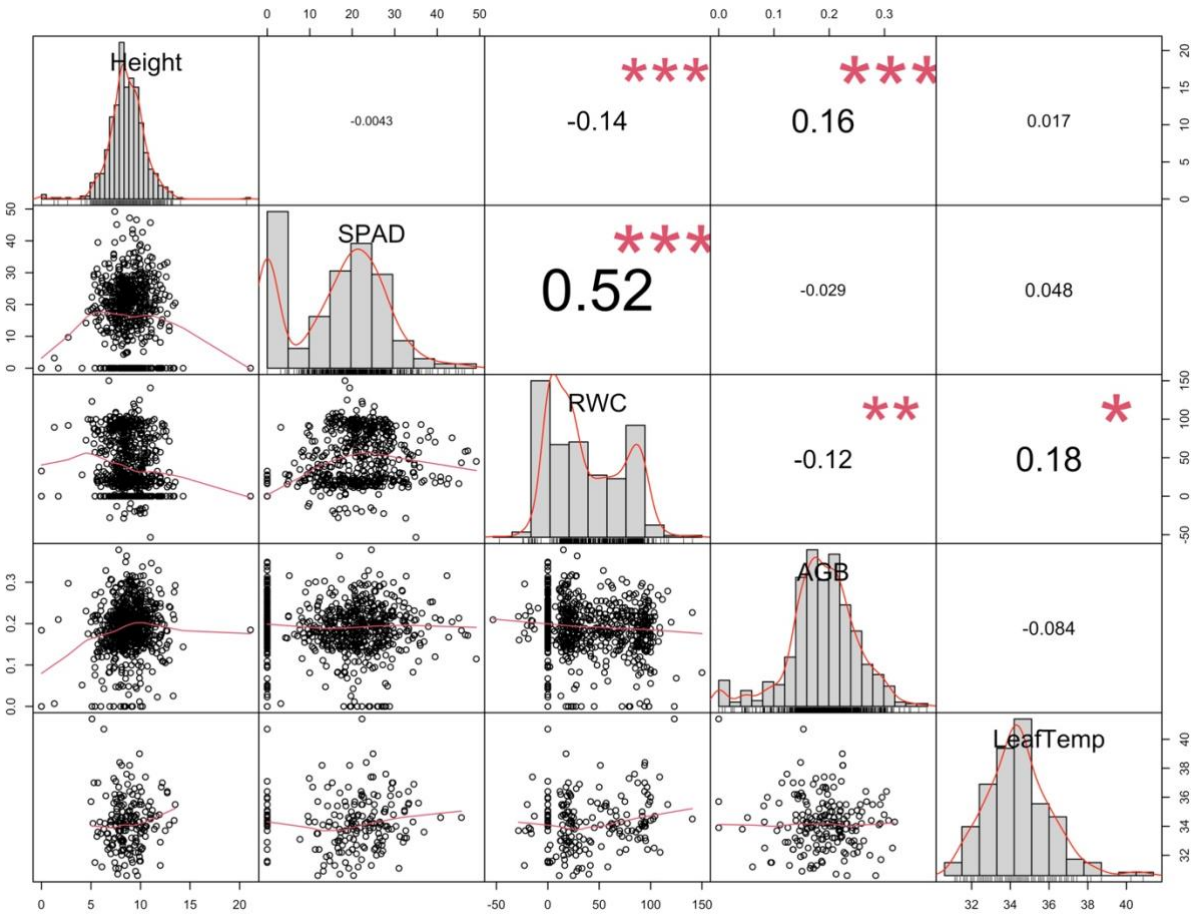
Height
SPAD
RWC
AGB
LeafTemp
-0.0043
-0.14
0.16
0.017
0.52
-0.029
0.048
-0.12
0.18
-0.084
***
***
***
**
*

B

C

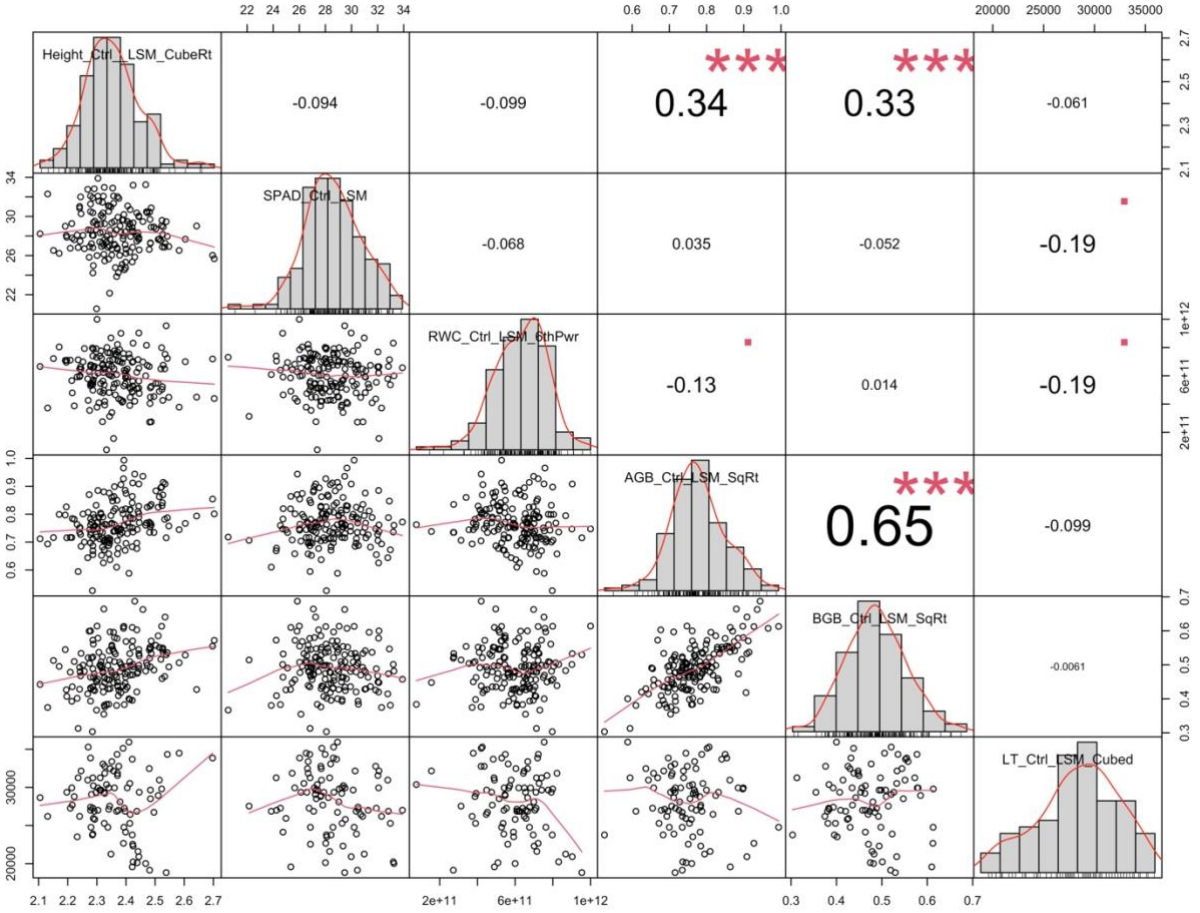
Height_Ctrl_LSM_CubeRt
SPAD_Ctrl_LSM
RWC_Ctrl_LSM_6thPwr
AGB_Ctrl_LSM_SqRt
BGB_Ctrl_LSM_SqRt
LT_Ctrl_LSM_Cubed
-0.094
-0.099
0.34
0.33
-0.061
-0.068
0.035
-0.052
-0.19
-0.13
0.014
-0.19
0.65
-0.099
-0.0061

D

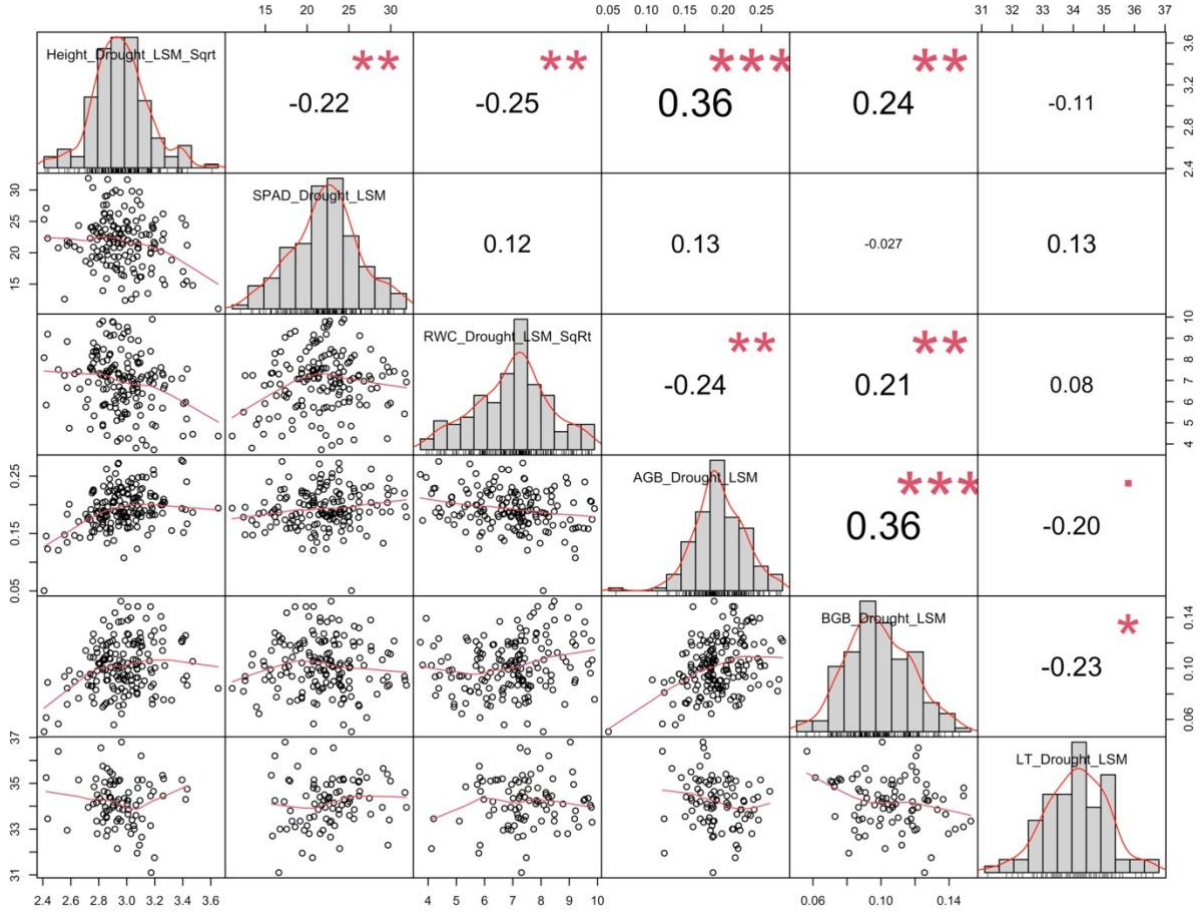
Height_Drought_LSM_Sqrt
SPAD_Drought_LSM
RWC_Drought_LSM_SqRt
AGB_Drought_LSM
BGB_Drought_LSM
LT_Drought_LSM
-0.22
-0.25
0.36
0.24
-0.11
0.12
0.13
-0.027
0.13
-0.24
0.21
0.08
0.36
-0.20
-0.23

Supplementary Figures 2A-E: Boxplots displaying average control (black) and drought stressed (blue) values for all measured morphological and physiological traits. **A**) aboveground biomass, **B**) height, **C**) foliar chlorophyll content, **D**) leaf temperature, **E**) relative water content.

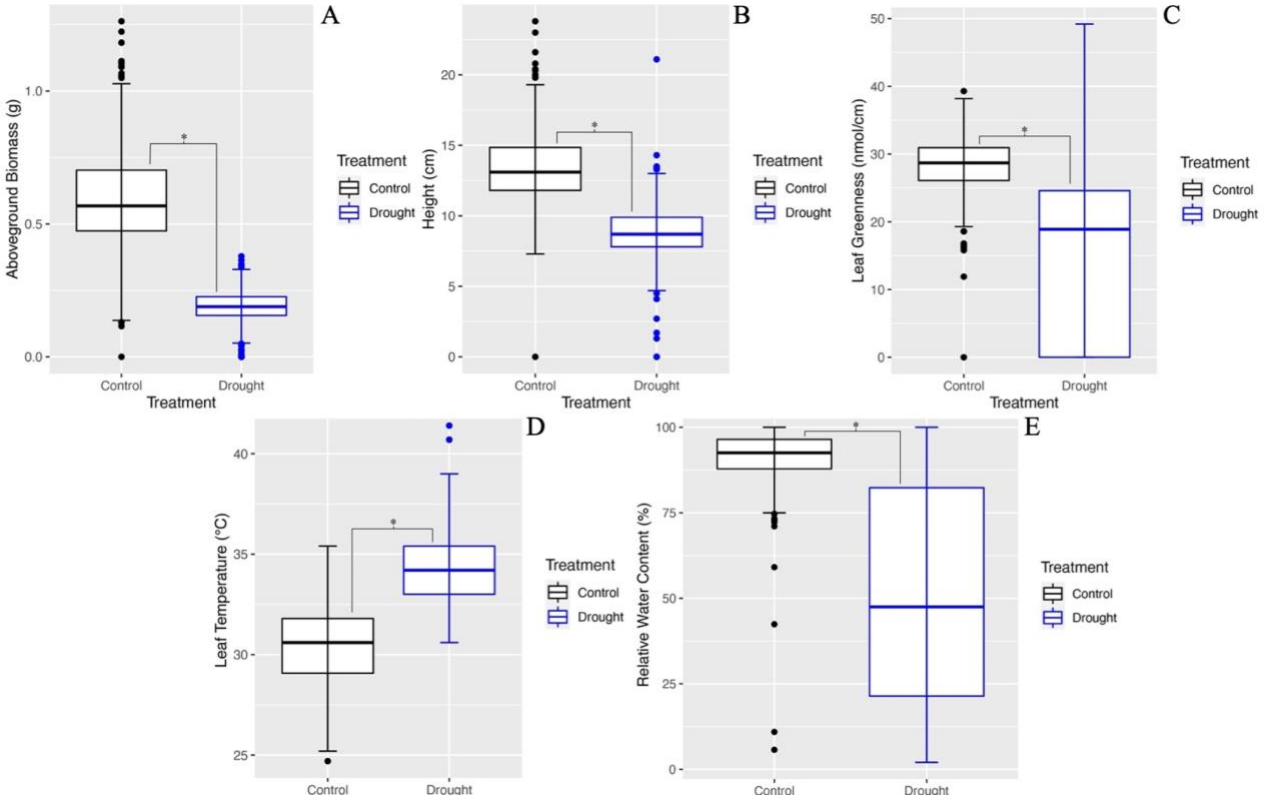

Supplementary Figure 3: Genetic map following removal of heterozygous and duplicate markers. Mapping position (in cM), is shown on the y-axis, and chromosome number is displayed across the x-axis.

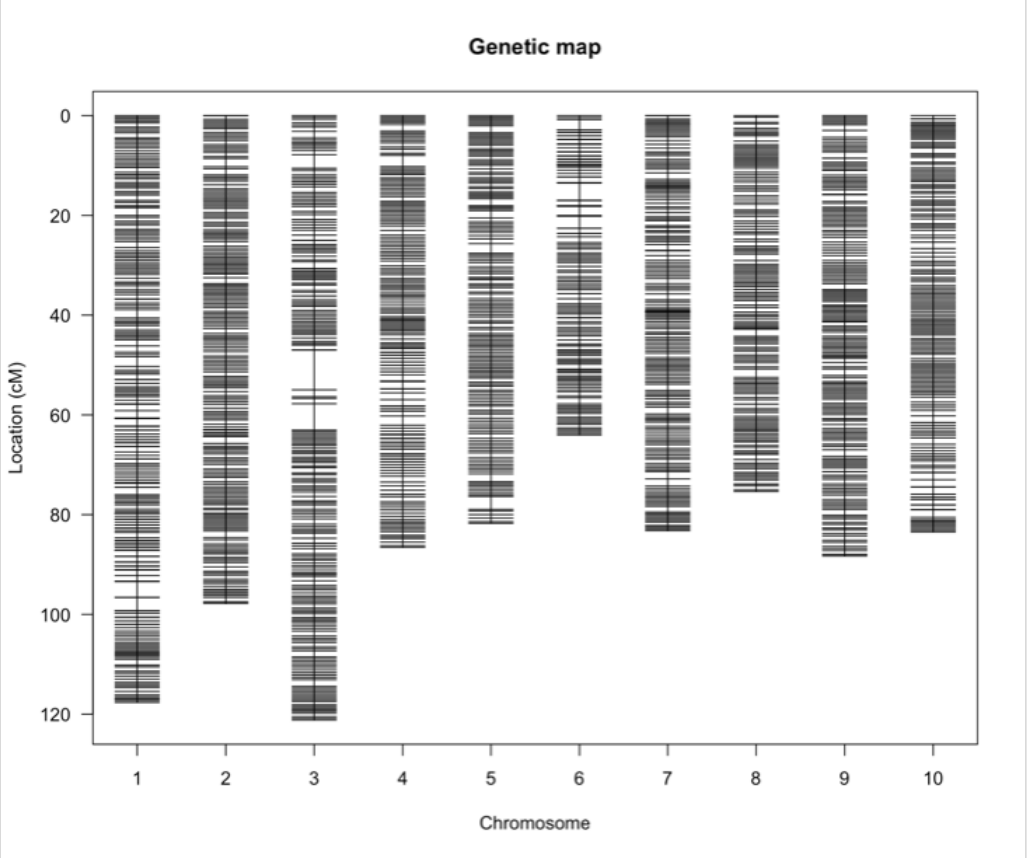

Supplementary Figure 4: Non-metric multidimensional scaling, paired with an analysis of similarity, reveals clustering of morphological traits (excluding leaf temperature) by treatment. Control = purple squares, Drought = black triangles.

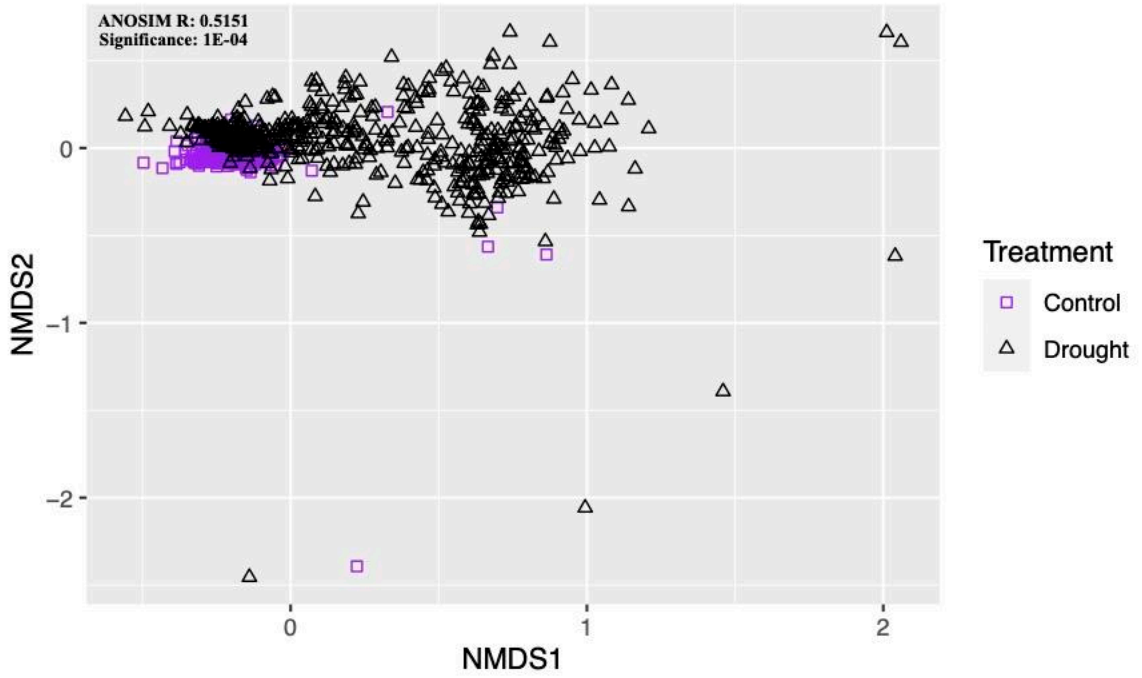

CHAPTER 5: QTL MAPPING IN A *SORGHUM* RECOMBINANT INBRED LINE POPULATION EMPHASIZES ROLE OF ROOT SYSTEM REORGANIZATION IN DROUGHT RESISTANCE

Melissa A. Lehrer, Rajanikanth Govindarajulu, Farren Smith, and Jennifer S. Hawkins

Abstract

Climate change induced environmental stressors, such as drought, significantly limit crop productivity. As moisture acquisition is critical during periods of drought, elucidating root system architectural responses that enhance water uptake will deepen our understanding of belowground drought tolerance strategies. Evaluation of a *Sorghum* recombinant inbred line (RIL) that was generated via a cross between domesticated *Sorghum bicolor* (TX7000 inbred) and its wild and weedy relative *Sorghum propinquum* under drought conditions resulted in the identification of five drought-specific quantitative trait loci (QTL) related to root system architecture (RSA). These QTL contained genes whose products were involved in hormone synthesis and signaling, suggesting that intricate and cascading signal transduction pathways play a role in mitigating drought stress through root-to-shoot communication. Further, co-localization of these QTL with a root biomass QTL detected in this same population under salinity stress indicates shared genetic control of belowground traits under osmotic stress. The allelic control of these traits reflects enhanced downward growth and maintenance of root biomass under osmotic stress, as influenced by *S. bicolor*. Our findings show that: 1) root systems undergo structural rearrangement upon exposure to osmotic stress, likely improving water uptake, and 2) phytohormones trigger cascading downstream physiological and molecular effects in response to drought.

Keywords: *Sorghum* recombinant inbred line, domestication, drought, osmotic stress, root system architecture, water acquisition, phytohormones, abscisic acid (ABA)

Introduction

Drought is one of the most important environmental constraints limiting crop productivity in many regions of the world (Uga et al., 2013). Therefore, it is crucial to shed light on the genetic underpinnings associated with drought tolerant phenotypes, specifically in agriculturally and economically important grain crops. Not only is it important to study these mechanisms aboveground, as the grain and biomass are the monetary and/or consumable components of cereals, but also belowground, as water and nutrient uptake are crucial for plant growth and development, especially under drought (Chen et al., 2020). Further, as the roots are the first organ to experience drought, they play the important role in modulating water uptake and sensing the onset of water limitation (Gewin, 2010, Chen et al., 2020). Thus, investigation of the drought-responsive changes to root system architecture (RSA) in drought conditions will provide a more thorough understanding of the phenotypic and genetic driving forces that enhance soil exploration and water acquisition (Koeveots et al., 2016).

Variation in nodal root angle impacts lateral soil exploration and significantly influences water uptake (Oyanagi, 1994; Kato et al., 2006, Hammer, 2009, Gewin, 2010, Singh et al., 2010, Mace, 2012). Further, Gewin (2010) found that deep root systems play a major role in the drought response, as they are better able to absorb water and nutrients compared to shallow root systems (Chen et al., 2020). Other RSA traits, like root number and positioning, can also impact water and nutrient uptake (Manschadi et al., 2006). In addition to these morphological mechanisms, root systems are involved in hormone synthesis and transport, which are essential in the drought response and can influence aboveground drought-responsive phenotypes via signal transduction (Chen et al., 2020).

In this work, a recombinant inbred line (RIL) population, generated via an interspecific cross between *Sorghum propinquum* (female parent) and *Sorghum bicolor* (TX7000, male parent) (Govindarajulu *et al*., 2021) was used to identify genetic controls of drought tolerance. *S. bicolor* is a domesticated grain crop, while *S. propinquum* is drought sensitive and displays phenotypes associated with wild grasses, like small seeds, narrow leaves, tillering (Govindarajulu *et al*., 2021). TX7000, an elite, grain producing line of *S. bicolor* from the durra landrace, displays pre-anthesis drought tolerance (Evans *et al.,* 2013, Henderson et al., 2020). As described in Lehrer et al. (in prep, Chapter 4), this RIL population has been successfully used to identify the allelic and potential genetic controls of the morphological and physiological strategies associated with domestication-derived drought resistance. Putative genetic controls uncovered within the QTL detected in Lehrer et al. in prep were found to be involved in root growth/development and hormone signaling. Therefore, these previous findings provide a foundation for expanding our analysis to belowground tissues and responses in this same *Sorghum* population under drought.

Methods and Materials

Plant Material:
A recombinant inbred line (RIL) population generated from an interspecific cross between *Sorghum propinquum* (courtesy William Rooney, Texas A&M University, College Station, TX, USA) and *Sorghum bicolor* (TX7000 inbred) was used to explore the genetic controls associated with the drought response. The RIL population consists of 168 $F_{3:6}$ lines, with 5.4% being F_3, 11.4% being F_4, 82.1% being F_5, and 1.1% being F_6. Each line was derived via the single seed descent method (Brim, 1966, Snape and Riggs, 1975).

Experimental Design and Conditions:
In a controlled greenhouse room, between two and four seeds of each RIL were organized into treatment groups (control and drought stressed) and randomly sown in 5 cm x 5 cm x 25 cm pots (Stuewe and Sons, Tangent, OR, USA). Each pot was filled with #4 silica sand with approximately one inch of Premier Pro-Mix BX MYCO soil on top (Premier Tech Horticulture, Quakertown, PA, USA); seeds were germinated in this soil layer. Conditions during germination were as follows: 27 °C day/23 °C night, 75% humidity, and approximately fifteen hours of natural light. During germination, and up to seventeen days post-sowing, all seedlings were watered once daily with tap water and fertilized once weekly with 80 PPM 20-20-20 NPK (Jack's Classic Water Soluble Fertilizer, Allentown, PA, USA). Between twelve and thirteen days post-sowing, all but one seedling was harvested from each pot; five replicates per RIL remained in each treatment group (1680 total plants). At seventeen days post-sowing, half of the replicates (drought stressed, DS), were left unwatered for the remainder of the study (until twenty-six days post-sowing). To prevent plant death during the three days of destructive harvest, all DS plants were watered lightly with tap water until collected (twenty-seven days post sowing).

Root Image Analysis and Phenotypic Measurements:
Control and DS root systems (four of the five replicates) were extracted from pots; the top layer of soil was removed with an air compressor, and any excess growing media was removed via shaking. Root systems were placed on a 18" x 12" black felt background and imaged with a Nikon D5100 camera in three different orientations to account for any asymmetrical growth (**Supplementary Figure 1**), hereafter referred to as A, B, and C. Following imaging, root systems were collected for belowground biomass.

Rhizovision Explorer (RVE) software (Version 2.0.2, Seethepalli et al., 2021) was used to identify drought-responsive changes to root system architecture (RSA); this data was collected from the images taken during the destructive harvest. In order to adjust for any lighting bias in the images due to time of day during the collection and imaging, the average number of pixels per inch (PPI) in each of three images (first image, middle image, last image) from each group of

thirty-six (**Supplementary Figure 2)** was determined via ImageJ; this PPI value was averaged and used in RVE to more accurately calculate the desired RSA traits. Traits extracted from RVE included: convex area (mm^2), root depth (mm), maximum width of the root system (mm), width-to-depth ratio, median root number, and average root diameter (mm). Belowground biomass was measured for plant tissue dried at 65°C for a minimum of 72 hours.

Statistical Analysis

All statistical analyses were performed on both control and DS RILs. There were four biological replicates of each RIL under both control and drought conditions included in the QTL analysis. All statistical analyses were performed using R version 1.4.1717 (R Core Team, 2013).
Least square means for each phenotype in each treatment group (control and DS) were calculated for each RIL. Normality of these data was assessed using both a Shapiro-Wilk test and Q-Q plots using the *stats* package in R (Version 4.1.0). Data that were not normally distributed were transformed as appropriate (**Table S1**) and used in statistical analyses and in the QTL analysis. Correlations of phenotypes (raw data and LSM data) in each treatment group were assessed via a Pearson's Correlation analysis using the *PerformanceAnalytics* package in R (version 2.0.4, R Core Team, 2013, Peterson and Carl, 2020, **Supplementary Figures 3A-D**).

Non-metric multidimensional scaling (NMDS) was performed on the raw phenotype data to identify any treatment effects. Clustering of the NMDS used Bray-Curtis dissimilarity when all phenotypes were included in the analysis. The NMDS, which was performed using the *vegan* packing in R (Version 2.5-7, Oksanen *et al.,* 2020), was coupled with an analysis of similarity (ANOSIM, significance assessed at alpha = 0.05), which adds statistical significance to the NMDS ordination. This analysis was performed twice: on the RSA traits collected from RVE in the A/B orientations and on the RSA traits collected from RVE in the C orientation, combined with belowground biomass. This separation was due to discrepancies in sample size. Further, a Kruskal-Wallis test was performed using the *stats* package in R to identify treatment effects for individual phenotypes; significance was assessed at $\propto = 0.05$. As all RSA traits could not be transformed to normality, the Kruskal-Wallis test, which is used to assess non-parametric data, was performed to identify treatment effects. Boxplots (**Supplementary Figures 4A-G)** were generated using *ggplot2* (version 3.3.5, Wickham, 2016)

Genetic Map Construction and QTL Analysis

Genetic map construction and the quantitative trait loci (QTL) analysis were performed as previously described in Lehrer et al. (in prep, Chapter 4).

Results

Root Image Analysis

Root images taken in the A and B orientations were to account for positional bias during growth; however, the results showed no significant difference between orientations A and B (as

determined via a Kruskal-Wallis test, **Supplementary Figures 7-8**). As such, these data were averaged and used in the downstream analyses. Additionally, given that images taken in the C orientation would inflate any lateral or area-related measurements of the root system due to the outward spread of the roots (**Supplementary Figure 1**), traits derived from C orientation images were used for median root number and average diameter only. All other traits (depth, maximum width, width-to-depth ratio, and convex area) were obtained from the average of the A and B orientations.

Genetic Map Construction

The genetic map for this study was generated as described in Lehrer et al. (in prep, Chapter 4) (**Supplementary Figure 5, Table S2)**.

Impact of Drought Exposure on Root System Architecture Traits

In response to drought, all root-related traits (i.e. root system architecture and belowground biomass) were reduced (**Table S3, Supplementary Figures 4A-G)**. Clustering of these traits, in the A/B and C orientations, respectively, in the NMDS provided additional support for the belowground growth strategies employed in response to drought exposure (**Supplementary Figures 8-9**).

Phenotype and QTL Results

Convex Area

In control plants, the average convex area (CA) of the root system was 19,832.9 mm^2 (range = 5,794.9 mm^2 to 64,471.8 mm^2). This trait was reduced by 35% in drought stressed plants to an average of 12,907 mm^2 (range = 1,377.9 mm^2 to 37,063.6 mm^2). In the drought population, a single QTL for this trait was identified on chromosome four. This QTL explained 11.4% of the phenotypic variation, and had an additive effect of 726.4, indicating that *S. bicolor* alleles positively influenced CA. Of the 103 genes located within this QTL, candidate genes involved in the drought response were associated with hormone responses (abscisic acid, jasmonic acid, salicylic acid, ethylene), hormone-mediated signaling pathways, response to osmotic stress, salt stress, water deprivation, shoot growth and development, and water channel activity (**Table S4**).

Maximum Width

Under well-watered conditions, maximum width (MW) of the root system ranged from 33.58 mm to 274.03 mm (average = 86.27 mm). In response to drought, this trait was reduced by 25.5% to an average of 64.29 mm (range = 21.09 mm to 208.33 mm). Two QTL were identified for MW, on chromosomes two and four, respectively. Together, these QTL explain 16.8% of the phenotypic variation, and had an average additive effect of -0.329, indicating that *S. bicolor* alleles negatively influenced MW. Of the 727 genes located within these two QTL, candidate genes involved in the drought response were associated with shoot growth and development, hormonal responses (abscisic acid, jasmonic acid, salicylic acid, ethylene, auxin, gibberellin),

hormone-mediated signaling pathways, root morphogenesis and development, responses to salt, osmotic, and heat stresses, water deprivation, water channel activity, and xylem development (**Table S4**).

Maximum Root Length (i.e. Depth)

In control plants, the average maximum depth of the root system was 323.51 mm (range = 215.55 mm to 430.25 mm). This trait was reduced by 8.42% in drought stressed plants, to an average of 296.29 mm (range = 76.51 mm to 430.33 mm). A single significant QTL, located on chromosome four, was identified in the control population. This QTL explained 13.4% of the phenotypic variation and had an additive effect of 0.195. This positive additive effect indicates that *S. bicolor* alleles positively influenced root system depth. No significant QTL were identified for root system depth in the drought population (**Table S4**).

Width-to-Depth Ratio (WDR)

Under control conditions, width-to-depth ratio (WDR) ranged from 0.085 to 0.993 (average = 0.268). In plants exposed to drought, WDR was reduced 16.9% to an average of 0.223 (0.063 to 1.263). In the drought population, two QTL for this trait were identified, one chromosome four and one on chromosome five. These QTL explained 11.52% of the phenotypic variation, and had an additive effect of −0.0005, indicating that *S. bicolor* alleles negatively influenced WDR. Of the 333 genes located within these QTL, candidate genes were associated with responses to water deprivation, osmotic, heat, and salinity stresses, root and root hair development, hormonal responses (abscisic acid, jasmonic acid, salicylic acid, ethylene, auxin), shoot development, and xylem development (**Table S4**).

Belowground Biomass (BGB)

Under control conditions, belowground biomass (BGB) ranged from 0.0301 g to 0.7383 g (average = 0.2462 g). In plants exposed to drought, BGB was reduced 58% to an average of 0.102 g (range = 0.0021 g to 0.2642 g). A single significant QTL, located on chromosome two, was identified in the control population. This QTL explained 6.5% of the phenotypic variation, and had an additive effect of 0.02403. This positive additive effect indicates that *S. bicolor* alleles positively influenced BGB. No significant QTL were identified for BGB in the drought population.

Median Root Number

In control plants, the median root number (MRN) ranged from 3 to 35 (average = 18.47). This trait was reduced by 60.1% in drought stressed plants (average = 7.36, range = 1 to 20). No significant QTL were identified for MRN in either the control of drought populations.

Average Root Diameter

Under control conditions, the average root diameter (ARD) of the root system was 1.23 mm (range = 0.22 mm to 2.92 mm). This trait was reduced by 12.73% in drought stressed plants, to

an average of 1.07 mm (range = 0.65 mm to 2.88 mm). No significant QTL were identified for ARD in either the control of drought populations.

Discussion

Categorization of *Sorghum* species and/or genotypes as drought tolerant is often based on morphological and physiological traits related to aboveground components (Serraj et al., 2004, Henderson et al., 2021, Demelash et al., 2021, Lehrer and Hawkins, in prep). Although aboveground strategies play a significant role in mitigating the drought response, belowground adjustments are equally important. Root system architecture (RSA) is a major factor contributing to moisture acquisition, and changes to RSA traits are essential under drought (Bengough et al., 2004, Demelash et al., 2021).

Since root growth requires photosynthetic assimilates that are synthesized from aboveground tissues, adjustments to root system architecture can be resource intensive (Ruan et al., 2013). Although these resources can be partitioned based on need (i.e. the limiting resource) or organism size, it has been shown that both approaches similarly impact aboveground growth (Eziz et al., 2017). Thus, the ability to enhance soil exploration under drought via modifications to RSA would facilitate drought resistance. *Sorghum* accessions that belong to the landrace durra, such as TX7000, have been shown to display aboveground phenotypes associated with drought tolerance, a byproduct of selection during domestication (Henderson et al., 2020). Therefore, it is sensible that *S. bicolor* alleles would control traits relating to RSA modification under drought due to their established control of aboveground morphology and physiology under osmotic stress (Henderson et al., 2020, Hostetler et al., 2021, Lehrer et al., in prep, Chapter 4). This premise is supported by our findings: the average negative additive effect for the QTL detected for maximum width (qMW_2.DS, qMW_4.DS) indicate that *S. bicolor* alleles were associated with a reduction in this trait. Additionally, *S. bicolor* alleles had an average negative additive effect on the QTL identified for width-to-depth ratio (qWDR_4.DS, qWDR_5.DS), suggesting that root system lateral growth is reduced in favor of downward growth. Further, there was a positive additive effect on the QTL discovered for convex area (qCA_4.DS). As convex area (CA) and belowground biomass are positively correlated (**Supplementary Figures 3A-D)**, CA is reflective of overall root growth. These results suggest that strategies corresponding with enhanced soil exploration under drought conditions are controlled by *S. bicolor* alleles and were likely a result of domestication.

Three QTL (qMW_4.DS, qWDR_4.DS, qCA_4.DS) co-localized on chromosome four, and the QTL detected for maximum depth in the control population (qDepth_4.Ctrl) overlaps with these loci (**Table 1, Figure 1**). This overlap may indicate that some of the genes within this shared region are architectural and are responsible for root growth and other developmental processes. However, the chromosomal region unique to the QTL detected in the drought population suggests there are also drought-responsive components, while the co-localization indicates that

these traits share genetic control. The drought-specific QTL on chromosome four identified in this study also co-localize with the root biomass QTL identified in this same *Sorghum* population under salinity stress (Hostetler et al., 2021). Further, similar to qCA_4.DS, there was a positive additive effect for this salt-specific QTL detected for root biomass in Hostetler et al. (2021), indicating that *S. bicolor* alleles increase this trait under both drought and salinity stress. The co-localization of the QTL described here, coupled with the positive additive effects for qCA_4.DS and the root biomass QTL in Hostetler et al. (2021), indicates the shared genetic and allelic control of belowground traits in this *Sorghum* population. Therefore, upon exposure to both drought and salinity stress, *S. bicolor* controls root system reorganization to facilitate water acquisition, further indicating that osmotic stress tolerance was a byproduct of selection during domestication.

Within the QTL on chromosome four, in the regions unique to the drought population, we identified genes associated with both above- and belowground responses to drought (**Table S4**). For example, gene products were involved in plant hormone biosynthesis and recognition, leaf senescence and morphogenesis, as well as lateral, adventitious, and overall root growth. Altogether, these findings indicate that gene products associated with enhanced water acquisition and hormone synthesis and signaling, which impact belowground phenotypes and are associated with drought resistance, are located within these three drought-specific QTL on chromosome four.

Two additional QTL identified in this study, located on chromosomes two (qMW_2.DS) and five (qWDR_5.DS), also contain genes with probable roles in the drought response, and encode: 1) pentatricopeptide repeat (PPR)-containing proteins, and 2) late embryogenesis abundant-like (LEA) proteins (**Table S4**). PPR-containing proteins play a role in plant developmental processes and are also involved in various abiotic stress responses (Chen et al., 2018). For example, a gene encoding a PPR-containing protein in *Sorghum* (Sobic.003G380100) was found to be upregulated in response to heat and combined heat and drought stresses (Johnson et al., 2014). Additionally, the *Sorghum* gene Sobic.004G282000 contains a PPR repeat that is highly homologous to several PPR-containing proteins in *Arabidopsis* that are involved in RNA modification (Ortiz and Salas-Fernandez, 2021). A mutation in this gene, *SLO2* (At2g13600), resulted in hypersensitivity to abscisic acid (ABA), accumulation of reactive oxygen species, and increased drought tolerance (Zhu et al., 2014). Further, the *Arabidopsis* gene SOAR1, another PPR-containing protein, was found to be involved in ABA signaling and tolerance to drought, salinity, and cold stresses (Jiang et al., 2015).

The interplay between the function of PPR-containing proteins and the functions of the genes identified in the QTL on chromosome four, specifically as it relates to hormone synthesis and responsiveness, emphasize the role of long-distance signaling in the drought response. This significance is further supported by: 1) the identification of genes associated with LEAs in the QTL on chromosomes two and five, and 2) the functions and inducibility of the LEA protein

genes themselves. Although they have a wide variety of functions, LEA proteins are mainly involved in the stabilization of membranes and proteins, often acting as molecular chaperones (Tunnacliffe and Wise, 2007). Additionally, Blackman et al. (1995) showed that LEA protein gene expression was inducible upon ABA exposure, and this expression improved cell integrity following desiccation stress (Blackman et al., 1995, Tunnacliffe and Wise, 2007). LEA protein gene expression is also induced by drought and salinity stresses (Tunnacliffe and Wise, 2007). The identification of genes involved in plant hormone biosynthesis and signaling, which are specific to the drought population, in combination with the genes induced by these hormones (i.e. LEAs), emphasizes the major role of fine-tuned and cascading hormone signaling under drought conditions.

Conclusions

The QTL detected for the RSA traits in the drought population in this study suggest that hormone synthesis and signaling play important roles in the drought response. In addition to mitigating drought stress through facilitating communication between the shoots and the roots, plant hormones also induce physiological processes and the expression of putative genes involved in drought resistance. More broadly, the co-localization of the QTL detected for RSA traits on chromosome four in this study (qMW_4.DS, qWDR_4.DS, qCA_4.DS) with the salt-stress associated root biomass QTL detected in Hostetler et al. (2021) reflects the shared genetic and allelic control of root architectural and biomass traits under osmotic stress, which are positively influenced by *S. bicolor*. As such, the enhanced water uptake associated with resistance to both drought and salinity stresses is likely a result of domestication and improvement.

References:

Bengough AG, Gordon DC, Al-Menaie H, Ellis RP, Allan D, Keith R, Thomas WTB, Forster BP. 2004. Gel observation chamber for rapid screening of root traits in cereal seedlings. Plant and Soil **262**, 63-70.

Blackman SA, Obendorf RL, Leopold AC. 1995. Desiccation tolerance in developing soybean seeds: The role of stress proteins. Physiologia Plantarum **93**, 630-638.

Brim CA. 1966. A Modified Pedigree Method of Selection in Soybeans ¹. Crop Science **6**, 220-220.

Chen G, Zou Y, Hu J, Ding Y. 2018. Genome-wide analysis of the rice PPR gene family and their expression profiles under different stress treatments. BMC genomics **19**, 720.

Chen X, Wu Q, Gao Y, Zhang J, Wang Y, Zhang R, Zhou Y, Xiao M, Xu W, Huang R. 2020. The Role of Deep Roots in Sorghum Yield Production under Drought Conditions. Agronomy **10**, 611.

Demelash H, Tadesse T, Menamo T, Menzir A. 2021. Determination of root system architecture variation of drought adapted sorghum genotypes using high throughput root phenotyping. Rhizosphere **19**, 100370.

Evans J, McCormick RF, Morishige D, Olson SN, Weers B, Hilley J, Klein P, Rooney W, Mullet J. 2013. Extensive variation in the density and distribution of DNA polymorphism in sorghum genomes. PloS One **8**, e79192.

Eziz A, Yan Z, Tian D, Han W, Tang Z, Fang J. 2017. Drought effect on plant biomass allocation: A meta-analysis. Ecology and Evolution **7**, 11002-11010.

Gewin V. 2010. Food: An underground revolution. Nature **466**, 552-553.

Govindarajulu R, Hostetler AN, Xiao Y, *et al.* 2021. Integration of high-density genetic mapping with transcriptome analysis uncovers numerous agronomic QTL and reveals candidate genes for the control of tillering in sorghum (M Hufford, Ed.). G3 Genes|Genomes|Genetics **11**, jkab024.

Hammer GL, Dong Z, McLean G, Doherty A, Messina C, Schussler J, Zinselmeier C, Paszkiewicz S, Cooper M. 2009. Can Changes in Canopy and/or Root System Architecture Explain Historical Maize Yield Trends in the U.S. Corn Belt? Crop Science **49**, 299-312.

Henderson AN, Crim PM, Cumming JR, Hawkins JS. 2020. Phenotypic and physiological responses to salt exposure in *Sorghum* reveal diversity among domesticated landraces. American Journal of Botany **107**, 983-992.

Hostetler AN, Govindarajulu R, Hawkins JS. 2021. QTL mapping in an interspecific sorghum population uncovers candidate regulators of salinity tolerance. Plant Stress **2**, 100024.

Jiang S-C, Mei C, Liang S, Yu Y-T, Lu K, Wu Z, Wang X-F, Zhang D-P. 2015. Crucial roles of the pentatricopeptide repeat protein SOAR1 in Arabidopsis response to drought, salt and cold stresses. Plant Molecular Biology **88**, 369-385.

Johnson SM, Lim F-L, Finkler A, Fromm H, Slabas AR, Knight MR. 2014. Transcriptomic analysis of Sorghum bicolor responding to combined heat and drought stress. BMC genomics **15**, 456.

Kato Y, Abe J, Kamoshita A, Yamagishi J. 2006. Genotypic Variation in Root Growth Angle in Rice (Oryza sativa L.) and its Association with Deep Root Development in Upland Fields with Different Water Regimes. Plant and Soil **287**, 117-129.

Koevoets IT, Venema JH, Elzenga JTheoM, Testerink C. 2016. Roots Withstanding their Environment: Exploiting Root System Architecture Responses to Abiotic Stress to Improve Crop Tolerance. Frontiers in Plant Science **07**.

Mace ES, Singh V, Van Oosterom EJ, Hammer GL, Hunt CH, Jordan DR. 2012. QTL for nodal root angle in sorghum (Sorghum bicolor L. Moench) co-locate with QTL for traits associated with drought adaptation. Theoretical and Applied Genetics **124**, 97-109.

Manschadi AM, Christopher J, deVoil P, Hammer GL. 2006. The role of root architectural traits in adaptation of wheat to water-limited environments. Functional Plant Biology **33**, 823.

Oksanen J, Blanchet FG, Friendly M, Kindt R, Legendre P, McGlinn D, Minchin PR, O'Hara RB, Simpson GL, Soylmos P, *et al.* 2019. *vegan: Community Ecology Package*.

Ortiz D, Salas-Fernandez MG. 2021. Dissecting the genetic control of natural variation in sorghum photosynthetic response to drought stress (J Kromdijk, Ed.). Journal of Experimental Botany, erab502.

Oyanagi A. 1994. Gravitropic response growth angle and vertical distribution of roots of wheat (Triticum aestivum L.). Plant and Soil **165**, 323-326.

Peterson B, Carl P. 2020. PerformanceAnalytics: Econometric Tools for Performance and Risk Analysis.

R Core Team. 2013. *R: A language and environment for statistical computing.* Vienna, Austria: R Foundation for Statistical Computing.

Ruan Y-L, Patrick JW, Shabala S, Slewinski TL. 2013. Uptake and regulation of resource allocation for optimal plant performance and adaptation to stress. Frontiers in Plant Science **4**.

Seethepalli A, Dhakal K, Griffiths M, Guo H, Freschet GT, York LM. 2021. RhizoVision Explorer: open-source software for root image analysis and measurement standardization (J Cahill, Ed.). AoB PLANTS **13**, plab056.

Serraj R, Krishnamurthy L, Kashiwagi J, Kumar J, Chandra S, Crouch JH. 2004. Variation in root traits of chickpea (Cicer arietinum L.) grown under terminal drought. Field Crops Research **88**, 115-127.

Singh V, van Oosterom EJ, Jordan DR, Messina CD, Cooper M, Hammer GL. 2010. Morphological and architectural development of root systems in sorghum and maize. Plant and Soil **333**, 287-299.

Snape JW, Riggs TJ. 1975. Genetical consequences of single seed descent in the breeding of self-pollinating crops. Heredity **35**, 211-219.

Tunnacliffe A, Wise MJ. 2007. The continuing conundrum of the LEA proteins. Naturwissenschaften **94**, 791-812.

Uga Y, Sugimoto K, Ogawa S, *et al.* 2013. Control of root system architecture by DEEPER ROOTING 1 increases rice yield under drought conditions. Nature Genetics **45**, 1097-1102.

Wickham H. **2016**. *ggplot2: Elegant Graphics for Data Analysis*. Verlag, New York: R Foundation for Statistical Computing.

Zhu Q, Dugardeyn J, Zhang C, *et al.* 2014. The Arabidopsis thaliana RNA Editing Factor SLO2, which Affects the Mitochondrial Electron Transport Chain, Participates in Multiple Stress and Hormone Responses. Molecular Plant **7**, 290-310.

Table 1: Summary of QTL identified in *Sorghum* RIL population under control and drought conditions, using transformed least square means. QTL were detected via Multiple QTL Mapping (MQM) in control and drought conditions. QTL are named using the following structure: q[Trait]_[Chr].[Trtmt]. PVE = percent variation explained

BGB = Belowground Biomass, **CA**= Convex Area, **MW** = Maximum Width, **WDR** = Width-to-Depth Ratio, **Ctrl** = Control, **DS** = Drought Stressed

Trait	Trtmt	QTL Name	Chr	Position (cM)	Bin (Max LOD)	LOD Score	p-value	PVE (%)	Additive Effect	Start (Mb)	Peak (Mb)	End (Mb)
BGB	Ctrl	qBGB_2.Ctrl	2	43.69	64.56	3.41	0.027	6.5	0.0240	62.61	64.56	88.86
CA	DS	qCA_4.DS	4	92.64	69.34	4.89	0.006	11.4	726.4	67.72	69.34	68.41
MW	DS	qMW_2.DS	2	86.91	72.19	3.40	0.034	10.9	-2.98	69.80	72.19	73.37
MW	DS	qMW_4.DS	4	92.64	67.87	3.60	0.023	5.9	2.32	66.84	67.87	68.47
Depth	Ctrl	qDepth_4.Ctrl	4	89.059	67.012	5.67	0.004	13.4	0.195	66.96	67.012	68.13
WDR	DS	qWDR_4.DS	4	92.64	67.87	3.58	0.025	6.8	0.008	66.74	67.87	68.29
WDR	DS	qWDR_5.DS	5	28.51	4.03	3.12	0.044	4.7	-0.009	3.27	4.03	4.45

Figure 1: Genetic map with QTL locations from 168 $F_{3:6}$ *Sorghum* RILs. Colored vertical lines display the position of each QTL for each trait in control and drought conditions. Closed black circles within each colored vertical line represent the peak of the QTL (in centimorgans, cM). The open spaces on each chromosome reflect the removal of duplicate and/or heterozygous markers; horizontal lines represent bins used as markers. The genetic map positions (in cM) are shown in the y-axis, while the chromosome number is located across the x-axis.

BGB = Belowground Biomass, **CA** = Convex Area, **MW** = Maximum Width, **WDR** = Width-to-Depth Ratio, **Ctrl** = Control, **DS** = Drought Stressed

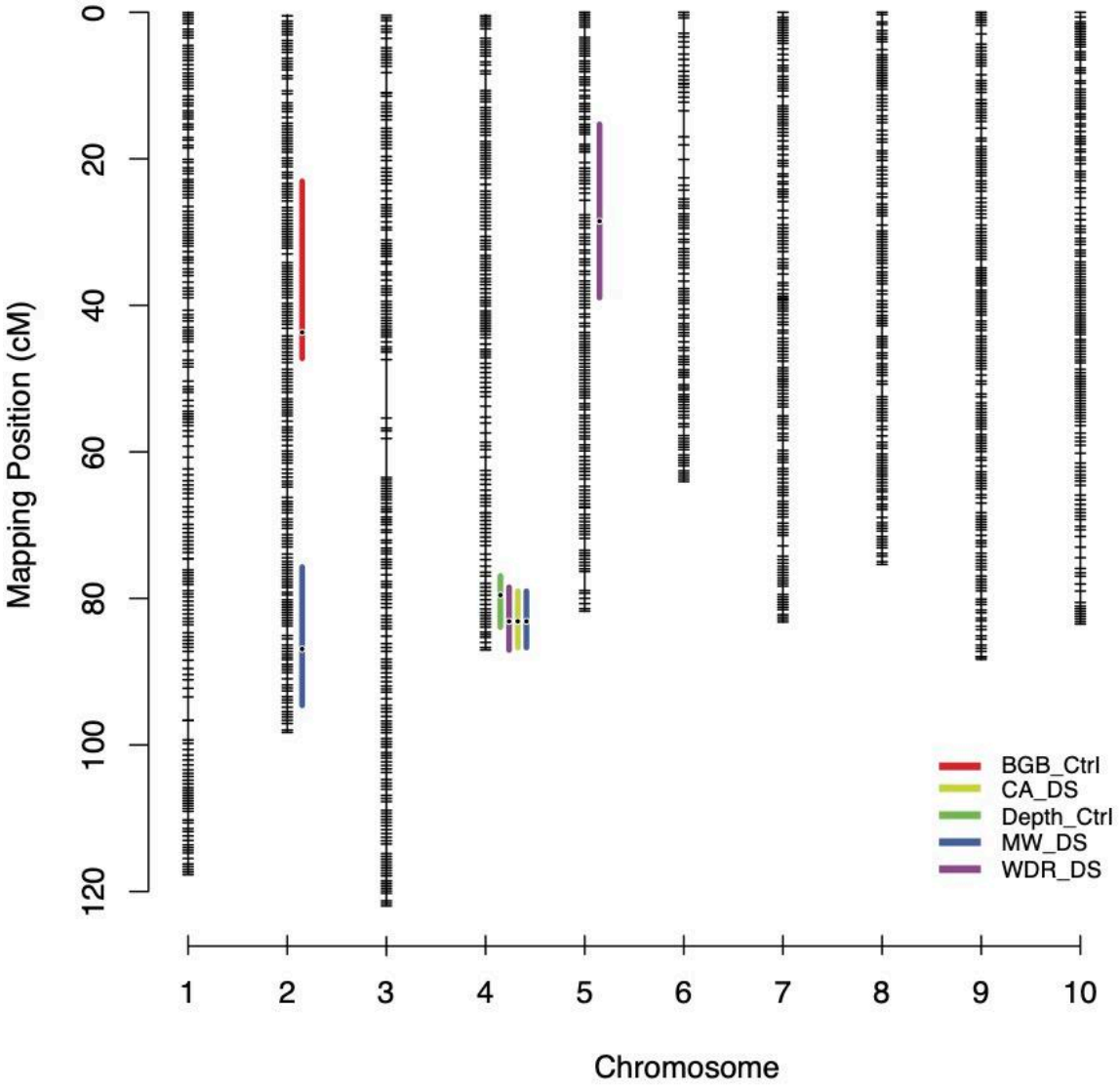

Table S1: Transformation of least square means values. Phenotypes were transformed to meet normality, and were used in the QTL analysis.

BGB = Belowground Biomass, **MW** = Maximum Width, **WDR** = Width-to-Depth Ratio, **CA** = Convex Area, **MRN** = Median Root Number, **ARD** = Average Root Diameter

Trait	Control Transformation	Shapiro-Wilk Test p-value	Drought Stressed Transformation	Shapiro-Wilk Test p-value
BGB (g)	Square Root	0.9394	None	0.5583
Depth (mm)	Square Root	0.06412	One outlier removed + 4th power	0.97251
MW (mm)	5th Root	0.971	None	0.7422
WDR	Six outliers removed	0.1756	4th root	0.07055
CA (mm^2)	Square Root	0.3043	None	0.564
MRN	None	0.971	None	0.2056
ARD (mm)	Five outliers removed	0.2634	Five outliers removed + square root	0.1852

Table S2: Genetic map summary. The genetic map consists of 10 total chromosomes and spans 899.4 cM with a total of 1991 bin markers. On average, markers are 0.4 cM apart with a maximum spacing of 8.0 cM.

Chromosome	Control Transformation	Shapiro-Wilk Test p-value	Drought Stressed Transformation	Shapiro-Wilk Test p-value
1	308	117.6	0.4	3.2
2	256	97.8	0.4	1.7
3	254	121.2	0.5	8.0
4	213	86.6	0.4	2.3
5	185	81.7	0.4	2.6
6	170	64.0	0.4	3.5
7	203	83.2	0.4	1.4
8	174	75.4	0.4	1.7
9	221	88.3	0.4	1.4
10	186	83.5	0.5	1.6
Overall	**2170**	**899.4**	**0.4**	**8.0**

Table S3: Summary statistics for phenotypic values for control and drought stressed populations. Statistical significance was assessed via Kruskal-Wallis test. S.D. = standard deviation.

BGB = Belowground Biomass, **MW** = Maximum Width, **WDR** = Width-to-Depth Ratio, **CA** = Convex Area, **MRN** = Median Root Number, **ARD** = Average Root Diameter

Trait	Control	S.D.	Drought Stressed	S.D.	Percent Change from Control (%)	Statistical Significance
BGB (g)	0.25	0.10	0.10	0.035	-58.48	***
Depth (mm)	323.51	28.00	296.29	37.031	-8.42	***
MW (mm)	86.27	26.73	64.30	18.3049	-25.47	***
WDR	0.27	0.0852	0.22	0.0846	-16.87	***
CA (mm^2)	19832.94	5794.94	12907.39	3760.48	-34.92	***
MRN	18.47	5.19	7.36	3.18	-60.13	***
ARD (mm)	1.23	0.22	1.07	1.21	-12.73	***

Table S4. Candidate genes identified for each QTL. Genes were identified within 1 logarithm of the odds (LOD) confidence interval for each QTL. Genes are organized by trait.

	QTL	Gene_ID	Sorghum_Annotation	Arabidopsis_Annotation	Rice_Annotation
1	qCA_4.DS	Sobic.004G348600	similar to Kinesin light chain–like	Tetratricopeptide repeat (TPR)–like superfamily protein	"tetratricopeptide repeat containing protein, putative, expressed"
2	qCA_4.DS	Sobic.004G348700	similar to Putative uncharacterized protein	HXXXD–type acyl–transferase family protein	"transferase family protein, putative, expressed"
3	qCA_4.DS	Sobic.004G348800	similar to LOB domain protein–like	lateral organ boundaries–domain 16	"DUF260 domain containing protein, putative, expressed"
4	qCA_4.DS	Sobic.004G349150			"tetratricopeptide repeat domain containing protein, expressed"
5	qCA_4.DS	Sobic.004G349175		"Signal transduction histidine kinase, hybrid–type, ethylene sensor"	"ethylene receptor, putative, expressed"
6	qCA_4.DS	Sobic.004G349300	similar to Receptor protein kinase–like	calmodulin–binding receptor–like cytoplasmic kinase 2	"tyrosine protein kinase domain containing protein, putative, expressed"
7	qCA_4.DS	Sobic.004G349550		MATE efflux family protein	"MATE efflux family protein, putative, expressed"
8	qCA_4.DS	Sobic.004G349900	similar to Hydroxyproline–rich glycoprotein–like	hydroxyproline–rich glycoprotein family protein (AT1G63720 Arabidopsis thaliana)	expressed protein
9	qCA_4.DS	Sobic.004G350100	similar to Putative uncharacterized protein	"Peptidase C12, ubiquitin carboxyl–terminal hydrolase 1"	"ubiquitin carboxyl–terminal hydrolase, family 1, putative, expressed"
10	qCA_4.DS	Sobic.004G350300	similar to NAC–like protein	NAC domain containing protein 2	"No apical meristem protein, putative, expressed"
11	qCA_4.DS	Sobic.004G350400	"weakly similar to Pectinesterase family protein, expressed"	Pectin lyase–like superfamily protein	"pectinesterase, putative, expressed"
12	qCA_4.DS	Sobic.004G350700	similar to Acyl–CoA binding protein–like	Galactose oxidase/kelch repeat superfamily protein	"kelch repeat protein, putative, expressed"
13	qCA_4.DS	Sobic.004G351200	similar to Aquaporin PIP1–5	plasma membrane intrinsic protein 1;4	"aquaporin protein, putative, expressed"
14	qCA_4.DS	Sobic.004G351800	PF12854//PF13041 – PPR repeat (PPR_1) // PPR repeat family (PPR_2) (1 of 18)	Tetratricopeptide repeat (TPR)–like superfamily protein	"PPR repeat containing protein, expressed"
15	qCA_4.DS	Sobic.004G352200	similar to Putative uncharacterized protein		expressed protein
16	qCA_4.DS	Sobic.004G352700	similar to Putative uncharacterized protein	NAD(P)–binding Rossmann–fold superfamily protein	"methionine adenosyltransferase regulatory beta subunit–related, putative, expressed"
17	qCA_4.DS	Sobic.004G353700	similar to Putative uncharacterized protein	Protein of unknown function (DUF789)	expressed protein
18	qCA_4.DS	Sobic.004G354000	similar to UDP–glucoronosyl/UDP–glucosyl transferase family protein–like	Tetratricopeptide repeat (TPR)–like superfamily protein	"OsSigP1 – Putative Type I Signal Peptidase homologue; employs a putative Ser/His catalytic dyad, expressed"
19	qCA_4.DS	Sobic.004G354200	similar to Putative uncharacterized protein	Endosomal targeting BRO1–like domain–containing protein	expressed protein
20	qCA_4.DS	Sobic.004G354301	PTHR12360:SF0 – PROTEIN SHUTTLE CRAFT (1 of 2)	NF–X–like 1	"NF–X1–type zinc finger protein, putative, expressed"
21	qCA_4.DS	Sobic.004G355000		sacI homology domain–containing protein / WW domain–containing protein	"SAC9, putative, expressed"
22	qCA_4.DS	Sobic.004G355200		transcription factor jumonji (jmjC) domain–containing protein	"jmjC domain containing protein, expressed"
23	qCA_4.DS	Sobic.004G355600	1.3.1.72 – Delta(24)–sterol reductase / Lanosterol Delta(24)–reductase (1 of 2)	cell elongation protein / DWARF1 / DIMINUTO (DIM)	"FAD–linked oxidoreductase protein, putative, expressed"
24	qCA_4.DS	Sobic.004G355700	similar to C2 domain–containing protein–like	Calcium–dependent lipid–binding (CaLB domain) family protein	"C2 domain containing protein, putative, expressed"
25	qCA_4.DS	Sobic.004G356300	similar to Membrane–associated salt–inducible protein–like	pentatricopeptide repeat 336	expressed protein
26	qCA_4.DS	Sobic.004G356500	similar to Protein BRICK1	"BRICK1, putative"	
27	qCA_4.DS	Sobic.004G356600	similar to Pentatricopeptide repeat–containing protein–like	Tetratricopeptide repeat (TPR)–like superfamily protein	expressed protein
28	qCA_4.DS	Sobic.004G356800	similar to Type A response regulator 3	response regulator 3	"OsRR3 type–A response regulator, expressed"
29	qCA_4.DS	Sobic.004G357100	similar to Putative uncharacterized protein	ARM repeat superfamily protein	expressed protein
30	qMW_2.DS	Sobic.002G330400	similar to Pentatricopeptide (PPR) repeat–containing protein–like protein	Pentatricopeptide repeat (PPR) superfamily protein	"pentatricopeptide, putative, expressed"
31	qMW_2.DS	Sobic.002G330500	similar to Isopentenyl pyrophosphate:dimethylallyl pyrophosphate isomerase	isopentenyl pyrophosphate:dimethylallyl pyrophosphate isomerase 2	"hydrolase, NUDIX family, domain containing protein, expressed"
32	qMW_2.DS	Sobic.002G330600	similar to Putative uncharacterized protein OJ1612_A04.102	eukaryotic translation initiation factor–related	"eukaryotic translation initiation factor–related, putative, expressed"
33	qMW_2.DS	Sobic.002G333300	weakly similar to Serine /threonine kinase precursor	receptor kinase 3	"serine/threonine–protein kinase receptor precursor, putative, expressed"
34	qMW_2.DS	Sobic.002G333400	similar to Putative S–receptor kinase KIK1	S–locus lectin protein kinase family protein	"KI domain interacting kinase 1, putative, expressed"
35	qMW_2.DS	Sobic.002G333500	similar to KI domain interacting kinase 1	S–locus lectin protein kinase family protein	"serine/threonine–protein kinase receptor precursor, putative, expressed"
36	qMW_2.DS	Sobic.002G334900	similar to S–domain receptor–like protein kinase precursor	S–locus lectin protein kinase family protein	"S–domain receptor–like protein kinase, putative, expressed"
37	qMW_2.DS	Sobic.002G336800		Tetratricopeptide repeat (TPR)–like superfamily protein	"PPR repeat domain containing protein, putative, expressed"
38	qMW_2.DS	Sobic.002G337400	similar to Putative uncharacterized protein	UDP–glucosyl transferase 88A1	"anthocyanidin 5,3–O–glucosyltransferase, putative, expressed"
39	qMW_2.DS	Sobic.002G337500	similar to Putative uncharacterized protein	UDP–glucosyl transferase 88A1	"anthocyanidin 5,3–O–glucosyltransferase, putative, expressed"
40	qMW_2.DS	Sobic.002G337700	similar to Putative uncharacterized protein	Protein kinase superfamily protein	"ABC1 family domain containing protein, putative, expressed"
41	qMW_2.DS	Sobic.002G337800	similar to Myb protein	MYB–like 102	"MYB family transcription factor, putative, expressed"
42	qMW_2.DS	Sobic.002G338000	similar to Chlorophyll a/b–binding protein CP29 precursor	light harvesting complex photosystem II	"chlorophyll A–B binding protein, putative, expressed"
43	qMW_2.DS	Sobic.002G338200	similar to Putative uncharacterized protein	PapD–like superfamily protein; Vesicle–associated protein 4–1	"MSP domain containing protein, putative, expressed"
44	qMW_2.DS	Sobic.002G338700		ARM repeat superfamily protein	"armadillo/beta–catenin repeat family protein, putative, expressed"
45	qMW_2.DS	Sobic.002G339200	Chlorophyll a–b binding protein 3, chloroplastic	light–harvesting chlorophyll B–binding protein 3	"chlorophyll A–B binding protein, putative, expressed"
46	qMW_2.DS	Sobic.002G339666	2.7.1.91 – Sphinganine kinase / Dihydrosphingosine kinase	sphingosine kinase 1	"diacylglycerol kinase, putative, expressed"
47	qMW_2.DS	Sobic.002G339900	similar to Putative uncharacterized protein	Protein of unknown function (DUF761)	"fiber expressed protein, putative, expressed"
48	qMW_2.DS	Sobic.002G340100	similar to ARF GAP–like zinc finger–containing protein–like	ARF–GAP domain 5	"GTPase–activating protein, putative, expressed"
49	qMW_2.DS	Sobic.002G340900	similar to Putative uncharacterized protein	HOPM interactor 7	"ATMIN7, putative, expressed"
50	qMW_2.DS	Sobic.002G341600	similar to Putative uncharacterized protein	alpha/beta–Hydrolases superfamily protein	"lipase, putative, expressed"
51	qMW_2.DS	Sobic.002G342100	similar to NAC transcription factor NAM–2	NAC domain containing protein 25	"no apical meristem protein, putative, expressed"
52	qMW_2.DS	Sobic.002G342800	Scarecrow–like protein 23	GRAS family transcription factor	"GRAS family transcription factor domain containing protein, expressed"
53	qMW_2.DS	Sobic.002G343500	similar to Putative uncharacterized protein	calmodulin–domain protein kinase 7	"CAMK_CAMK_like.34 – CAMK includes calcium/calmodulin depedent protein kinases, expressed"

54	qMW_2.DS	Sobic.002G344400	similar to Putative uncharacterized protein	late embryogenesis abundant protein–related / LEA protein–related	"RCLEA2 – Root cap and Late embryogenesis related family protein precursor, putative, expressed"
55	qMW_2.DS	Sobic.002G344700	similar to Remorin–like protein	Remorin family protein	"remorin, putative, expressed"
56	qMW_2.DS	Sobic.002G345300	Zinc finger AN1 and C2H2 domain–containing stress–associated protein, Stress response, Regulation of the expression of stress–associated gene	"zinc finger (C2H2 type, AN1–like) family protein"	"ZOS7–05 – C2H2 zinc finger protein, expressed"
57	qMW_2.DS	Sobic.002G347000	similar to Putative uncharacterized protein	Transducin/WD40 repeat–like superfamily protein; COMPASS–like H3K4 histone methylase component WDR5B	"WD domain, G–beta repeat domain containing protein, expressed"
58	qMW_2.DS	Sobic.002G347300	similar to Putative uncharacterized protein	Copper amine oxidase family protein; Primary amine oxidase 1	"copper methylamine oxidase precursor, putative, expressed"
59	qMW_2.DS	Sobic.002G348600	similar to Putative uncharacterized protein	RING/FYVE/PHD zinc finger superfamily protein	"zinc finger family protein, putative, expressed"
60	qMW_2.DS	Sobic.002G348900	similar to Putative uncharacterized protein	"cytochrome P450, family 87, subfamily A, polypeptide 6", CYP89A5 Arabidopsis thaliana	"cytochrome P450, putative, expressed"
61	qMW_2.DS	Sobic.002G349000	similar to Putative uncharacterized protein	Nucleotide–sugar transporter family protein; CMP–sialic acid transporter 3	"UAA transporter family domain containing protein, expressed"
62	qMW_2.DS	Sobic.002G349500	similar to Putative uncharacterized protein	leucine–rich repeat transmembrane protein kinase family protein	"inactive receptor kinase At2g26730 precursor, putative, expressed"
63	qMW_2.DS	Sobic.002G350500		related to AP2 11; Ethylene–responsive transcription factor RAP2–11	"AP2 domain containing protein, expressed"
64	qMW_2.DS	Sobic.002G351300	similar to Putative uncharacterized protein	Plant protein of unknown function (DUF946)	expressed protein
65	qMW_2.DS	Sobic.002G351801		SBP (S–ribonuclease binding protein) family protein	expressed protein
66	qMW_2.DS	Sobic.002G352700	similar to Putative uncharacterized protein	Target SNARE coiled–coil domain protein	expressed protein
67	qMW_2.DS	Sobic.002G353200	similar to Putative uncharacterized protein	Brassinosteroid signalling positive regulator (BZR1) family protein	"BES1/BZR1 homolog protein, putative, expressed"
68	qMW_2.DS	Sobic.002G353500	similar to Os06g0186900 protein	P–loop containing nucleoside triphosphate hydrolases superfamily protein; RuvB–like protein 1	"ruvB–like 2, putative, expressed"
69	qMW_2.DS	Sobic.002G353700	similar to Zinc finger protein–like protein	C2H2–like zinc finger protein; indeterminate(ID)–domain 16	"ZOS7–06 – C2H2 zinc finger protein, expressed"
70	qMW_2.DS	Sobic.002G353900	similar to Os07g0582400 protein	polyol/monosaccharide transporter 5	"transporter family protein, putative, expressed"
71	qMW_2.DS	Sobic.002G354000	similar to Os07g0582400 protein	polyol/monosaccharide transporter 5	"transporter family protein, putative, expressed"
72	qMW_2.DS	Sobic.002G354100	similar to Os07g0582400 protein	polyol/monosaccharide transporter 5	"transporter family protein, putative, expressed"
73	qMW_2.DS	Sobic.002G354200		polyol/monosaccharide transporter 5	"transporter family protein, putative, expressed"
74	qMW_2.DS	Sobic.002G354300	similar to Putative uncharacterized protein	polyol/monosaccharide transporter 5	"polyol transporter 5, putative, expressed"
75	qMW_2.DS	Sobic.002G354400	weakly similar to Putative uncharacterized protein	polyol/monosaccharide transporter 5	"polyol transporter 5, putative, expressed"
76	qMW_2.DS	Sobic.002G354600	similar to Putative uncharacterized protein OJ1127_E01.105	Mitochondrial transcription termination factor family protein	"mTERF family protein, expressed"
77	qMW_2.DS	Sobic.002G357600	similar to Lipase (Class 3) family–like protein	alpha/beta–Hydrolases superfamily protein	"lipase class 3 family protein, putative, expressed"
78	qMW_2.DS	Sobic.002G357800	similar to Short–root protein–like	GRAS family transcription factor (SHR)	"SHR, putative, expressed"
79	qMW_2.DS	Sobic.002G357900	similar to Putative uncharacterized protein OJ1047_C01.5	Nucleotide–diphospho–sugar transferase family protein (RRA3)	expressed protein
80	qMW_2.DS	Sobic.002G358800	similar to Putative uncharacterized protein	interferon–related developmental regulator family protein / IFRD protein family	"interferon–related developmental regulator, putative, expressed"
81	qMW_2.DS	Sobic.002G359000	similar to Os07g0588200 protein	formin homolog 6	"formin, putative, expressed"
82	qMW_2.DS	Sobic.002G359100	similar to Putative uncharacterized protein	Plant protein of unknown function (DUF936); CORD2	expressed protein
83	qMW_2.DS	Sobic.002G359200	similar to Transcription factor (BHLH)–like protein	basic helix–loop–helix (bHLH) DNA–binding superfamily protein	"helix–loop–helix DNA–binding domain containing protein, expressed"
84	qMW_2.DS	Sobic.002G359300		C2H2 and C2HC zinc fingers superfamily protein	"ZOS7–07 – C2H2 zinc finger protein, expressed"
85	qMW_2.DS	Sobic.002G360100	weakly similar to Putative uncharacterized protein	zinc–finger protein 1; salt tolerance zinc finger	"ZOS3–11 – C2H2 zinc finger protein, expressed"
86	qMW_2.DS	Sobic.002G360701	weakly similar to Os09g0325700 protein	protein phosphatase 2CA; highly ABA–induced PP2C protein 2	"protein phosphatase 2C, putative, expressed"
87	qMW_2.DS	Sobic.002G361400	similar to Putative uncharacterized protein	FRIGIDA–like protein	"frigida, putative, expressed"
88	qMW_2.DS	Sobic.002G362900	similar to Putative uncharacterized protein	Protein kinase superfamily protein	"IBS1, putative, expressed"
89	qMW_2.DS	Sobic.002G363100		eukaryotic elongation factor 5A–1	"eukaryotic translation initiation factor 5A, putative, expressed"
90	qMW_2.DS	Sobic.002G363901		NDR1/HIN1–like 25; Late embryogenesis abundant (LEA) hydroxyproline–rich glycoprotein family	"harpin–induced protein 1 domain containing protein, expressed"
91	qMW_2.DS	Sobic.002G366000	similar to Os07g0600700 protein	plasmodesmata callose–binding protein 3	"X8 domain containing protein, expressed"
92	qMW_2.DS	Sobic.002G366800	weakly similar to Os07g0602600 protein	glycine–rich RNA–binding protein 3	"RNA recognition motif containing protein, putative, expressed"
93	qMW_2.DS	Sobic.002G366900	similar to Putative receptor–like protein kinase	receptor–like protein kinase 2	"receptor–like protein kinase precursor, putative, expressed"
94	qMW_2.DS	Sobic.002G367000	similar to Putative glycerophosphoryl diester phosphodiesterase	PLC–like phosphodiesterases superfamily protein	"glycerophosphoryl diester phosphodiesterase family protein, putative, expressed"
95	qMW_2.DS	Sobic.002G367100	similar to Putative uncharacterized protein OSJNBb0018H10.21	ABI five binding protein 2	"protein of unknown function DUF1675 domain containing protein, expressed"
96	qMW_2.DS	Sobic.002G367400	similar to Os07g0603600 protein	methyl esterase 11	"esterase, putative, expressed"
97	qMW_2.DS	Sobic.002G367900	similar to Putative uncharacterized protein	Eukaryotic aspartyl protease family protein	"aspartic proteinase nepenthesin precursor, putative, expressed"
98	qMW_2.DS	Sobic.002G369800	similar to Putative transcription factor	"nuclear factor Y, subunit B3"	"histone–like transcription factor and archaeal histone, putative, expressed"
99	qMW_2.DS	Sobic.002G370300		Pectin lyase–like superfamily protein	"pectinesterase, putative, expressed"
100	qMW_2.DS	Sobic.002G370900	similar to Putative membrane protein	alpha/beta–Hydrolases superfamily protein (WAV2)	"OsPOP16 – Putative Prolyl Oligopeptidase homologue, expressed"
101	qMW_2.DS	Sobic.002G371000	similar to Putative nucleic acid binding protein	alfin–like 5	"PHD finger protein, putative, expressed"
102	qMW_2.DS	Sobic.002G372300		RELA/SPOT homolog 2	"HD domain containing protein, putative, expressed"
103	qMW_2.DS	Sobic.002G372300		RELA/SPOT homolog 3	"HD domain containing protein, putative, expressed"
104	qMW_2.DS	Sobic.002G372700	similar to Putative ES2 protein	DGCR14–related	"DGCR14, putative, expressed"
105	qMW_2.DS	Sobic.002G373200		strictosidine synthase–like 5/Calcium–dependent phosphotriesterase superfamily protein	"strictosidine synthase, putative, expressed"
106	qMW_2.DS	Sobic.002G373600	similar to Putative uncharacterized protein	inter–alpha–trypsin inhibitor heavy chain–related	"von Willebrand factor type A domain containing protein, expressed"
107	qMW_2.DS	Sobic.002G373800	similar to Elongation factor 1–delta 1	Translation elongation factor EF1B/ribosomal protein S6 family protein	"elongation factor protein, putative, expressed"

108	qMW_2.DS	Sobic.002G374900	similar to Putative uncharacterized protein	40s ribosomal protein SA B	"ribosomal protein S2, putative, expressed"
109	qMW_2.DS	Sobic.002G375100	similar to Putative uncharacterized protein	40s ribosomal protein SA B	"ribosomal protein S2, putative, expressed"
110	qMW_2.DS	Sobic.002G375400	weakly similar to EREB–like protein	Integrase–type DNA–binding superfamily protein; ethylene response factor	"AP2 domain containing protein, expressed"
111	qMW_2.DS	Sobic.002G375900	similar to Putative glycerophosphoryl diester phosphodiesterase 2	PLC–like phosphodiesterase family protein	"glycerophosphoryl diester phosphodiesterase family protein, putative, expressed"
112	qMW_2.DS	Sobic.002G375900	similar to Putative glycerophosphoryl diester phosphodiesterase 2	SHV3–like 1	"glycerophosphoryl diester phosphodiesterase family protein, putative, expressed"
113	qMW_2.DS	Sobic.002G376100	similar to Leucine–rich repeat transmembrane protein kinase 1–like protein	STRUBBELIG–receptor family 6	"STRUBBELIG–RECEPTOR FAMILY 6 precursor, putative, expressed"
114	qMW_4.DS	Sobic.004G336500		AUX/IAA transcriptional regulator family protein	"OsIAA9 – Auxin–responsive Aux/IAA gene family member, expressed"
115	qMW_4.DS	Sobic.004G336700	similar to Putative SPATULA	basic helix–loop–helix (bHLH) DNA–binding superfamily protein; phytochrome interacting factor 3	"helix–loop–helix DNA–binding domain containing protein, expressed"
116	qMW_4.DS	Sobic.004G337800	similar to Putative uncharacterized protein	"UDP–glucose:glycoprotein glucosyltransferases;transferases, transferring hexosyl groups;transferases, transferring glycosyl groups"	"UDP–glucose glycoprotein glucosyltransferase 1 precursor, putative, expressed"
117	qMW_4.DS	Sobic.004G337925		Zinc finger (C3HC4–type RING finger) family protein	"zinc finger family protein, putative, expressed"
118	qMW_4.DS	Sobic.004G338400	similar to Putative uncharacterized protein	LIGHT–DEPENDENT SHORT HYPOCOTYLS–like protein (DUF640)	"DUF640 domain containing protein, putative, expressed"
119	qMW_4.DS	Sobic.004G339300	similar to Putative uncharacterized protein	P–loop containing nucleoside triphosphate hydrolases superfamily protein	"ABC transporter, ATP–binding protein, putative, expressed"
120	qMW_4.DS	Sobic.004G339600	similar to Ankyrin repeat protein–like	Ankyrin repeat family protein	"ankyrin repeat domain containing protein, expressed"
121	qMW_4.DS	Sobic.004G340100		Octicosapeptide/Phox/Bem1p family protein	"PB1 domain containing protein, expressed"
122	qMW_4.DS	Sobic.004G340200	similar to Cinnamoyl CoA reductase	cinnamoyl coa reductase 1	"dehydrogenase, putative, expressed"
123	qMW_4.DS	Sobic.004G340300	similar to Cinnamoyl CoA reductase	cinnamoyl coa reductase 1	"dehydrogenase, putative, expressed"
124	qMW_4.DS	Sobic.004G341900		phospholipid sterol acyl transferase 1	"lecithine cholesterol acyltransferase, putative, expressed"
125	qMW_4.DS	Sobic.004G342000	similar to Putative uncharacterized protein	Fatty acid hydroxylase superfamily	"WAX2, putative, expressed"
126	qMW_4.DS	Sobic.004G343200	similar to Alcohol dehydrogenase class–3 (EC 1.1.1.1) (Alcohol dehydrogenase class–III) (S–(hydroxymethyl)glutathione dehydrogenase)	GroES–like zinc–binding dehydrogenase family protein	"dehydrogenase, putative, expressed"
127	qMW_4.DS	Sobic.004G343500		Peptidase S41 family protein	"OsCttP2 – Putative C–terminal processing peptidase homologue, expressed"
128	qMW_4.DS	Sobic.004G343700	similar to Putative receptor protein kinase PERK1	Protein kinase superfamily protein	"serine/threonine–protein kinase, putative, expressed"
129	qMW_4.DS	Sobic.004G344100	similar to Putative uncharacterized protein	GDSL–like Lipase/Acylhydrolase superfamily protein; Li–tolerant lipase 1 (LTL1)	"GDSL–like lipase/acylhydrolase, putative, expressed"
130	qMW_4.DS	Sobic.004G344600	similar to ABC1–like	Protein kinase superfamily protein	" ELMO/CED–12 family protein, putative, expressed"
131	qMW_4.DS	Sobic.004G344901		myosin XI B	"Myosin head domain containing protein, expressed"
132	qMW_4.DS	Sobic.004G345600	similar to Auxin–responsive protein IAA10	auxin–induced protein 13	"OsIAA10 – Auxin–responsive Aux/IAA gene family member, expressed"
133	qMW_4.DS	Sobic.004G345800	"similar to Chromosome chr5 scaffold_2, whole genome shotgun sequence"	peroxisomal 3–ketoacyl–CoA thiolase 3 (PED1/PKT3)	"3–ketoacyl–CoA thiolase, peroxisomal precursor, putative, expressed"
134	qMW_4.DS	Sobic.004G346000	similar to Os02g0817900 protein	"cytochrome P450, family 97, subfamily A, polypeptide 3"	"cytochrome P450, putative, expressed"
135	qMW_4.DS	Sobic.004G346200	similar to Putative uncharacterized protein	SLOW GROWTH 1; Pentatricopeptide repeat (PPR) superfamily protein	"tetratricopeptide–like helical, putative, expressed"
136	qMW_4.DS	Sobic.004G347600		vacuolar ATP synthase subunit H family protein	"vacuolar ATP synthase subunit H, putative, expressed"
137	qMW_4.DS	Sobic.004G348700	similar to Putative uncharacterized protein	HXXXD–type acyl–transferase family protein	"transferase family protein, putative, expressed"
138	qMW_4.DS	Sobic.004G348800	similar to LOB domain protein–like	lateral organ boundaries–domain 16	"DUF260 domain containing protein, putative, expressed"
139	qMW_4.DS	Sobic.004G349175		"Signal transduction histidine kinase, hybrid–type, ethylene sensor"	"ethylene receptor, putative, expressed"
140	qMW_4.DS	Sobic.004G349900	similar to Hydroxyproline–rich glycoprotein–like	hydroxyproline–rich glycoprotein family protein	expressed protein
141	qMW_4.DS	Sobic.004G350100	similar to Putative uncharacterized protein	"Peptidase C12, ubiquitin carboxyl–terminal hydrolase 1"	"ubiquitin carboxyl–terminal hydrolase, family 1, putative, expressed"
142	qMW_4.DS	Sobic.004G350300	similar to NAC–like protein	NAC domain containing protein 2	"No apical meristem protein, putative, expressed"
143	qMW_4.DS	Sobic.004G350700	similar to Acyl–CoA binding protein–like	Galactose oxidase/kelch repeat superfamily protein	"kelch repeat protein, putative, expressed"
144	qMW_4.DS	Sobic.004G351100	similar to Os02g0823000 protein	SIGNAL PEPTIDE PEPTIDASE–LIKE 2	"signal peptide peptidase–like 2B, putative, expressed"
145	qMW_4.DS	Sobic.004G351200	similar to Aquaporin PIP1–5	plasma membrane intrinsic protein 1;4	"aquaporin protein, putative, expressed"
146	qMW_4.DS	Sobic.004G351800	PF12854//PF13041 – PPR repeat (PPR_1) // PPR repeat family (PPR_2)	Tetratricopeptide repeat (TPR)–like superfamily protein	"PPR repeat containing protein, expressed"
147	qMW_4.DS	Sobic.004G352301		Remorin family protein	"remorin C–terminal domain containing protein, putative, expressed"
148	qMW_4.DS	Sobic.004G352500	similar to Os04g0137500 protein	vacuolar ATPase subunit F family protein	"vacuolar ATP synthase subunit F, putative, expressed"
149	qMW_4.DS	Sobic.004G353700	similar to Putative uncharacterized protein	Protein of unknown function (DUF789)	expressed protein
150	qMW_4.DS	Sobic.004G354200	similar to Putative uncharacterized protein	Endosomal targeting BRO1–like domain–containing protein	expressed protein
151	qMW_4.DS	Sobic.004G354301	PTHR12360:SF0 – PROTEIN SHUTTLE CRAFT	NF–X–like 1	"NF–X1–type zinc finger protein, putative, expressed"
152	qMW_4.DS	Sobic.004G355000		sacI homology domain–containing protein / WW domain–containing protein	"SAC9, putative, expressed"
153	qMW_4.DS	Sobic.004G355700	similar to C2 domain–containing protein–like	Calcium–dependent lipid–binding (CaLB domain) family protein	"C2 domain containing protein, putative, expressed"
154	qMW_4.DS	Sobic.004G356500	similar to Protein BRICK1	"BRICK1, putative"	
155	qMW_4.DS	Sobic.004G356600	similar to Pentatricopeptide repeat–containing protein–like	Tetratricopeptide repeat (TPR)–like superfamily protein	expressed protein
156	qMW_4.DS	Sobic.004G357100	similar to Putative uncharacterized protein	ARM repeat superfamily protein	expressed protein
157	qMW_4.DS	Sobic.004G357200	weakly similar to Putative uncharacterized protein	CCCH–type zinc finger family protein	"zinc finger C–x8–C–x5–C–x3–H type family protein, expressed"
158	qMW_4.DS	Sobic.004G357700	similar to AGO1 homologous protein	Stabilizer of iron transporter SufD / Polynucleotidyl transferase	"PINHEAD, putative, expressed"
159	qWDR_4.DS	Sobic.004G335700	similar to Putative uncharacterized protein	S–adenosyl–L–methionine–dependent methyltransferases superfamily protein	"methyltransferase, putative, expressed"
160	qWDR_4.DS	Sobic.004G336000	similar to Putative heat shock protein dnaJ	Molecular chaperone Hsp40/DnaJ family protein	"chaperone protein dnaJ, putative, expressed"
161	qWDR_4.DS	Sobic.004G336500	PF02309 – AUX/IAA family (AUX_IAA)	AUX/IAA transcriptional regulator family protein	"OsIAA9 – Auxin–responsive Aux/IAA gene family member, expressed"

162	qWDR_4.DS	Sobic.004G337500	similar to Os02g0806400 protein	GATA transcription factor 12	"GATA zinc finger domain containing protein, expressed"
163	qWDR_4.DS	Sobic.004G337800	similar to Putative uncharacterized protein	"UDP–glucose:glycoprotein glucosyltransferases;transferases, transferring hexosyl groups;transferases, transferring glycosyl groups"	"UDP–glucose glycoprotein glucosyltransferase 1 precursor, putative, expressed"
164	qWDR_4.DS	Sobic.004G337925	PTHR10579//PTHR10579:SF50 – CALCIUM–ACTIVATED CHLORIDE CHANNEL REGULATOR	Zinc finger (C3HC4–type RING finger) family protein	"zinc finger family protein, putative, expressed"
165	qWDR_4.DS	Sobic.004G338400	similar to Putative uncharacterized protein	LIGHT–DEPENDENT SHORT HYPOCOTYLS–like protein (DUF640)	"DUF640 domain containing protein, putative, expressed"
166	qWDR_4.DS	Sobic.004G338900	PTHR23177//PTHR23177:SF28 – MKIAA1688 PROTEIN	PAK–box/P21–Rho–binding family protein; ROP–interactive CRIB motif–containing protein 5	"P21–Rho–binding domain containing protein, putative, expressed"
167	qWDR_4.DS	Sobic.004G339600	similar to Ankyrin repeat protein–like	Ankyrin repeat family protein	"ankyrin repeat domain containing protein, expressed"
168	qWDR_4.DS	Sobic.004G340100		Octicosapeptide/Phox/Bem1p family protein	"PB1 domain containing protein, expressed"
169	qWDR_4.DS	Sobic.004G340200	similar to Cinnamoyl CoA reductase	cinnamoyl coa reductase 1	"dehydrogenase, putative, expressed"
170	qWDR_4.DS	Sobic.004G340300	similar to Cinnamoyl CoA reductase	cinnamoyl coa reductase 1	"dehydrogenase, putative, expressed"
171	qWDR_4.DS	Sobic.004G341700	similar to OSIGBa0157K09–H0214G12.8 protein	LEUNIG_homolog	"transcriptional corepressor LEUNIG, putative, expressed"
172	qWDR_4.DS	Sobic.004G341900	PSAT1	phospholipid sterol acyl transferase 1	"lecithine cholesterol acyltransferase, putative, expressed"
173	qWDR_4.DS	Sobic.004G342000	similar to Putative uncharacterized protein	Fatty acid hydroxylase superfamily	"WAX2, putative, expressed"
174	qWDR_4.DS	Sobic.004G343200	similar to Alcohol dehydrogenase class–3 (EC 1.1.1.1) (Alcohol dehydrogenase class–III) (S–(hydroxymethyl)glutathione dehydrogenase)	GroES–like zinc–binding dehydrogenase family protein	"dehydrogenase, putative, expressed"
175	qWDR_4.DS	Sobic.004G343500	Carboxyl–terminal–processing peptidase 2, chloroplastic	Peptidase S41 family protein	"OsCttP2 – Putative C–terminal processing peptidase homologue, expressed"
176	qWDR_4.DS	Sobic.004G343700	similar to Putative receptor protein kinase PERK1	Protein kinase superfamily protein	"serine/threonine–protein kinase, putative, expressed"
177	qWDR_4.DS	Sobic.004G343800	similar to Putative uncharacterized protein	C2 calcium/lipid–binding plant phosphoribosyltransferase family protein	"anthranilate phosphoribosyltransferase, putative, expressed"
178	qWDR_4.DS	Sobic.004G344100	similar to Putative uncharacterized protein	GDSL–like Lipase/Acylhydrolase superfamily protein; LTL1 (Li–tolerant lipase 1)	"GDSL–like lipase/acylhydrolase, putative, expressed"
179	qWDR_4.DS	Sobic.004G344600	similar to ABC1–like	Protein kinase superfamily protein	" ELMO/CED–12 family protein, putative, expressed"
180	qWDR_4.DS	Sobic.004G344901	PTHR13140//PTHR13140:SF382 – MYOSIN	myosin XI B	"Myosin head domain containing protein, expressed"
181	qWDR_4.DS	Sobic.004G345600	similar to Auxin–responsive protein IAA10	auxin–induced protein 13	"OsIAA10 – Auxin–responsive Aux/IAA gene family member, expressed"
182	qWDR_4.DS	Sobic.004G345800	"similar to Chromosome chr5 scaffold_2, whole genome shotgun sequence"	peroxisomal 3–ketoacyl–CoA thiolase 3	"3–ketoacyl–CoA thiolase, peroxisomal precursor, putative, expressed"
183	qWDR_4.DS	Sobic.004G346000	similar to Os02g0817900 protein	"cytochrome P450, family 97, subfamily A, polypeptide 3"	"cytochrome P450, putative, expressed"
184	qWDR_4.DS	Sobic.004G347600	V–type proton ATPase subunit H	vacuolar ATP synthase subunit H family protein	"vacuolar ATP synthase subunit H, putative, expressed"
185	qWDR_4.DS	Sobic.004G347900	similar to Putative uncharacterized protein P0474F11.3	Protein kinase superfamily protein	"protein kinase APK1A, chloroplast precursor, putative, expressed"
186	qWDR_4.DS	Sobic.004G348600	similar to Kinesin light chain–like	Tetratricopeptide repeat (TPR)–like superfamily protein	"tetratricopeptide repeat containing protein, putative, expressed"
187	qWDR_4.DS	Sobic.004G348800	similar to LOB domain protein–like	lateral organ boundaries–domain 16	"DUF260 domain containing protein, putative, expressed"
188	qWDR_4.DS	Sobic.004G349175	PTHR24423//PTHR24423:SF489 – TWO–COMPONENT SENSOR HISTIDINE KINASE	"Signal transduction histidine kinase, hybrid–type, ethylene sensor"	"ethylene receptor, putative, expressed"
189	qWDR_4.DS	Sobic.004G349900	similar to Hydroxyproline–rich glycoprotein–like	hydroxyproline–rich glycoprotein family protein	expressed protein
190	qWDR_4.DS	Sobic.004G350300	similar to NAC–like protein	NAC domain containing protein 2	"No apical meristem protein, putative, expressed"
191	qWDR_4.DS	Sobic.004G351200	similar to Aquaporin PIP1–5	plasma membrane intrinsic protein 1–4; plasma membrane intrinsic protein 1C (PIP 1–3)	"aquaporin protein, putative, expressed"
192	qWDR_4.DS	Sobic.004G351800	PF12854//PF13041 – PPR repeat (PPR_1) // PPR repeat family (PPR_2)	Tetratricopeptide repeat (TPR)–like superfamily protein	"PPR repeat containing protein, expressed"
193	qWDR_4.DS	Sobic.004G352301		Remorin family protein	"remorin C–terminal domain containing protein, putative, expressed"
194	qWDR_4.DS	Sobic.004G352500	similar to Os04g0137500 protein	vacuolar ATPase subunit F family protein	"vacuolar ATP synthase subunit F, putative, expressed"
195	qWDR_4.DS	Sobic.004G353700	similar to Putative uncharacterized protein	Protein of unknown function (DUF789); plant/protein (DUF789)	expressed protein
196	qWDR_4.DS	Sobic.004G354000	similar to UDP–glucoronosyl/UDP–glucosyl transferase family protein–like	Tetratricopeptide repeat (TPR)–like superfamily protein	"OsSigP1 – Putative Type I Signal Peptidase homologue; employs a putative Ser/His catalytic dyad, expressed"
197	qWDR_4.DS	Sobic.004G354200	similar to Putative uncharacterized protein	Endosomal targeting BRO1–like domain–containing protein	expressed protein
198	qWDR_4.DS	Sobic.004G354301	PTHR12360:SF0 – PROTEIN SHUTTLE CRAFT	NF–X–like 1	"NF–X1–type zinc finger protein, putative, expressed"
199	qWDR_4.DS	Sobic.004G354600			Tetratricopeptide–like helical domain containing protein
200	qWDR_4.DS	Sobic.004G355000		sacI homology domain–containing protein / WW domain–containing protein	"SAC9, putative, expressed"
201	qWDR_5.DS	Sobic.005G036500	"similar to Second messenger–dependent protein kinase, putative"	Protein kinase superfamily protein; root hair specific 3	"AGC_PVPK_like_kin82y.1 – ACG kinases include homologs to PKA, PKG and PKC, expressed"
202	qWDR_5.DS	Sobic.005G036600	"similar to Calmodulin–binding family protein, putative, expressed"	IQ calmodulin–binding motif family protein	"calmodulin–binding protein, putative, expressed"
203	qWDR_5.DS	Sobic.005G036800	"similar to Calmodulin–binding family protein, putative, expressed"	IQ calmodulin–binding motif family protein	"calmodulin–binding protein, putative, expressed"
204	qWDR_5.DS	Sobic.005G036900		late embryogenesis abundant protein–related / LEA protein–related	"RCLEA6 – Root cap and Late embryogenesis related family protein precursor, expressed"
205	qWDR_5.DS	Sobic.005G037200	similar to Putative anthocyanin 5–aromatic acyltransferase	HXXXD–type acyl–transferase family protein	"transferase family protein, putative, expressed"
206	qWDR_5.DS	Sobic.005G038400	similar to Cen–like protein FDR1	centroradialis; PEBP (phosphatidylethanolamine–binding protein) family protein	"RCN1 Centroradialis–like1 homogous to TFL1 gene; contains Pfam profile PF01161: Phosphatidylethanolamine–binding protein, expressed"
207	qWDR_5.DS	Sobic.005G043000	"similar to Transposon protein, putative, mutator sub–class"	Double Clp–N motif–containing P–loop nucleoside triphosphate hydrolases superfamily protein	"heat shock protein–related, putative, expressed"
208	qWDR_5.DS	Sobic.005G044000	"similar to Harpin–induced protein 1 (Hin1), putative"	NDR1/HIN1–like 1	"harpin–induced protein 1 domain containing protein, expressed"
209	qWDR_5.DS	Sobic.005G044600	"similar to Pyridine nucleotide–disulphide oxidoreductase family protein, putative"	FAD/NAD(P)–binding oxidoreductase family protein	"pyridine nucleotide–disulphide oxidoreductase family protein, putative, expressed"
210	qWDR_5.DS	Sobic.005G044700		MAP kinase kinase 9	"STE_MEK_ste7_MAP2K.3 – STE kinases include homologs to sterile 7, sterile 11 and sterile 20 from yeast, expressed"
211	qWDR_5.DS	Sobic.005G045000	"similar to Digalactosyldiacylglycerol synthase 1, putative, expressed"	UDP–Glycosyltransferase superfamily protein	"digalactosyldiacylglycerol synthase, chloroplast precursor, putative, expressed"
212	qWDR_5.DS	Sobic.005G045100	similar to Expressed protein	transcription factor–related (LHW)	"helix–loop–helix DNA–binding protein, putative, expressed"
213	qWDR_5.DS	Sobic.005G046100	similar to BZIP transcriptional activator RSG–related	VIRE2–interacting protein 1 (VIP1)	"bZIP transcription factor domain containing protein, expressed"
214	qWDR_5.DS	Sobic.005G046700	similar to Cortical cell–delineating protein	Bifunctional inhibitor/lipid–transfer protein/seed storage 2S albumin superfamily protein	"LTPL141 – Protease inhibitor/seed storage/LTP family protein precursor, expressed"

Supplementary Figure 1: Root Imaging Orientations. During the destructive harvest, root systems were imaged in three orientations to adjust for any asymmetrical growth. Following extraction from pots and removal of excess growing media, root systems were placed on a black felt background and imaged (Orientation A). Root systems were then rotated 90° and imaged again (Orientation B). Lastly, root systems were spread out and imaged one last time (Orientation C).

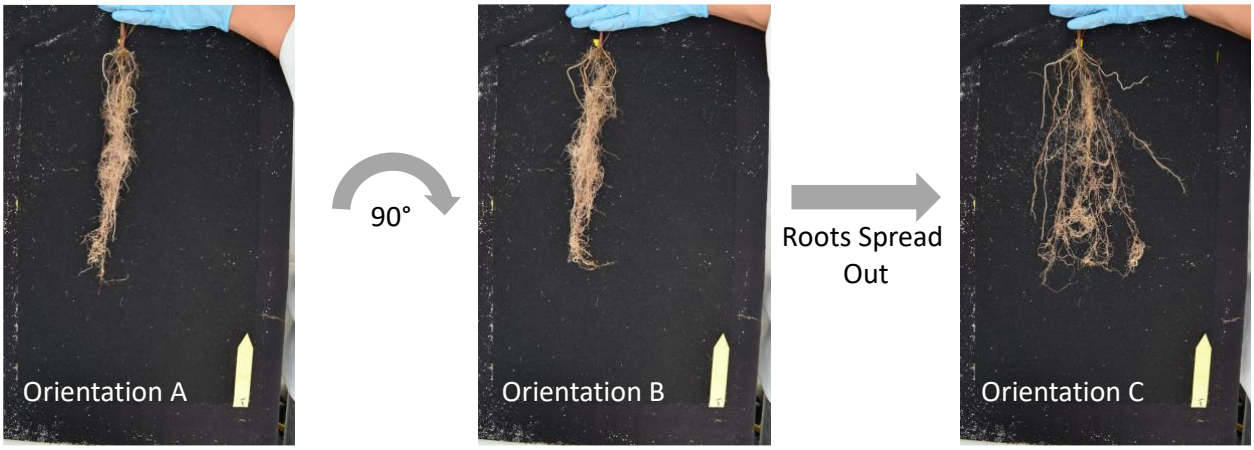

Supplementary Figure 2: Overhead view of plant pot organization. The setup consisted of forty-eight total boxes containing approximately thirty-six plants in each. Boxes were split into two groups of twenty-four, one for each treatment group (control and drought stressed); seeds for each recombinant inbred line were randomly sown in each pot.

Supplementary Figures 3A-D: Pearson correlations on raw phenotypes (**A, B**) and transformation least squared mean values (**C, D**) for the control (**A, C**) and drought (**B, D**) populations.

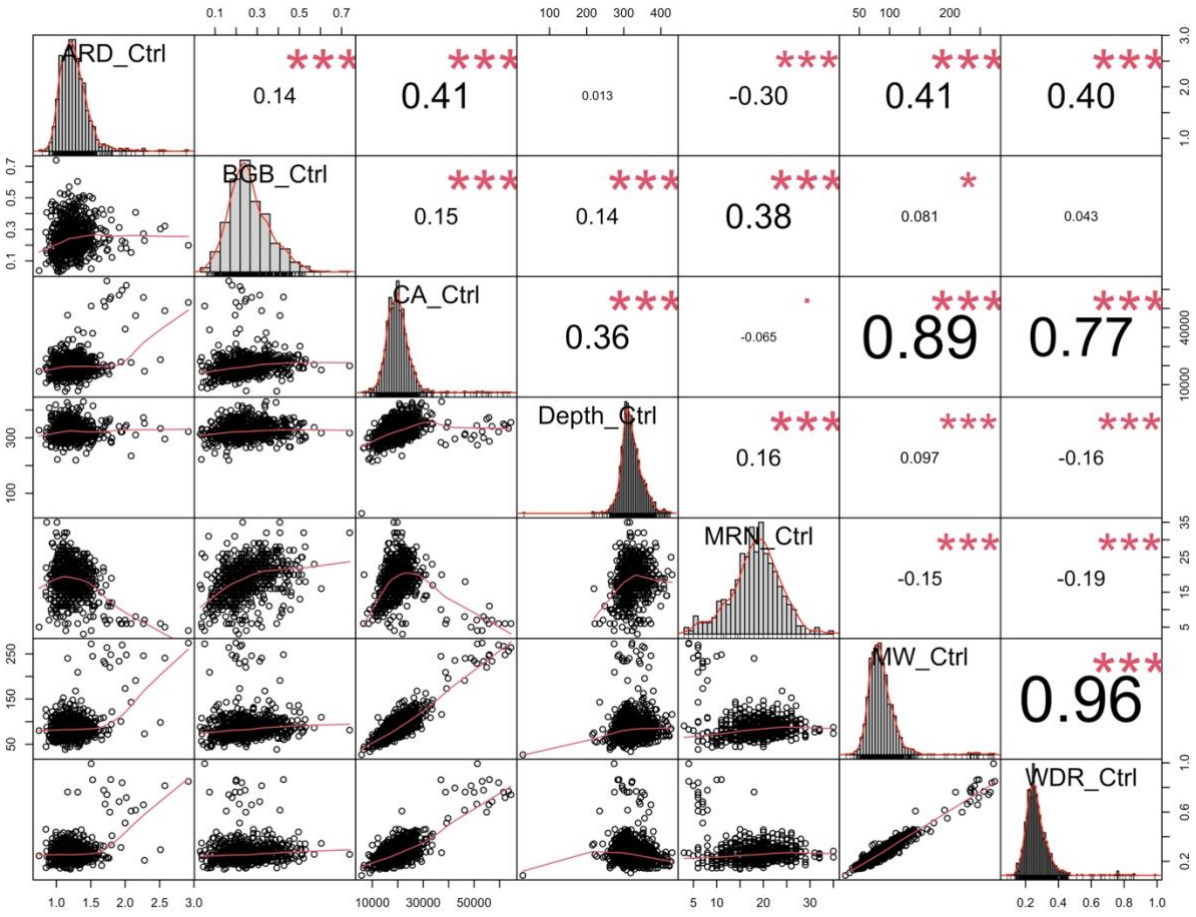

A

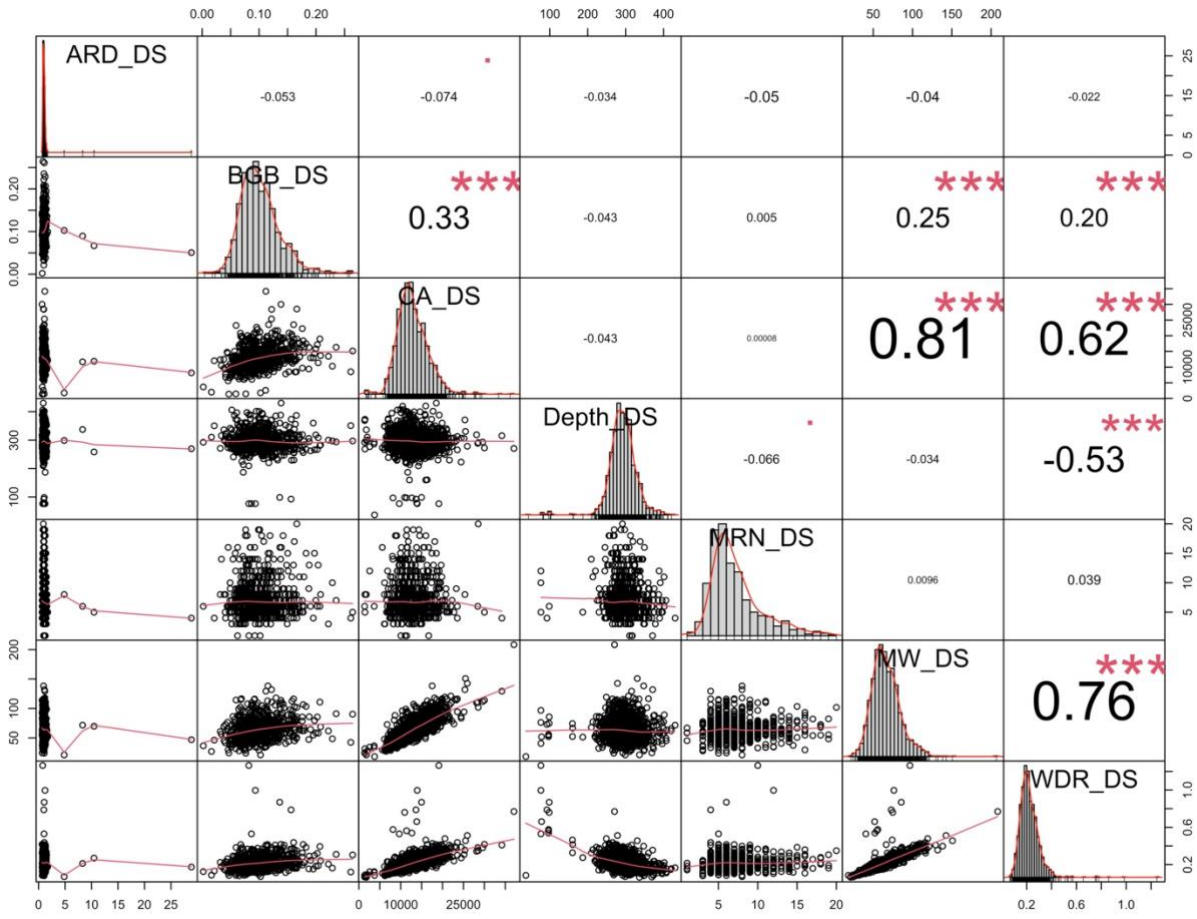
ARD_DS
BGB_DS
CA_DS
Depth_DS
MRN_DS
MW_DS
WDR_DS
-0.053
-0.074
-0.034
-0.05
-0.04
-0.022
0.33
-0.043
0.005
0.25
0.20
0.81
0.62
-0.066
-0.034
-0.53
0.0096
0.039
0.76

B

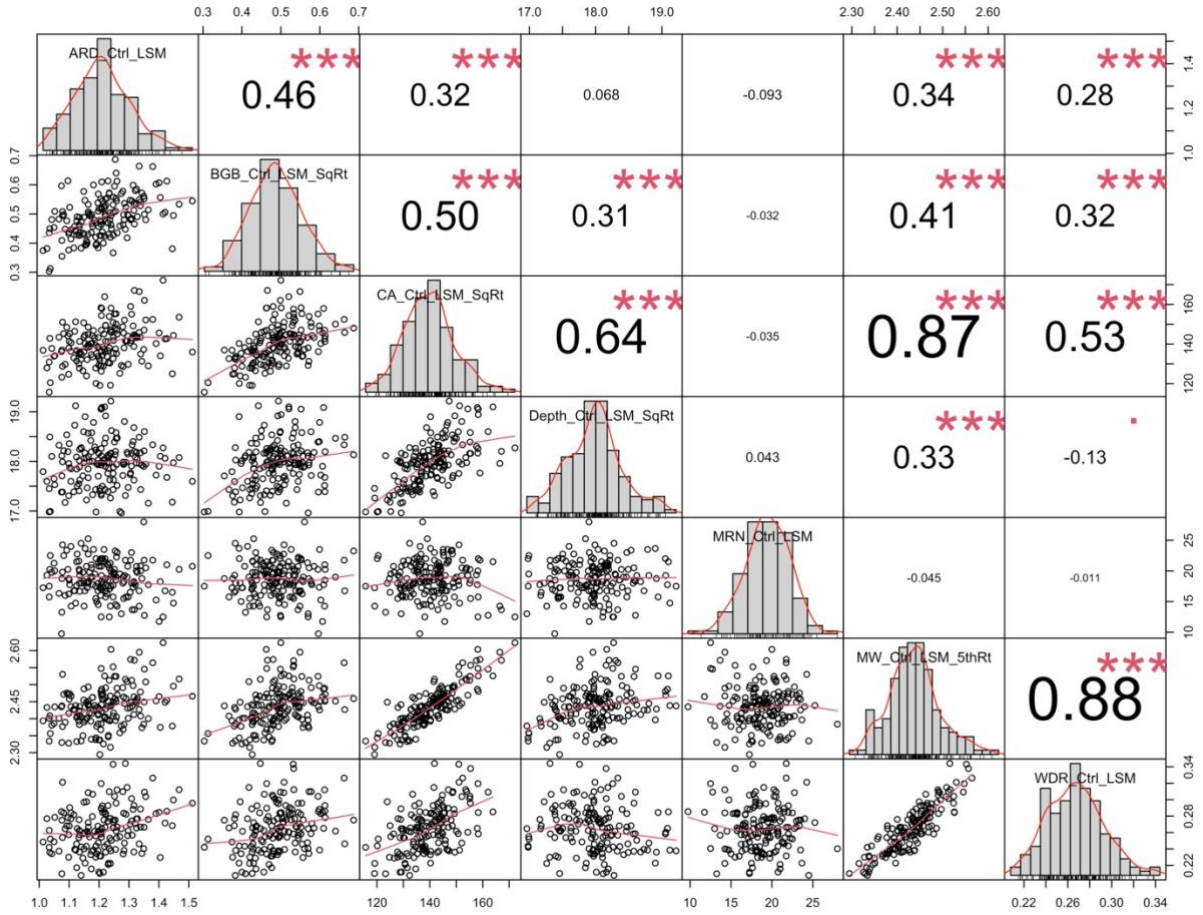
ARD_Ctrl_LSM
BGB_Ctrl_LSM_SqRt
CA_Ctrl_LSM_SqRt
Depth_Ctrl_LSM_SqRt
MRN_Ctrl_LSM
MW_Ctrl_LSM_5thRt
WDR_Ctrl_LSM
0.46
0.32
0.068
-0.093
0.34
0.28
0.50
0.31
-0.032
0.41
0.32
0.64
-0.035
0.87
0.53
0.043
0.33
-0.13
-0.045
-0.011
0.88

C

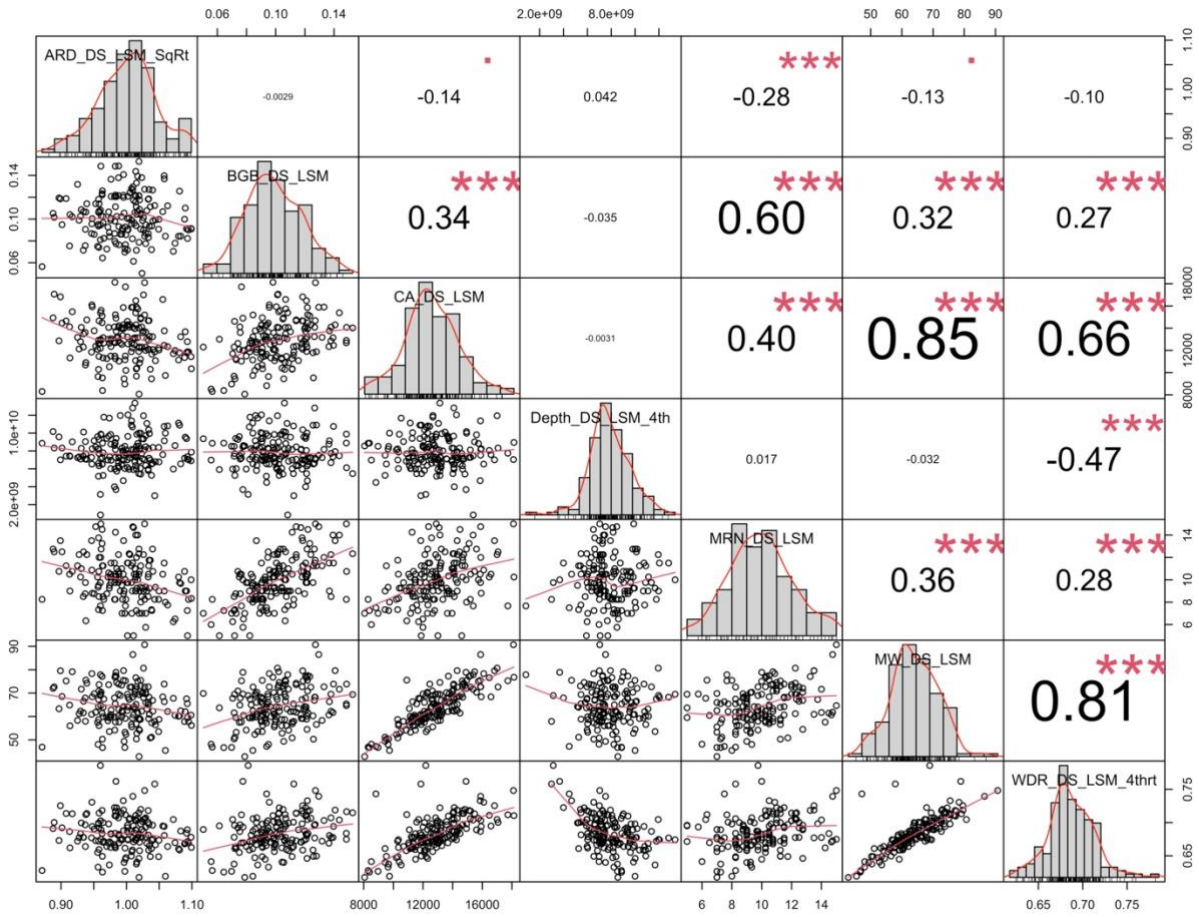
ARD_DS_LSM_SqRt
BGB_DS_LSM
CA_DS_LSM
Depth_DS_LSM_4th
MRN_DS_LSM
MW_DS_LSM
WDR_DS_LSM_4thrt
-0.14
0.042
-0.28
-0.13
-0.10
0.34
-0.035
0.60
0.32
0.27
0.40
0.85
0.66
0.017
-0.032
-0.47
0.36
0.28
0.81

D

Supplementary Figures 4A-G: Boxplots displaying average control (black) and drought stressed (blue) values for all measured belowground traits. **A**) root diameter, **B**) belowground biomass, **C**) convex area **D**) maximum width, **E**) median root number, **F**) root depth, **G**) width-to-depth-ratio.

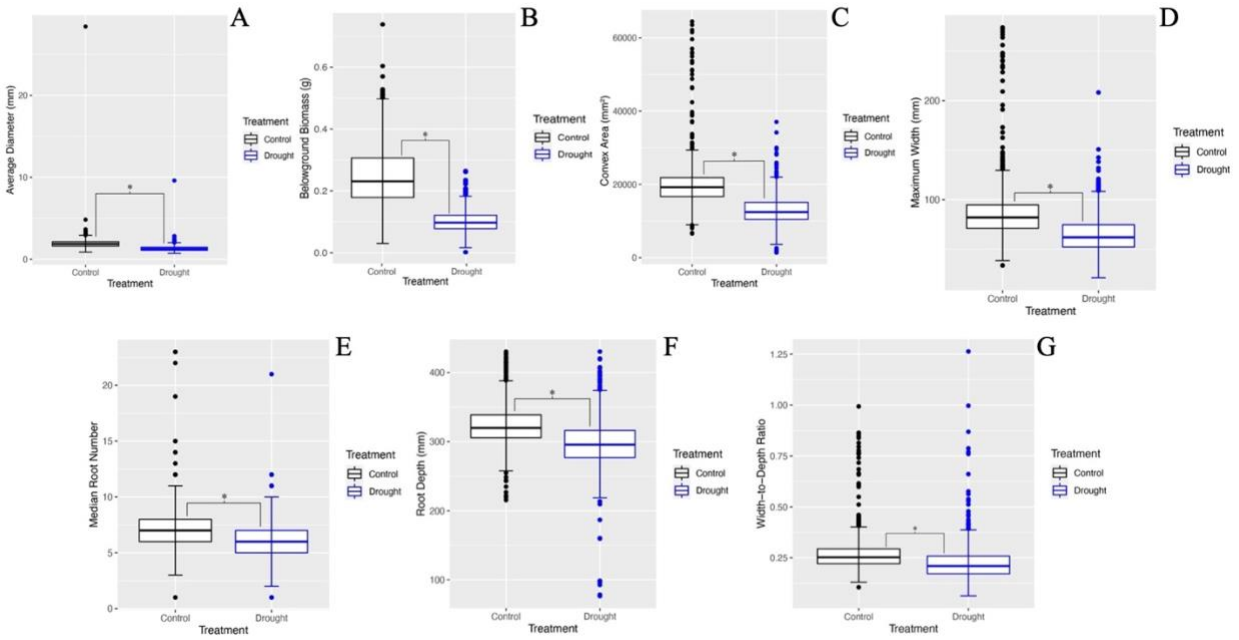

Supplementary Figure 5: Genetic map following removal of heterozygous and duplicate markers. Mapping position (in cM), is shown on the y-axis, and chromosome number is displayed across the x-axis.

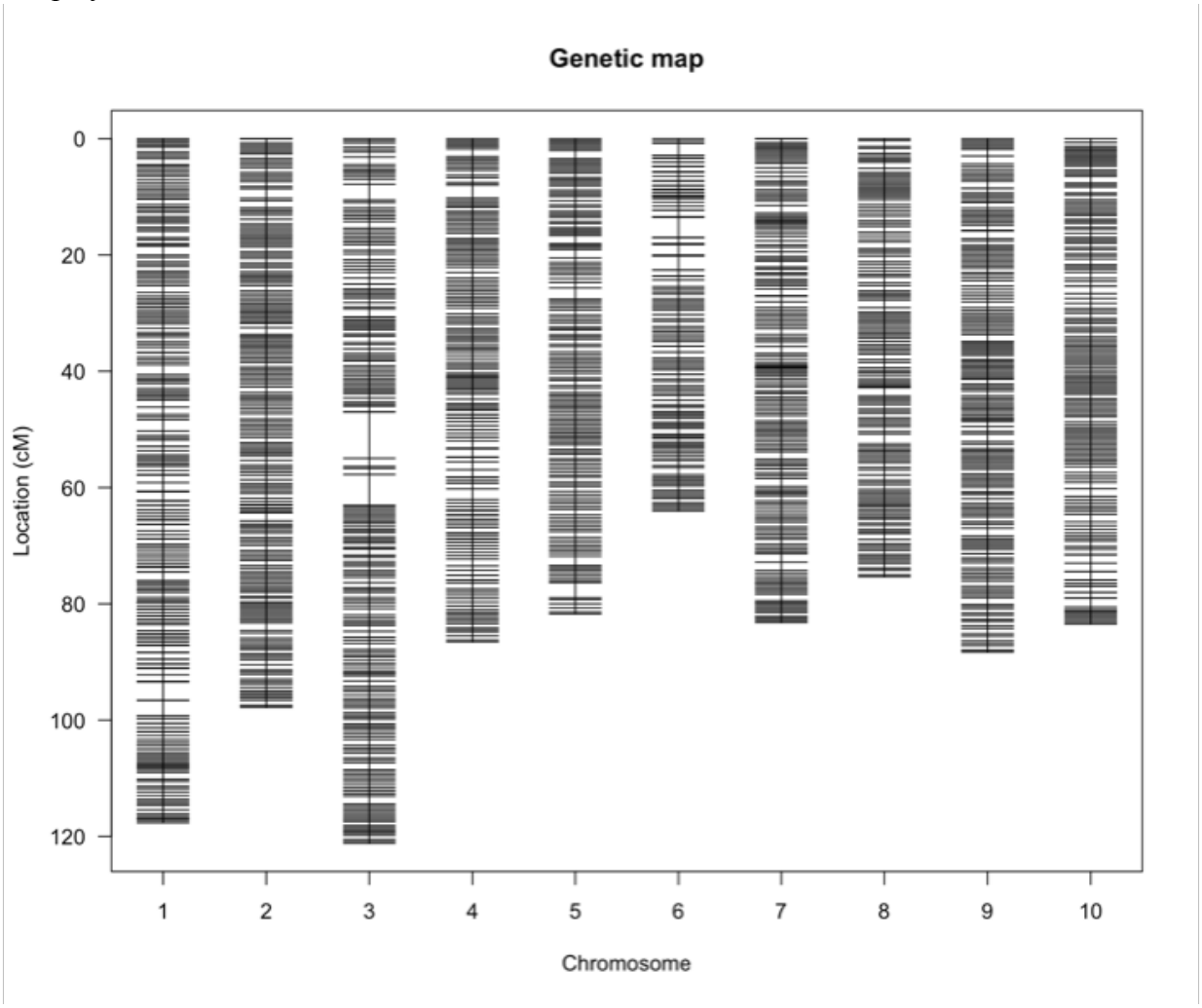

Supplementary Figures 6A-F: Comparison of root system architecture (RSA) traits in A and B orientations in the control population. RSA traits extracted from the A and B orientations from Rhizivision Explorer were compared via Kruskal-Wallis test to determine if there was any bias due to asymmetrical growth. A p-value less than 0.05 and/or small effect sizes indicated minimal positional effects. A Orientation = brown, B Orientation = orange.

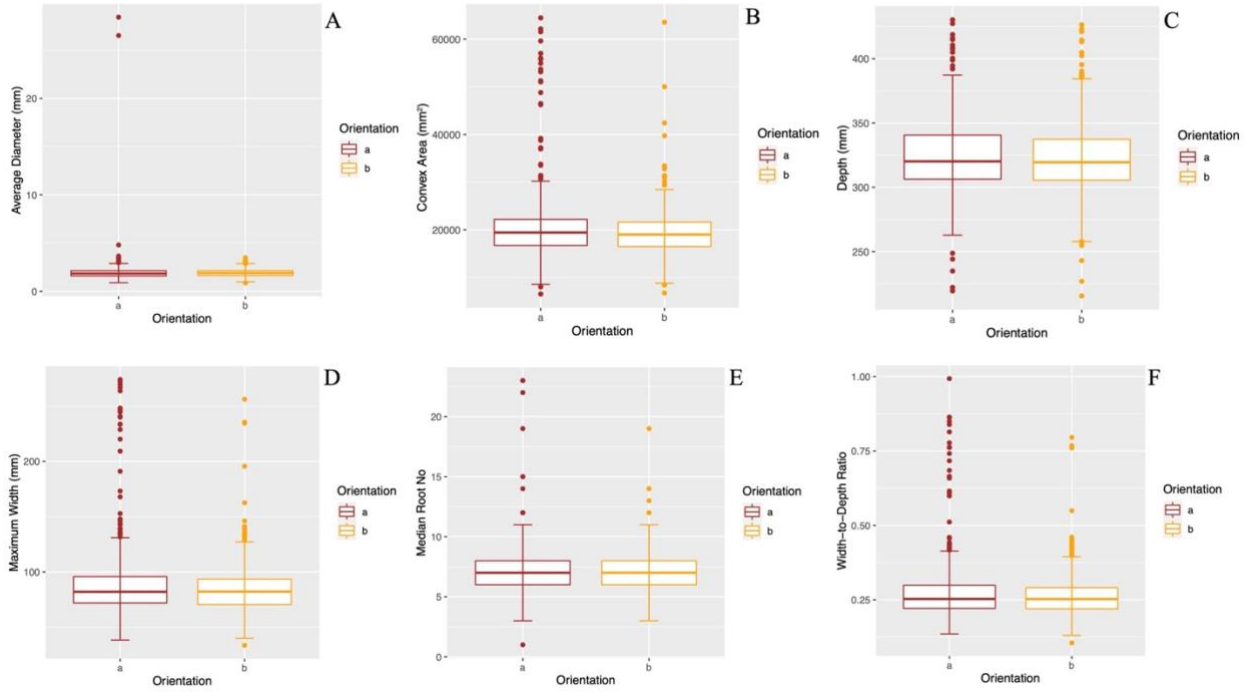

Supplementary Figures 7A-F: Comparison of root system architecture (RSA) traits in A and B orientations in the drought population. RSA traits extracted from the A and B orientations from Rhizivision Explorer were compared via Kruskal-Wallis test to determine if there was any bias due to asymmetrical growth. A p-value less than 0.05 and/or small effect sizes indicated minimal positional effects. A Orientation = blue, B Orientation = gray.

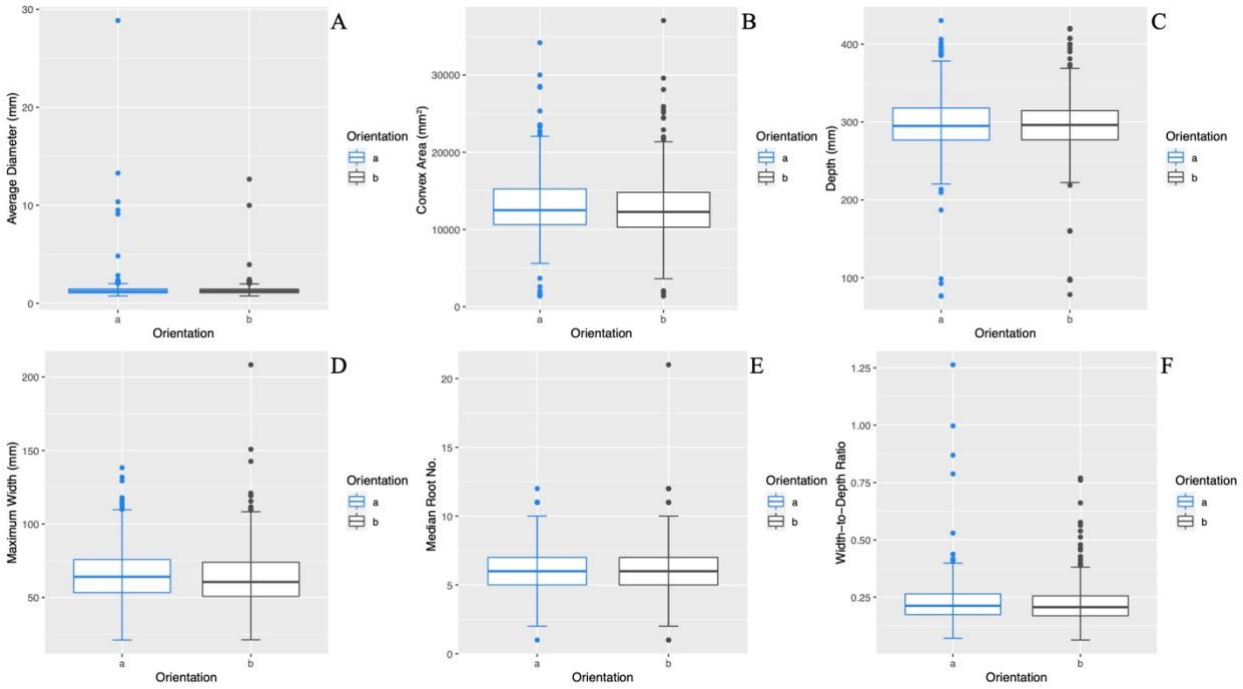

Supplementary Figure 8: Non-metric multidimensional scaling, paired with an analysis of similarity, reveals clustering of belowground traits by treatment in the A/B Orientations. Control = purple squares, Drought = black triangles.

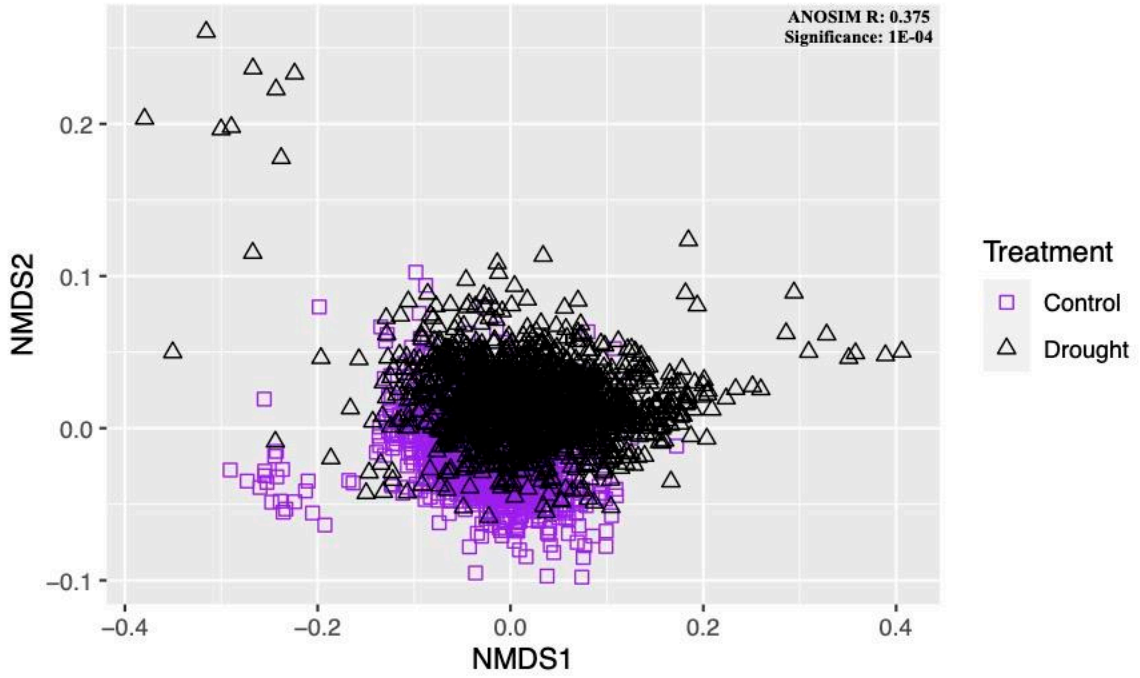

Supplementary Figure 9: Non-metric multidimensional scaling, paired with an analysis of similarity, reveals clustering of belowground traits by treatment in the C Orientation. Control = purple squares, Drought = black triangles.

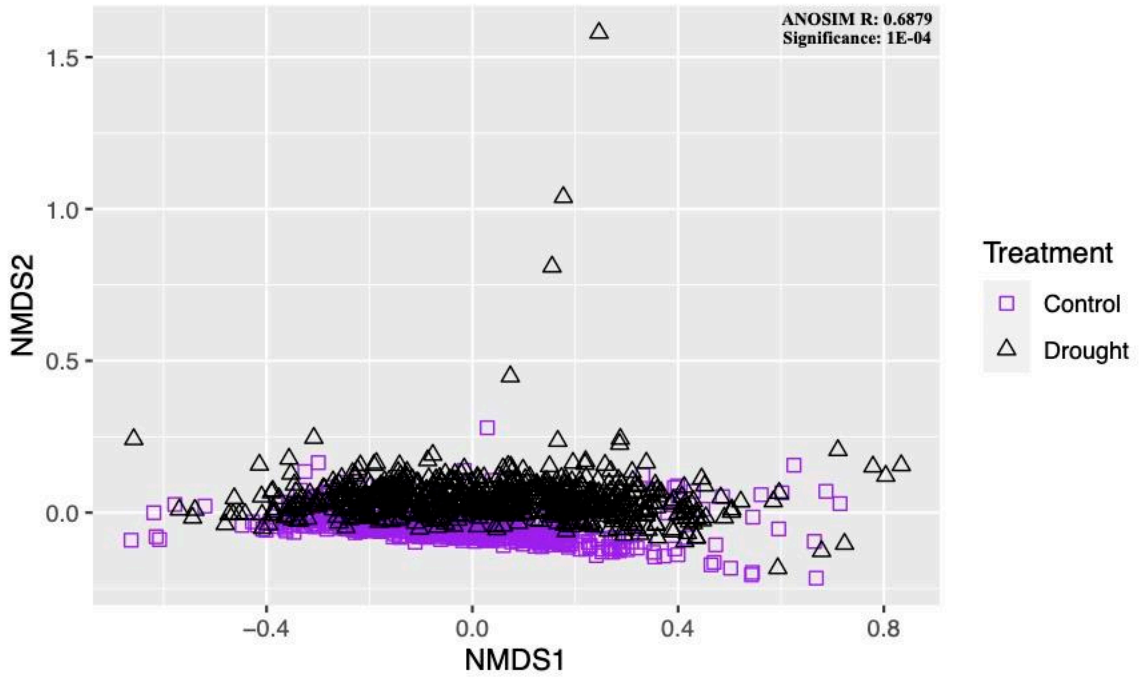

CHAPTER 6: CONCLUSIONS

Drought, having both climatic and anthropogenic origins, severely impedes plant growth and development, ultimately impacting crop productivity (Turral et al., 2011, Van Loon et al., 2016, USGCRP, 2017, Gupta et al., 2020). As reviewed in **Chapter 2**, a complex network of morphological and physiological strategies are employed in response to drought that either enhance water acquisition and/or prevent transpirational water loss, both working to maintain the plant's water status (Ali et al., 2009, Singh et al., 2010, Uga et al., 2013, Redillas et al., 2012, Borrell et al., 2014, Johnson et al., 2014, Liu et al., 2014, Uga et al., 2015, Zhang et al., 2015, Liang et al., 2016, Dinneny, 2019, Ndlovu et al., 2021). Additional physiological mechanisms, such as hormone signaling, can contribute to drought resistance by modulating growth, triggering stomatal closure, and inducing the expression of drought-responsive genes (Kalladan et al., 2017, Kundu and Gantait, 2017, McAdam and Brodribb, 2018, Goche et al., 2020).

Although drought is transient, it can be experienced multiple times throughout a growing season. To mimic these conditions in a greenhouse setting, two *Sorghum bicolor* accessions that vary in the pre- and post-flowering responses to drought were exposed to repeated and prolonged drought and rewatering, as described in **Chapter 3**. In this work, morphological and physiological traits were quantified over developmental time to identify strategies associated with long-term drought exposure, while modifications to plant vasculature were measured following this prolonged exposure. Our findings revealed that growth-related and physiological approaches both work to preserve hydraulic safety, but through different mechanisms. For example, the pre-flowering drought tolerant accession, TX7078, maintained height and transpiration rate near control levels and displayed a reduction in vascular bundle number. Additionally, decreases in height and transpiration rate occurred in the pre-flowering drought sensitive accession, BTx642; however, vascular bundle number was maintained at control levels. There were no accession-specific changes to metaxylem area. Although the proportion of height maintained was significantly different between these two accessions, TX7078 is naturally shorter compared to BTx642, under both control and drought conditions. Transpiration rate was maintained at or near control levels in TX7078, suggesting that its naturally shorter stature and hydraulic path are inherently less prone to hydraulic damage (Cochard, 2002, Tang and Boyer, 2008). In contrast, the taller height and longer hydraulic path of BTx642 make this accession more susceptible to xylem embolism. Thus, a modified transpiration rate was required in BTx642 to impede conductance between the roots and the shoots, working to minimize the risk of hydraulic damage (Tang and Boyer, 2008). Further, the maintenance of vascular bundle number in BTx642 ensured the availability of usable xylem in the event that embolism formation rendered some vessels non-functional, a redundancy not required in TX7078. Altogether, our findings emphasized the tight control of stomatal aperture that is needed to minimize xylem embolism risk when morphological and histological adaptations are insufficient.

Following the identification of the strategies associated with long-term drought exposure in Chapter 3, **Chapter 4** aimed to discover the evolutionary origin of these responses via quantitative trait loci (QTL) mapping. In this chapter, a *Sorghum* recombinant inbred line (RIL) population, generated from a cross between domesticated *S. bicolor* (TX7000 inbred) and its wild relative *S. propinquum*, was evaluated under drought stress. In addition to delineating the genetic controls of both the osmotic and ionic phases of the salt stress response, this population also provided the opportunity to explore genetic controls of drought tolerance selected during domestication (Henderson et al., 2020, Hostetler et al., 2021). Eight QTL unique to the drought population were detected for both morphological (aboveground biomass and height) and physiological (relative water content, RWC and leaf temperature) traits. The additive effects for the morphological QTL indicated that *S. bicolor* alleles enhanced aboveground biomass and reduced height under stress conditions, highlighting the impact of grain *Sorghum* varieties (i.e. TX7000) on drought-responsive phenotypes. Within these QTL, genes involved in reproductive processes were identified. Gene products involved in these processes may promote early flowering under drought, a common drought escape mechanism. The maintenance of grain yield via early flowering is a drought-adaptive strategy likely resulting from domestication. Physiologically, leaf temperature was increased by *S. bicolor* alleles in stress conditions, while RWC was increased by *S. propinquum* alleles. These allelic effects reflect the variability in belowground growth patterns between the parents of the RIL population that impact water management under drought. For example, *S. bicolor*, with a modest root system, controls transpirational water loss via induction of stomatal closure, as inferred from measurements of leaf temperature. In contrast, *S. propinquum* controls water uptake, and ultimately RWC, due to its extensive root system and enhanced water acquisition. Thus, both above- and belowground responses impact water management through different species-specific strategies. Candidate genes within these QTL, through their involvement in hormone signaling, may play roles in these physiological water regulation processes. Not only are phytohormones important through their impact on root development and water acquisition, but also through their influence on aboveground responses, such as stomatal closure. Therefore, our findings stress the roles of above- and belowground responses in regulating transpirational water loss and enhancing water uptake through species-specific approaches.

The relationship between above- and belowground traits, particularly through hormone signaling and water management as suggested in Chapter 4, encouraged the design of an experiment aimed at uncovering the genetic controls of the belowground drought response (**Chapter 5)**. Using the same *Sorghum* RIL population and experimental design, five QTL unique to drought-responsive traits were detected for root system architecture (RSA). The QTL detected for convex area, maximum root system width, and width-to-depth ratio co-localized with a root biomass QTL detected in this same population evaluated under salinity stress on chromosome four (Hostetler et al., 2021). This suggested that these belowground traits share genetic control. Further, these RSA traits were modified by the domesticated parent to favor vertical growth and biomass

enhancement, indicating that *S. bicolor* is proficient at water uptake under both drought and salinity stresses. Genes within these three drought-specific QTL play roles in root development and hormone synthesis/recognition, likely contributing to the role of water acquisition and signal transduction in drought resistance uncovered in Chapter 4. Within the two remaining drought-specific QTL, we found genes that were associated with hormone signaling, specifically relating to abscisic acid (ABA). For example, genes encoding pentatricopeptide repeat (PPR)-containing proteins were discovered; PPR's have established roles in ABA signaling in *Arabidopsis*, and were also found to be up-regulated in response to drought and heat stresses in *Sorghum* (Johnson et al., 2014, Jiang et al., 2015). Additionally, Late Embryogenesis Abundant-like (LEA) proteins, which are induced upon exposure to ABA and osmotic stress and act as molecular chaperones, were also identified within these QTL (Blackman et al., 1995, Tunnacliffe and Wise, 2007). Altogether, these findings emphasize that *S. bicolor* alleles improve water acquisition through control of root system reorganization in response to both drought and salinity stress and suggest an essential role of hormone synthesis and signaling on drought-responsive gene expression and physiological responses.

The work summarized above identified loci selected upon during domestication and improvement that facilitated drought tolerance. As described in Henderson et al. 2020, tolerance to salinity stress was found to be a product of domestication. As drought and salt stress both have osmotic components, drought tolerance was also likely acquired via domestication. Further, *S. bicolor* accessions from the landrace durra, such as TX7000, were found to be most tolerant to osmotic stress (Henderson et al., 2020). The accessions used in Chapter 3, in addition to displaying variable pre- and post-flowering responses to drought, are members of two different landraces; BTx642 belongs to the durra landrace, whereas TX7078 is a member of the kafir landrace (Menz et al., 2004). Therefore, the use of these accessions allowed for the disentanglement of landrace-specific traits under drought, as they relate to domestication and improvement in the same *Sorghum* species. Further, the RIL population used to QTL map drought-responsive changes in above- and belowground traits in Chapters 4 and 5 provided the opportunity to explore allelic and genetic controls derived from domestication. The positive control of *S. bicolor* alleles on these traits, namely the maintenance of grain yield and enhancement of water acquisition under drought, suggests that these are adaptive mechanisms acquired during *Sorghum* domestication (Woodhouse and Hufford**,** 2019).

In summary, my dissertation work contributes to and expands upon species- and accession-specific contributions to drought tolerance in an agriculturally important grain crop. Not only does my dissertation work refine our current understanding of the mechanisms that control drought responses over developmental time, but also sheds light on the histological mechanisms associated with prolonged drought exposure, which are understudied in grasses. The findings of this dissertation work suggest that morphological and physiological drought responsive strategies may work independently to achieve the same long-term goal of preventing hydraulic damage.

Additionally, my dissertation work demonstrates: 1) the impact of grain *Sorghum* varieties on drought-responsive phenotypes, which preferentially maintain grain-related traits, and 2) the influence of *S. bicolor* alleles on drought-responsive RSA modification, which favor downward growth and enhance root biomass. The QTL detected in this work shed light on the roles of both belowground (i.e. water acquisition) and aboveground (i.e. water loss prevention) drought-responsive strategies from a domestication perspective. Therefore, our findings can be used in breeding programs to enhance drought resistance and agronomic traits in *Sorghum*.

References:

Ali M, Abbas A, Niaz S, Zulkiffal M, Ali S. Morpho-physiological Criteria for Drought Tolerance in Sorghum (Sorghum bicolor) at Seedling and Post-anthesis Stages. ResearchGate.

Blackman SA, Obendorf RL, Leopold AC. 1995. Desiccation tolerance in developing soybean seeds: The role of stress proteins. Physiologia Plantarum **93**, 630-638.

Borrell AK, Mullet JE, George-Jaeggli B, van Oosterom EJ, Hammer GL, Klein PE, Jordan DR. 2014. Drought adaptation of stay-green sorghum is associated with canopy development, leaf anatomy, root growth, and water uptake. Journal of Experimental Botany **65**, 6251-6263.

Cochard H. 2002. Xylem embolism and drought-induced stomatal closure in maize. Planta **215**, 466-471.

Dinneny JR. 2019. Developmental Responses to Water and Salinity in Root Systems. Annual Review of Cell and Developmental Biology **35**, 239-257.

Goche T, Shargie NG, Cummins I, Brown AP, Chivasa S, Ngara R. 2020. Comparative physiological and root proteome analyses of two sorghum varieties responding to water limitation. Scientific Reports **10**, 11835.

Gupta A, Rico-Medina A, Caño-Delgado AI. 2020. The physiology of plant responses to drought. Science **368**, 266-269.

Hostetler AN, Govindarajulu R, Hawkins JS. 2021. QTL mapping in an interspecific sorghum population uncovers candidate regulators of salinity tolerance. Plant Stress **2**, 100024.

Jiang S-C, Mei C, Liang S, Yu Y-T, Lu K, Wu Z, Wang X-F, Zhang D-P. 2015. Crucial roles of the pentatricopeptide repeat protein SOAR1 in Arabidopsis response to drought, salt and cold stresses. Plant Molecular Biology **88**, 369-385.

Johnson SM, Lim F-L, Finkler A, Fromm H, Slabas AR, Knight MR. 2014. Transcriptomic analysis of Sorghum bicolor responding to combined heat and drought stress. BMC Genomics **15**, 456.

Kalladan R, Lasky JR, Chang TZ, Sharma S, Juenger TE, Verslues PE. 2017. Natural variation identifies genes affecting drought-induced abscisic acid accumulation in *Arabidopsis thaliana*. Proceedings of the National Academy of Sciences **114**, 11536-11541.

Kundu S, Gantait S. Abscisic acid signal crosstalk during abiotic stress response | Request PDF. ResearchGate.

Liang X, Erickson JE, Vermerris W, Rowland DL, Sollenberger LE, Silveira ML. 2017. Root architecture of sorghum genotypes differing in root angles under different water regimes. Journal of Crop Improvement **31**, 39-55.

Liu P, Yin L, Deng X, Wang S, Tanaka K, Zhang S. 2014. Aquaporin-mediated increase in root hydraulic conductance is involved in silicon-induced improved root water uptake under osmotic stress in Sorghum bicolor L. Journal of Experimental Botany **65**, 4747-4756.

McAdam SAM, Brodribb TJ. 2018. Mesophyll Cells Are the Main Site of Abscisic Acid Biosynthesis in Water-Stressed Leaves. Plant Physiology **177**, 911-917.

Menz M, Klein R, Unruh N, Rooney W, Klein P. Mullet J. 2004. Genetic Diversity of Public Inbreds of Sorghum Determined by Mapped AFLP and SSR Markers. Crop Science, 44(4).

Ndlovu E, van Staden J, Maphosa M. 2021. Morpho-physiological effects of moisture, heat and combined stresses on Sorghum bicolor [Moench (L.)] and its acclimation mechanisms. Plant Stress **2**, 100018.

Redillas MCFR, Jeong JS, Kim YS, Jung H, Bang SW, Choi YD, Ha S-H, Reuzeau C, Kim J-K. 2012. The overexpression of *OsNAC9* alters the root architecture of rice plants enhancing drought resistance and grain yield under field conditions: *OsNAC9* improves drought resistance and grain yield in rice. Plant Biotechnology Journal **10**, 792-805.

Singh V, van Osterom E, Jordan D, Messina C, Cooper M, Hammer G. Morphological and architectural development of root systems in sorghum and maize. ResearchGate.

Tang AC, Boyer JS. 2008. Xylem tension affects growth-induced water potential and daily elongation of maize leaves. Journal of Experimental Botany **59**, 753-764.

Tunnacliffe A, Wise MJ. 2007. The continuing conundrum of the LEA proteins. Naturwissenschaften **94**, 791-812.

Turral H, Burke JJ, Faurès J-M. 2011. *Climate change, water and food security*. Rome: Food and Agriculture Organization of the United Nations.

Uga Y, Kitomi Y, Ishikawa S, Yano M. 2015. Genetic improvement for root growth angle to enhance crop production. Breeding Science **65**, 111-119.

Uga Y, Sugimoto K, Ogawa S, *et al.* 2013. Control of root system architecture by DEEPER ROOTING 1 increases rice yield under drought conditions. Nature Genetics **45**, 1097-1102.

U.S. Global Change Research Program, Wuebbles DJ, Fahey DW, Hibbard KA, Dokken DJ, Stewart BC, Maycock TK. 2017. *Climate Science Special Report: Fourth National Climate Assessment, Volume I*. U.S. Global Change Research Program.

Van Loon A. Drought in the Anthropocene. ResearchGate.

Woodhouse MR, Hufford MB. 2019. Parallelism and convergence in post-domestication adaptation in cereal grasses. Philosophical Transactions of the Royal Society B: Biological Sciences **374**, 20180245.

Zhang F, Zhang K, Du C, Li J, Xing Y, Tang L, Li Y. Effect of Drought Stress on Anatomical Structure and Chloroplast Ultrastructure in Leaves of Sugarcane. ResearchGate.

ACKNOWLEDGEMENTS

I would like to begin by thanking my Ph.D. advisor, Dr. Jennifer Hawkins. I first met Jen during my in-person interview at WVU in May 2015. I had graduated from Roanoke College a few days earlier, and was excited to see what the next few years of my life would look like; who knew I'd be working with plants! Following that visit, I knew WVU was the place for me. My journey in Jen's lab has had many ups and downs, but Jen always encouraged me to learn something new from every failure. I'm so lucky that she let me learn from those experiences and be very independent in my research, because I know the challenges I've overcome shaped me into the person and scientist I am today. Even though Jen gave me a lot of freedom and flexibility in my research, she always knew when it was time to reel me back in. Jen was always supportive of my career goals (even when they changed!), and encouraged me to participate in various extracurricular organizations/committees, unrelated to my dissertation work, in support of my professional development. Without a doubt, I know my experience at WVU would be far different without her as my advisor and mentor, and I would not change any aspect of this journey.

Next, I would like to thank my dissertation committee members, Dr. Vagner Benedito, Dr. Eddie Brzostek, Dr. Jonathan Cumming, and Dr. Tim Driscoll, for their feedback and time (and patience!) throughout my graduate career. I have thoroughly enjoyed all of our conversations about my research and am thankful for the confidence they have instilled in me.

There are many members of the Biology Department that I would like to thank. First, is Mickey Sackett. This department would not function without Mickey, so she deserves MANY thanks. Mickey has always been like a mother to the graduate students, and has always been there for anything I may have needed, administrative or personal; I will miss her dearly. Next, I would like to thank Mike McKinstry. Mike is one of the smartest, kindest, and most wonderful people I have ever met, and it has been such a joy to develop a friendship with him over the past few years. I often laugh when thinking about all of the chats (some may call them rants) I've had with him and Christine. I'd also like to thank Dr. Dana Huebert Lima. She has been a wonderful mentor and friend, and has provided me with many opportunities to hone my pedagogical skills. I will miss her and her kiddos immensely. Dr. Jen Gallagher has also played such a large role in my life at WVU. I rotated in her research lab during my first semester at WVU. Even though I didn't stay in her lab for my graduate studies, she has always continued to treat me as one of her own. Her support throughout my graduate career has been much appreciated. Lastly, I have to thank my wonderful and amazing boss, Ryan Percifield. I've been so lucky to work with Ryan in the Genomics Core over the past two years and have learned so much during this time. He is such a kind and understanding person and goes out of his way to help me with both Genomics Core work and dissertation-related projects. Fortunately for me, he is more than happy to be thanked in homemade chocolate chip cookies :)

I'd like to thank my amazing lab members, especially my best friend Jazz Freeman, for their constant support, encouragement, and willingness to always commiserate with me. I am beyond thankful to have a friend like Jazz. She is one of my biggest supporters (and just **gets** me), and there aren't words to describe how much I appreciate her family essentially taking me in as their fourth daughter. I also want to give Farren Smith a huge shout out, not only for being a great friend, but because much of this dissertation work would have been impossible without her help. Same goes for Dr. Raj Govindarajulu, whose computational guidance and advice saved me countless hours of work. I cannot forget Emmy Braun, Noah Collie, Dr. Ashley Hostetler, and Dr. Dhanu Ramachandran: thank you for wonderful memories that I will cherish for a lifetime.

My two best friends, Dr. Michael Ayers and Dr. Apoorva Ravishankar, have been my anchors throughout graduate school. They have been my voices of reason and encouragement, and I do not know how I survived without them both in Morgantown. I am so thankful for video chatting!

I'd like to thank my boyfriend, Dave. He's only been with me on this journey for about two years, but he's definitely gotten a taste of what a graduate school experience is like. His level-headedness is often what I need when I am feeling incredibly stressed and overwhelmed. Thank you for always being you, for knowing how to make me laugh, and for supporting me through the tail-end of this journey.

Lastly, I would like to thank my family. My dad and stepmom have always provided me with moral support from afar. Whenever my phone rings between 4-5pm, I can guarantee that it's my dad calling on his way home from work to check in on me. My sister, Cassandra, my closest confidant, understands me like no one else can. She drove to Morgantown at 2am to help me move into my apartment when I first came to WVU. If that doesn't describe how great she is, I don't know what will. Although she now works night shifts as a nurse (in Washington state no less) and our schedules are kind of backwards, I know she will always be there for me. Finally, my wonderful mother. She'll answer her phone even at all hours, even when she's working, to make sure I'm okay (the perks of being the youngest child), and will always listen to me read through various graduate school documents (even if she does not always understand the concepts). She celebrates my successes and comforts me when I am struggling. Even though she's in Florida, her support has never wavered.